THE INVESTIGATION OF NEW BIOCHEMICAL ASSAYS AND FUNCTIONS OF THE HISTONE ACETYLTRANSFERASES

by

LIZA NGO

(Under the Direction of Y. George Zheng)

ABSTRACT

Post-translational modifications (PTMs) are important tasks given to enzymes that are responsible for adding specific moieties onto proteins and have been dubbed as writers in the epigenetic code. Of the modifications, lysine acetylation is a common and vital modification that regulates many processes that occur in the cell. Histone acetyltransferases (HATs) are writers whose canonical function is to transfer the acetyl moiety from acetyl CoA to the ε-amino group of lysine residues. This modification on histone and non-histone proteins has also been linked to a number of diseases. Despite the many efforts to discover HAT inhibitors, currently, there are no FDA (Food and Drug Administration) approved drugs that target this type of enzyme. To aid in the discovery of drugs, that target HATs, the goal of this work is to investigate new assays and catalytic functions of HATs. More specifically, the focus will be on HAT1 because this enzyme has been associated with various devastating diseases such as cardiovascular disease and cancer; however, it is poorly studied in comparison to the other HATs. This work will aim to develop a biochemical assay that can detect HAT activity and is compatible with high throughput screening, as well as fill in the gap in knowledge about novel cofactors and substrates of HAT1. Results show that the developed scintillation proximity assay (SPA) is efficient and suitable to

detect HAT activity for inhibition screenings. Using the SPA, a potent inhibitor was identified for HAT1 that was competitive towards both substrate and cofactor. To expand our understanding of HAT1 activity, a novel crotonylation activity was also discovered to occur on and by this enzyme. Lastly, as a proof of concept, we showed that a rationally designed biorthogonal probe was able to label substrates of HAT1. Overall, this study was able to enhance our understanding of HAT1 activity and aided in the future development of therapeutics that target this enzyme.

INDEX WORDS: Epigenetics, HAT1, p300, Histone Acetyltransferase, Scintillation Proximity Assay (SPA), HAT1 Bioorthogonal probe, Crotonylation, Autocrotonylation, Bisubstrate inhibitor

THE INVESTIGATION OF NEW BIOCHEMICAL ASSAYS, AND FUNCTIONS OF THE HISTONE ACETYLTRANSFERASES

by

LIZA NGO

Bachelors of Science, Georgia State University, 2012

Masters, Georgia State University, 2013

A Dissertation Submitted to the Graduate Faculty of The University of Georgia in Partial Fulfillment of the Requirements for the Degree

DOCTOR OF PHILOSOPHY

ATHENS, GEORGIA

2018

THE INVESTIGATION OF NEW BIOCHEMICAL ASSAYS AND FUNCTIONS OF THE HISTONE ACETYLTRANSFERASES

by

LIZA NGO

Major Professor:	Y. George Zheng
Committee:	Shelley B. Hooks
	Eileen J. Kennedy
	Arthur Roberts
	Kojo A. Mensa-Wilmot

Electronic Version Approved:

Suzanne Barbour
Dean of the Graduate School
The University of Georgia
December 2018

DEDICATION

I would like to dedicate this to my family and friends. Their love, advice, and support mean more to me than words can ever express. I am forever grateful and blessed to have them in my life.

ACKNOWLEDGEMENTS

I would like to acknowledge and thank my major advisor, Dr. Y. George Zheng for the opportunity to work in his laboratory as well as for his support, guidance, and wisdom throughout my academic study. Being a part and working on projects in his laboratory really fueled my fire for science and has given me the skills to strengthen my foundation for my future endeavors. I would also like to thank my committee Dr. Shelley B. Hooks, Dr. Eileen J. Kennedy, Dr. Arthur Roberts, and Dr. Kojo A. Mensa-Wilmot for their helpful suggestions and critiques.

I would also like to acknowledge all the Zheng laboratory members who have been a part of my graduate career and whom has made this endeavor fun and enjoyable. I appreciate the suggestions, discussion, and help each member has made in my graduate studies. The Zheng laboratory members are not only dear colleagues but have become cherished friends.

Lastly, I would like to thank the staff, faculty, other graduate students in the Pharmaceutical and Biomedical Science department, the staff in the Proteomics and Mass Spectrometry Facility, as well as our collaborators for also helping me in my graduate studies.

TABLE OF CONTENTS

Page

LIST OF ABBREVIATIONS

2-[4-((bis[(1-tert-butyl-1H-1,2,3-triazol-4-yl)methyl]amino)methyl)-1H-1,2,3-triazol-1-yl]acetic acid (BTTAA)

3-Az sodium salt (Na 3-AZ)

4-Az sodium salt (Na 4-AZ)

Acetyl-coenzymeA (Ac-CoA)

Antisilencing function 1 (Asf1)

ATB-binding cassette transporter A1 (ABCA1)

Biotinylated H4-20 peptide (H4-20 BTN)

Di methylflormamide (DMF)

Diethylamino-3-(4'-maleimidylphenyl)-4-methylcoumarin (CPM)

Dimethyl sulfoxide (DMSO)

Dimethyldioxocyclohexylidene (Dde)

Dissociation-enhanced lanthanide fluorescence immunoassay (DELFIA)

Epithelial cell line of human esophageal carcinoma (Eca-109 cell)

Fast protein liquid chromatography (FPLC)

Food and Drug Administration (FDA)

Gcn5-related N-acetyltransferases (GNAT)

General Control Nonderepressible (GCN5)

High-performance liquid chromatography (HPLC)

High-throughput screening (HTS)

Histone acetyltransferase (HAT)

Histone acetyltransferase 1 (HAT1)

Histone acetyltransferase binding to ORC (HBO1)

Histone deacetylase (HDACs)

Histone H4 1-20 amino acid peptide (H4-20)

HIV Tat-interacting 60kDa protein (TIP60)

Homologous recombination (HR)

Human immunodeficiency virus (HIV),

Isopropyl β-D-1-thiogalactopyranoside (IPTG)

Lysine (Lys)

Males absent on the first (MOF)

Matrix assisted laser desorption/ionization (MALDI)

Monocytic leukemia zinc finger (MOZ)

Monocytic leukemia zinc finger protein-related factor (MORF)

Mouse Vasa homologue (MVH)

N-(9-fluorenyl) methoxycarbonyl (Fmoc)

N, N'-Diisopropylcarbodiimide (DIC)

Nuclear receptor coactivator 3 (ACTR/NCOA3)

Nuclear receptor cofactors (NRCF)

O-(1H-6-Chlorobenzotriazole-1-yl)-1,1,3,3-tetramethyluronium hexafluorophosphate (HCTU)

p300/CBP associated factor (PCAF)

Peroxisome-proliferator-activated receptor gamma coactivator-1α (PGC-1α)

Phenylmethanesulfonyl fluoride (PMSF)

Plant homeodomain-linked (PhD)

Polyvinyl toluene (PVT)

Post-translational modifications (PTMs)

Promyelocytic leukemia zinc finger protein (PLZF)

protein arginine methyltransferase 1 (PRMT1)

Scintillation proximity assay (SPA)

Sirtuin-3 (SIRT3)

Sodium crotonate (NaCro)

Sodium dodecyl sulfate polyacrylamide gel electrophoresis (SDS-PAGE)

Steroid receptor coactivator (SRC)

Sulfate-polyacrylamide gel electrophoresis (SDS-PAGE)

Transcription Factor IIIC (TFIIIC)

Trifluoroacetic acid (TFA)

Tritium (^{3}H)

LIST OF TABLES

Page

LIST OF FIGURES

Page

CHAPTER 1

INTRODUCTION

1.1 Modifications to histones and its impact on biological functions

Eukaryotic organisms organize DNA to chromatin structures using a compaction system involving highly basic histone proteins. Chromatin is made up of repeating units of nucleosomes, which consist of 145-147 base pairs of DNA left-handedly wrapped twice around the exterior of a histone core octamer.[1] The nucleosomes are connected through histone H1 to form the "beads on the string" construct and aids in the higher compaction of the DNA. The histone octamer comprises of two sets of the histone H2A, H2B, H3 and H4. Each core histone consists of flanking N -terminal tails which can undergo various post-translational modifications (PTMs), such as acetylation, methylation, phosphorylation, ubiquitination, and glycosylation, at numerous sites (**Figure 1.1**).[2] These PTMs are ways that organisms can react to external or internal stimuli. Of the modifications, acetylation is a common as well as important modifications found on histone tails and is also linked to several diseases.[3 4]

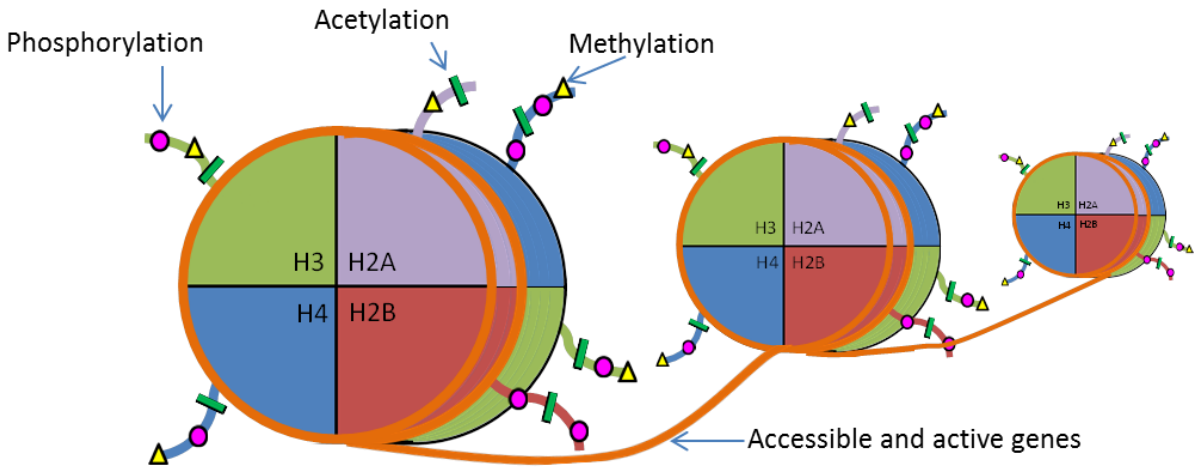

Figure 1.1: Open chromatin, in which genes are easily accessible for transcription. Nucleosome with DNA strand (orange) wrapped twice around a histone octamer with N-terminal tails containing post translational modifications (squares, triangle, circles indicate PTMs).

Different enzymes mediate the various post-translational modifications. The acetylation modification to histone proteins by Histone acetyltransferases (HATs) was discovered by Allfrey et.al in 1964.[5] HAT enzymes transfer the acetyl group from acetyl-coenzymeA (Ac-CoA) to the ε-amino group of lysine residues on histone and non-histone proteins (**Figure 1.2**). The removal of the acetyl group on lysine is done by histone deacetylase (HDACs). Sternglanz et al. identified the first histone acetyltransferase,HAT1, in 1995 through an in vitro screening of 250 mutant strains of budding yeast.[6] One mutant strain from the screening showed a 40% reduction in acetyltransferase activity in comparison to the wildtype. The gene was identified and cloned then later expressed in *E. coli*. HAT1 extracts from the E. *coli* expression demonstrated elevated levels of acetyltransferase activity, thus validating the identified gene and the intrinsic HAT1 function. Since the discovery of HAT 1, there has been an extensive

increase in the field study of HATs resulting in the identification of other HAT members and their function. For example, in 1996, Allis et al. showed that histone acetylation by HAT enzymes played a role in gene activation.[7] Since those initial discoveries, there have been more findings of histone acetylation by various HATs and its involvement in cellular activities such as cell signaling, cell proliferation, DNA repair, DNA replication, chromatin maturation and dynamics, nucleosome assembly, gene transcription, and gene silencing.[8-12] There have also been numerous efforts to investigate these enzymes to better understand their role in cells, diseases, and a as a therapeutic target.[4]

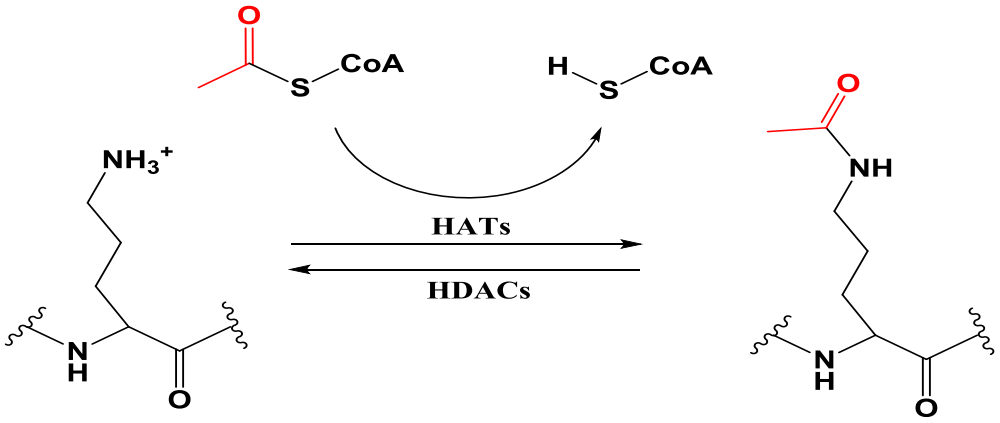

Figure 1.2: The canonical function of HATs. HATs acetylate histone and non-histone proteins by transferring the acetyl group from Ac-CoA to ε-amino group of lysine residues. Through HDACs, acetyl groups are removed from lysine residues

1.2 Histone acetyltransferases (HATs)

HATs are categorized into type A and type B based on the localization and function of the enzymes in the cell.[13] Type A HATs are localized in the nucleus and catalyze the acetylation reaction in events relating to transcription, however, type B HATs have been found in both the nucleus and cytoplasm and typically only acetylate newly synthesized histones that are not yet

part of a nucleosome.[14] HATs are divided into three major families based on their homology and acetylation mechanisms.[15] The Gcn5-related N-acetyltransferases (GNAT) family include members such as PCAF (p300/CBP associated factor), GCN5 (general control nonderepressible 5) and HAT1 (histone acetyltransferase 1) which have similarity to GCN5 and composed of several conserved domains.[16-17] Enzymes like GCN5 and PCAF in this family also have a bromodomain that bind to acetylated modifications. Likewise, CBP and p300 have a bromodomain, however, are in the p300/CBP family.[18] The MYST family named after its founding members human MOZ (monocytic leukemia zinc finger), yeast YBF2/SAS3, yeast SAS2, and human TIP60 (HIV Tat-interacting 60kDa protein) is known for having a conserved MYST domain which includes an acetyl-CoA binding motif and a zinc finger.[19] In addition to those domains, MYST enzyme TIP60 and MOF also have a chromodomain that binds to methylated lysine residues while MOZ and MORF have a PhD (plant homeodomain-linked) domain that binds to sequence specific methylated lysine and arginine as well as acetylated lysine residues.[20-21] The other three MYST enzymes found in human are MOF (males absent on the first), HBO1 (histone acetyltransferase binding to ORC), and MORF (monocytic leukemia zinc finger protein-related factor).[18] GNAT, p300/CBP, and MYST are the canonical HAT families and all of the HATs listed are type A HATs while HAT1 is a type B HAT (**Figure 1.3**).[22]

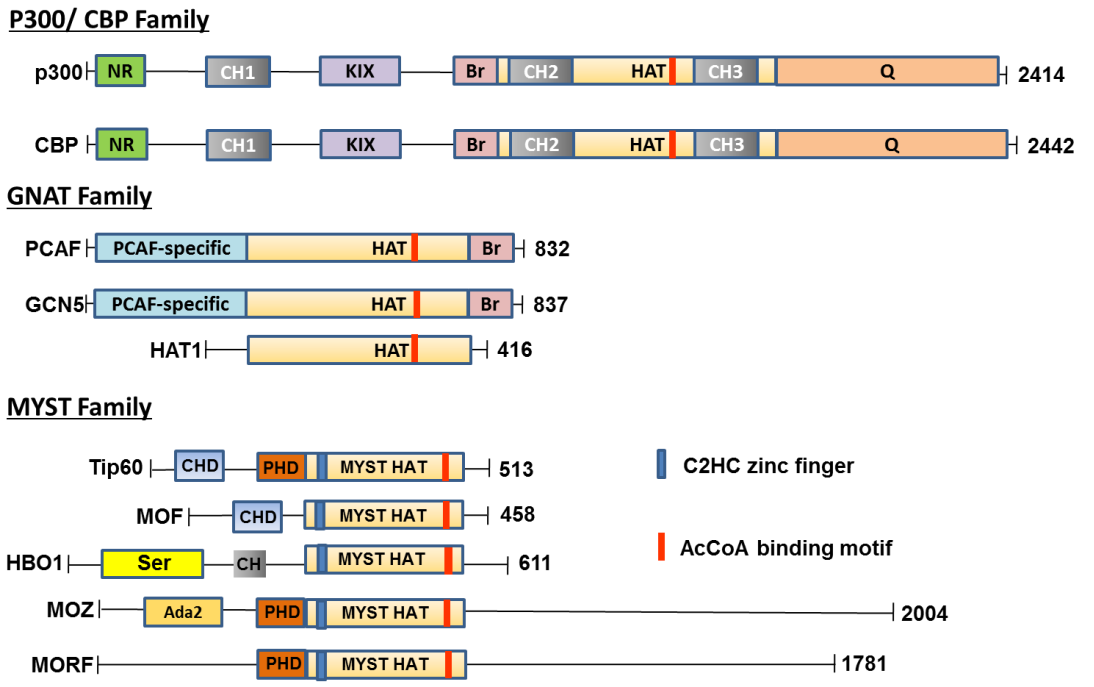

Figure 1.3: Functional domains of canonical human HAT families.

1.3 HAT1 localization and function

HAT1 is an evolutionary conserved enzyme from yeast to humans and is considered a type B HAT.[23-24] It is localized in both the cytoplasm and nucleus. In the cytoplasm HAT1 is known to acetylate newly synthesized histone H4 at the evolutionary conserved lysine 5 and 12, H2A at lysine 5 and to maintain the acetylation marks on histone H3 at lysine 9, 18, and 27 during replication-coupled chromatin assembly.[25-27] The acetylation marks of histone H5 at lysine 5 and 12 are evolutionarily conserved, however, its function is unclear and has been shown to be nonessential in yeast.[28] Although HAT1 is conserved from yeast to humans, it may be playing a redundant role in chicken cells and yeast because when HAT1 is depleted there is not a significant effect in the overall proliferation or viability; however, in mammalian cell models and mice models, there is a notable effect that is lethal.[25, 29-30]

In the nucleus HAT1 is involved in forming various complexes. It is a part of a trimeric NuB4 complex in yeast models with other members such as HAT2 (a homolog of the humans protein RbAp46) which binds to HAT1 and Hif1 (a homolog of the mammalian protein NASP).[14, 31] The chaperone, HAT2, increases HAT1 activity by ~10-fold and Hif1is a histone H3-H4 specific histone chaperone.[32] Association of HAT1 with the formation of the NuB4 complex was the first indication that HAT1 had a role in chromatin assembly process.[32] Another chaperone that is associated with HAT1 is Asf1 (antisilencing function 1). Asf1 plays a role in DNA replication, repair, and transcription through aiding in assembling or disassembling of chromatin, and binds to the HAT1 and HAT2 complex by interacting with H3-H4.[14]

In mammalian cell models, when HAT1 is knocked down the cells were more sensitive to DNA-damaging agents. HAT1 is shown to be vital for homologous recombination which uses genetic information obtained from an undamaged sister chromatid or chromosomal homologue to repair a break, but not non-homologous end joining which directly ligates DNA ends. When there is a DNA double-strand break, the role of HAT1 in the repair response is enriching H4K5/K12-acetylated H3.3 at the site by forming a complex with the chaperone, HIRA, to aid in histone turnover. This process marks the damaged area which then allows the repair factors, RAD51and RAD 50,which interact with HAT1 to start the homologous recombination (HR) repair process.[33]

1.4 HAT1 structure

Human HAT1 is a member of the GNAT superfamily and its crystal structure with a resolution of 1.9-Å was solved by Wu et al. The structure illustrates HAT1 binding to both histone H4 1-20 amino acid peptide (H4-20) and AcCoA (AcCoA consist of an adenine and ribose ring as well as a pyrophosphate, pantotheine, and acetyl group). Structure analysis

demonstrate that this elongated enzyme has three domains consisting of an N-terminal domain (residues 23-136), central or GNAT domain (residues 137-270), and the C-terminal domain (residues 271-341).[34]

The AcCoA binding site lies in a canyon formed from the central and the C-terminal domains, and for the cofactor to fit properly in the active site a kink must be formed in the pantotheine arm **(Figure 1.4** (AcCoA in purple)). The pantotheine moiety is stabilized through hydrogen bonding with Ile243 and van der Waals interaction with the conserved Leu242. The adenine and the ribose ring form hydrophobic interaction with Lys284 and stacking interactions with Phe288 respectively. Van der Waals interaction with Leu285and hydrophobic interactions with residues Gly249, Gly253, Gly251 and Ala254are formed with the pyrophosphate group. Stabilization of the acetyl moiety is done through hydrophobic interaction with residues Ile186, Pro278 and Tyr282. This allows the carbonyl carbon of the acetyl moiety to be placed with a distance of ~4.3 Å to the ε-amino group of the H4-20 substrate. The substrate binding site lies in the N-terminal and the central domain and is heavily negatively charged. Anchoring of the H4-peptide into the active site is achieved through a network of hydrogen bonding including Arg17 and Arg19 of the peptide and resides Glu54, Asp62 and Glu64 of HAT1. It is important to note, that Glu64 is a conserved residue that plays a critical role in substrate binding specificity (PDB: 2P0W).[34]

Fourteen amino acids of H4-20 form interactions with residues in the binding site of HAT1 located in the central as well as the N-terminal domains (**Figure 1.4** (H4-20 in green)). These domains span across the surface of HAT1 and consist of mostly negative charged residues. Because these residues are on the surface of HAT1 it has been proposed that HAT1 can accept larger substrates in that site. Although a majority of the substrate binds on the

surface, a notable structure of HAT1 is a 5-6Å wide opening that was observed to only allow the insertion of two residues (Gly11 and Lys12). The opening eventually gets narrower and the conserved residue Glu276 of HAT1enhances specifically by interacting with Lys12 and only letting it pass through. For acetylation to occur, both Glu187 and Glu276 act as a general base while Asp277 deprotonates Lys12 for the nucleophilic attack on AcCoA. [34]

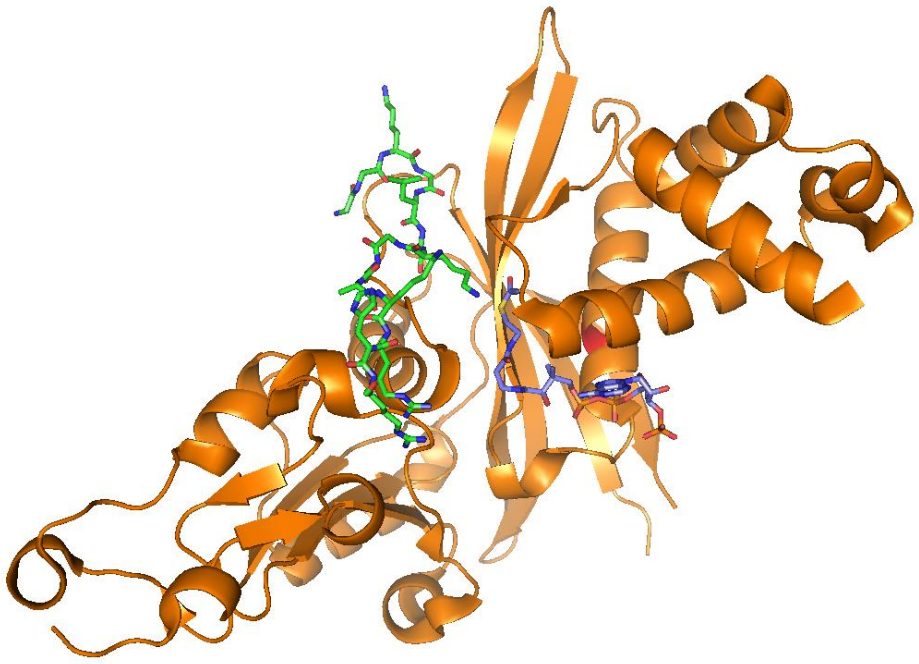

Figure 1.4: Crystal structure of HAT1 (PDB: 2P0W). Histone H4 (1-20) peptide is depicted in green and AcCoA is depicted in purple.

1.5 HAT1 link to diseases

Cancer formation and progression can occur due to the dysregulation of post transcriptional modifying proteins that are responsible for gene transcription, cell differentiation, proliferation and apoptosis. HAT1 has not only been linked to various diseases

such as cardiovascular diseases, colorectal cancer, liver cancer and lung cancer but also in the regulation of the immune response.[26, 35-36] In some instances, it is not only the aberrant expression of HAT1 but also its localization that can aid in the disease progression. These diseases have no cure or have poor treatment regimens therefore these studies demonstrate the role of HAT1 and how it can be a potential target in the design of better therapeutic agents as well as a biomarker.

HAT1 plays a role in cardiovascular disease by regulating the excessive cholesterol accumulation in macrophages. ATB-binding cassette transporter A1 (ABCA1) maintains the cellular cholesterol homeostasis by mediating the formation of high density lipoprotein to inhibit the development of atherosclerosis. Authors were able to show that mRNA and protein expression of ABCA1 was promoted by HAT1; and that atherosclerosis production was stimulated due to miR-486 targeting 3' UTR of HAT1, which resulted in a decrease in histone acetylation which caused the repression of ABCA1- mediated cholesterol efflux.[37]

Besides atherosclerosis, HAT1 acetyltransferase activity can modulate the NF-κB response by acetylating the transcription factor, promyelocytic leukemia zinc finger protein (PLZF). Part of regulating diseases is regulating the inflammation during the innate immune response. After HAT1 becomes activated through phosphorylation at S361 by CaMK2 from Toll-like or tumor necrosis factor receptors signaling, it can then acetylate the transcriptional regulator, PLZF at K277. Acetylated PLZF then forms a complex with HDAC3 and NF-κB p50 which can then negatively regulate NF-κB-mediated transactivation and represses the inflammatory response. The activation of PLZF-HDAC3- NF-κB by HAT1 repress the inflammatory response and limits the endotoxic shock and thus the mortality of mice.[38]

HAT1 has also been shown to be overexpressed at the mRNA level as well as the protein level in colorectal cancer and esophageal carcinoma.[39-40] Seiden-Long et al. studied the transcriptional changes that occurred due to Ki-ras oncogene and HGF/Met signaling in colon cancer. HAT1 was among the transcripts identified in the microarray, and the in vitro and in vivo expression profiling showed significant HAT1 gene expression changes. Tissue array immunohistochemistry of normal colonic mucosa, primary colorectal carcinoma, and metastatic tumors showed the increased expression of HAT1 in tumors to be more diffused throughout the tissue. When comparing the distribution of HAT1, it was found that in normal tissues HAT1 was more localized in the nucleus at the crypt base; however, in primary and metastatic tumors there was a drastic increase in cytoplasmic HAT1.[39] HAT1 was identified as being involved in esophageal carcinoma through RNAi screening. It was found that the mRNA expression level of HAT1 was statistically higher in the primary adjacent and tumor tissues than in normal esophageal tissues. Knockdown studies of HAT1 demonstrated a significant decrease in Eca-109 cell (epithelial cell line of human esophageal carcinoma) viability by 39% and that there was an induction of G2/M cell cycle arrest leading to growth inhibition. Immunohistochemistry of 167 esophageal carcinoma tissue samples showed that high expression of HAT1 mainly in the nucleus and that it was significantly correlated with reduced tumor differentiation.[40]

Lacking certain dietary supplements has been correlated with the induction of liver tumor formation in male rats.[41] Liver tumors also showed a significantly higher expression of HAT1 than the control liver tissue. This observation was noticed in a study looking at alterations in histone modification during methyl deficient metabolic stress. It was also observed that there was a decrease in HAT1 expression during methyl deprivation periods.[41]

The cooperativity between modifications is a topic that should be investigated and may provide an explanation as to why there is a change in HAT1 levels.

More recently, HAT1 has been shown to be overexpressed in samples from patients with hepatocellular carcinoma at both the mRNA and protein levels. In investigating hepatocellular carcinoma samples, it was determined that HAT1 has a role in cell growth and regulation of glucose metabolism because a knockdown of HAT1 caused a decrease in cell growth and glucose consumption. It was also suggested that in liver cancer HAT1 might act as an oncogenic protein due to its role in treatment resistance, preventing apoptosis, as well as promoting cell proliferation in vitro and in vivo.[35]

1.6 Assays to detect HAT activity in a high throughput fashion

Many diseases affecting millions of lives have been correlated to abnormal HATs activity. As stated before HATs act as oncogenes through chromosomal translocation mutations, deregulation, or overexpression.[42] The diseases linked to HATs often have a poor prognosis and lack treatment options. Drugs targeting the HAT opposing enzyme, HDAC, have been approved for clinical trials as well as for human use.[43] Thus, showing the therapeutic benefits of targeting enzymes involved in epigenetic modifications. The quest to find HAT inhibitors has not led to any approved therapeutics due to undesired pharmacokinetic properties, lack of selectivity, or potency.[44-45] In this drug development effort, a reliable, robust and cost-efficient biochemical method that can screen numerous HAT inhibitor compounds is critically needed. Methods currently used to detect HAT activity in a high throughput manner fall into two major categories: radiometric and fluorescence.

The radioactive filter binding assay can be considered the gold standard because of its higher sensitivity over the other methods.[46-47] It is not as time-consuming as the fluorography

assay which requires mixture separation by gel electrophoresis and radiographic film development. This assay switched from using individual filter binding papers to filters papers in a 96-well plate format, which aided in the slight decrease of radioactive waste. Despite these amenable attributes, the primary limitation for the filter binding assay is the requirement of the repeated washing and drying steps which is not only time-consuming but also causes more accumulation of radioactive wastes over other methods.[48] This technical hindrance also poses a significant challenge for this method to be used in a high-throughput format however this method is worth mentioning because of its gold standard status.

A radiometric assay that is suitable for high throughput screening was designed by Turlais et al. The flash plate assay detects HAT activity by utilizing radioactive isotopes and a solid scintillant coated 96-well plate. When the scintillant is in close proximity of the tritium labeled substrate the scintillant is excited and will emit light for detection. For this assay, the enzyme, tritium labeled Ac-CoA, and histone are reacted in the well and to quench the reaction excess buffer is added to dilute the reaction. Antibodies were used in their original design to attach the histone protein to the plate surface; however, it was discovered that the histones have an intrinsic ability to bind to the wells and excite the scintillant.[49] Although this assay has potential to be an effective high throughput assay, the homogeneity of the reaction mixture is questioned due to the intrinsic ability of the histone protein to bind to the well surface (**Figure 1.5A**).

Using radioactive assays provides more extensive background to noise ratio; however, the waste generated is not environmentally friendly. An alternative is the use of fluorescence probes incorporated into the assay. When HAT enzymes transfer the acetyl group from Ac-CoA to the lysine residue CoA is released as a byproduct. Probes such as -diethylamino-3-(4'-

maleimidylphenyl)-4-methylcoumarin (CPM) can then be used to measure the amount of byproduct produced.[50] Upon reacting with the thiol group on CoA, CPM gives off a strong fluorescence which can be detected at an excitation and emission wavelength of 382 nm and 482 nm respectively. This assay is robust and can be used in a microplate format thus allowing the use of high throughput automation. Limitations include the CPM interacting with thiol groups; therefore, this assay should be avoided it the tested molecules have a free thiol or if the reaction conditions contain reagents such as dithiothreitol. Also, the testing of fluorescent inhibitor compound should be cautioned because it can result in false data (**Figure 1.5B**).[51]

The previous two methods discussed require recombinant protein as the enzyme source; however, the cell-based ELISA provides a high throughput assay utilizing various cell lines. Tumor cells lines are incubated with the compound in a 96 well format. Then, the cells are fixed to the well and after various washing and blocking steps; the primary antibody followed by the europium-labeled secondary antibody is added. After the addition of the enhancement solution, the fluorescence is measured at 615 nm. The reported coefficient of variation for the reproducibility of this assay is between 10-15%. Other colorimetric and chemiluminescent reagents can also be used; however, DELFIA (dissociation-enhanced lanthanide fluorescence immunoassay) was used in the study and was noted to be a sensitive and robust reagent. Disadvantages of this assay include many washing steps which can hinder HTS by decreasing efficiency, as well as the use of antibodies that can vary from batch to batch and have non-specific binding (**Figure 1.5C**).[48]

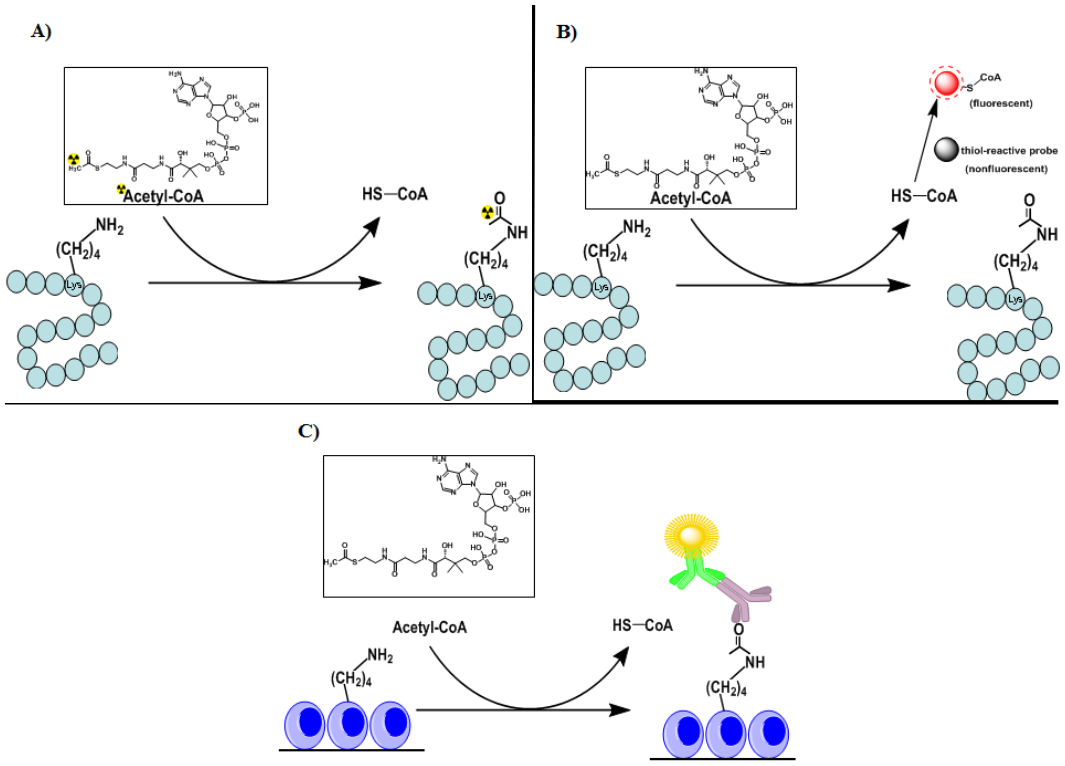

Figure 1.5: Biochemical assays to detect HAT activity. A) Radiometric assay; B) CPM assay; C) Cell-based ELISA

1.7 Inhibitors of HATs

In the above section, a few diseases linked to HAT enzymes were discussed, however, in actuality the list of diseases correlated to HATs is far greater.[42] HDAC, the opposing enzyme to HATs, has had remarkable success in inhibitor discovery. The therapeutics drugs targeting HDACs, Vorinostat, and Romidepsin, have surpassed clinical trials and are approved for human use in cutaneous and peripheral T-cell lymphoma.[52] These drugs provide a proof of concept on targeting epigenetic proteins as a practical approach to treat diseases. It is also thought that since acetylation is a reversible event that targeting it could result in lower toxicity.[53] Many groups have identified potent HAT inhibitors using approaches like rational design, small molecule

high-throughput screening, and plant extract screening. The HAT inhibitors identified fall into three major categories: CoA bisubstrate inhibitors, natural product, and small molecules.

Bisubstrate inhibitors were the designed to mimic the ternary complex formation that occurs upon the binding of the histone substrate and cofactor to the enzyme. The peptides varying in length can cause a difference in potency. H3-20-K14CoA imitates the first twenty amino acids on the amino terminus of H3 with the addition of CoA on lysine 14. The IC_{50} of this inhibitor for PCAF is reported to be 0.3 µM and highest potency was observed with peptides lengths greater than 12 but less than 20 amino acids.[54] Kinetics of this inhibitor for PCAF revealed that it was a competitive and noncompetitive inhibitor against Ac-CoA and H3-20 respectively.[54] H4-20-K16CoA had CoA was conjugated to lysine 16 and was an inhibitor that targeted TIP60 and its yeast orthologue Esa1. IC_{50} of this inhibitor for TIP60 and Esa1 was 17.3 µM and 5.5 µM respectively.[55] Similar to H3-20-K14CoA, this inhibitor is a competitive for AcCoA and noncompetitive against H4-20 peptide. The smaller bisubstrate inhibitor, lys-CoA, with an IC_{50} of 0.5 µM and was found to be a selective inhibitor for p300 over PCAF.[56]

The acetyl transfer mechanism of p300 explains why it does not interact with the long peptide inhibitor, H3-20-CoA, and why Lys CoA is a 20-fold better inhibitor for this enzyme. Theorell-Chance catalytic mechanism is the acetyl transfer mechanism of p300. This mechanism does not require a stable ternary complex formation; therefore, when the peptide weakly binds to the enzyme after Ac-CoA has bound the lysine will react with the acetyl group then quickly leaves. On the other hand, H3-20-CoA was found to be a potent and selective inhibitor for PCAF (IC_{50}: 28 nM), and it is because this enzyme tends to form stable complexes thus it will arrange higher affinity interaction with the substrate (**Figure1.6**).[57]

Despite the potency of these inhibitors for their respective HAT enzyme, pharmacokinetic properties such as poor cell permeability and metabolically instability prevent these bisubstrate inhibitors from being potential therapeutics.[58] Efforts have been made to eliminate the negatively charged phosphates in the CoA moiety but the results show a significant decrease in inhibition potency.[59] Removal of the 3'phosphate group of Lys-CoA resulted in the inhibitor 3'dephospho-Lys-CoA which increased the IC_{50} by 33-fold to 1.6 μM.[59] Further reduction of the CoA moiety leaving just the cysteamine-beta-alanine portion enhanced sensitization to chemotherapy and cellular uptake presumably by the polyamine transporter.[60]

Natural products have also been screened and explored as HAT inhibitors. Anacardic acid extracted from the shell liquid of a cashew nut was the first natural product inhibitor for p300. It inhibited p300 and PCAF activity with IC_{50} values of 8.5 μM and 5 μM respectfully, and was found to be a p300 noncompetitive inhibitor against Ac-CoA.[61] The limitations for anacardic acid as a potential therapeutic is that it has poor specificity as well as cell permeability. Garcinol, a polyisoprenylated benzophenone derivative, is isolated from the Garcinia indica fruit rind. It has known antioxidant properties and anticancer activity because in the presence of garcinol proto-oncogenes are down-regulated. On the downside Garcinol is not specific because it can inhibit both p300 ($IC_{50} \approx 7$ μM) and PCAF ($IC_{50} \approx 5$ μM) with similar potencies.[62] This inhibitor also has poor cell permeable capabilities. Curcumin, the yellow pigmented turmeric spice is from the root of *Curcuma longa L.* It has been reported that curcumin has other pharmacological effects such as anti-tumor, anti-inflammatory, and anti-infectious activities.[63] Of the HAT enzymes, this inhibitor is specific for p300/CBP with an IC_{50} of 25 μM and is cell permeable.[64] Curcumin can conjugate to p300/CBP due to the two Michael acceptor functionalities in its structure, and based on kinetic studies this inhibitor binds in an

allosteric site and not in either substrate or cofactor pocket.[64-65] Although curcumin has specificity for a certain HAT enzyme it can still bind to other targets like DNA methyltransferase 1 and HDAC making its target in disease models unknown.[66] Overall, anacardic acid, garcinol and curcumin have limitations such as being moderately potent and lacking selectivity. Despite these limitations, these inhibitors can be used as templates to synthesize inhibitors based off of its specific HAT activity modulation properties.[67] From these natural products analog derivatives have been synthesized with the goal of improving selectivity, inhibition potency, and cell permeability properties (**Figure 1.6**).[66]

Small molecules are another class of compounds to classify HAT inhibitors. The discovery of small molecules as HAT inhibitors emerge from the screening of large compound libraries. Isothiazolones have biological functions such as antibacterial and antiparasitic properties. In addition to those properties, isothiazolones and its derivatives were detected as HAT inhibitors through virtual screening as well as biochemical inhibitor assays.[68] The optimization of these small molecules led to IC_{50} values in the low micromolar range for PCAF (IC_{50} 1 μM) and p300 (IC_{50} 0.5 μM); however, the mechanism of inhibition was through covalent interaction. It was determined that the S-N bond reacted with the thiol of the cysteine in the active site resulting in low micromolar inhibition.[68] A decrease in the general bioreactivity of later optimized pyridoisothiazolones inhibitors was observed in addition to the submicromolar inhibition of PCAF and antiproliferative properties in epithelial cell lines.[69] Of the pyridoisothiazolones tested, PU141 specifically targeted CBP and p300, while PU139 targeted other HATs including GCN5, PCAF, CREB and p300.[70] Both of these inhibitors were more specific for HATs than of other cysteine-containing or dependent enzymes.[70] Although these inhibitors cause histone hypoacetylation, optimization is still required to enhance potency,

pharmacokinetic properties and selectivity among the HATs. NU9056 is an isothiazole that was discovered to be a TIP60 specific inhibitor with an IC_{50} of 2 μM. When tested with other HATs the selectivity for TIP60 was 16.5, 29 and >50 fold greater than for PCAF, p300 and GCN5 respectfully. In addition to decreasing the levels of androgen receptor, prostate-specific antigen, p53 and p21 protein levels, this small molecule also inhibited the proliferation of prostate cancer cells.[71] The most potent HAT inhibitor specific for p300 is C646 which was discovered through in silico screening. C646 is a competitive inhibitor against Ac-CoA and has an IC_{50} of 1.6 μM.[72] When tested among other HATs, such as PCAF, GCN5, and MOZ, C646 was more selective for p300. Studies demonstrate the inhibitors ability to induce caspase-dependent apoptosis in androgen-dependent and independent prostate cancer cell lines.[73] The potential of C646 as a therapeutic is very high, and animal studies shows this inhibitor is effective when locally administered; however, the downside is that it becomes inactivated in serum (**Figure 1.6**).[73-74]

The poor pharmacokinetics of these inhibitors is not the only challenge in the discovery of therapeutics targeting HATs. Another issue involves compounds disguising as an inhibitor by having Pan Assay INterference compoundS (PAINS) properties. PAINS compounds impersonate potential leads and provide false positives by having spontaneous reactions under assay conditions through the reactive moiety that can cause covalent modifications or redox effects, chelation, autofluorescence, or degradation.[75-76] Counter-screens have shown that most of the reported HAT inhibitors are PAINS.[77] For example, some of the compounds mentioned above such as C646, NU9056 and curcumin went through a biochemical counter screen and results showed that they were reactive towards thiols.[77] This issue has made the efficacy of

some of the published HAT inhibitors doubtful; thus, more efforts should be made to identify compounds with ideal pharmacokinetic parameters and do not contain PAINS moiety.

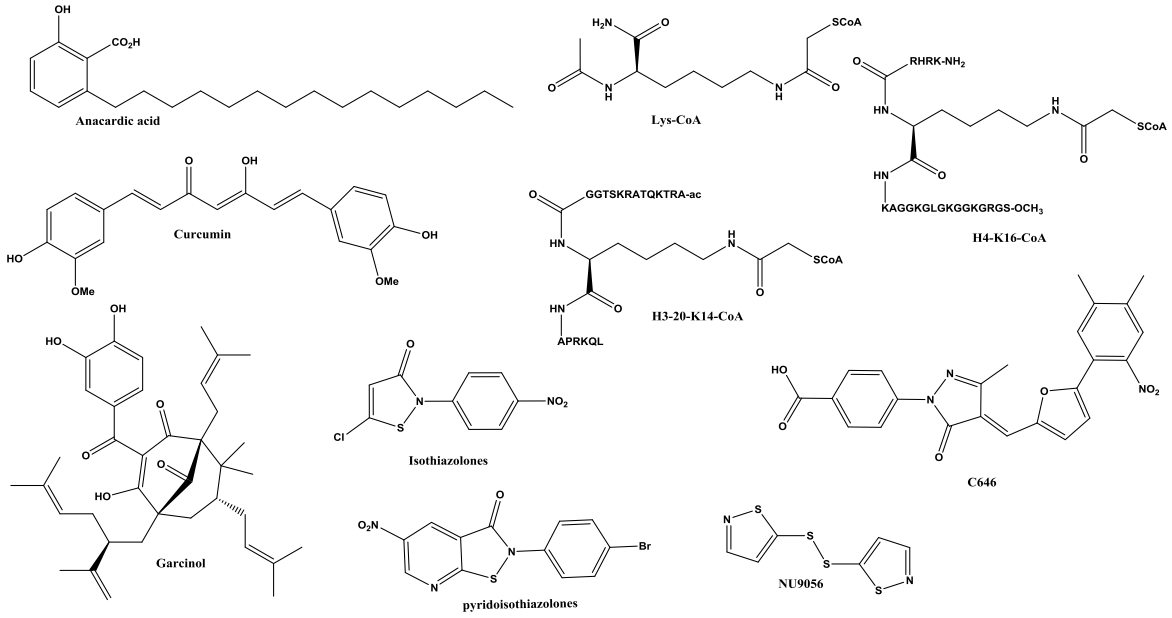

Figure 1.6: Selected HAT inhibitors which include natural products, bisubstrate inhibitors, and synthetic small molecules.

1.8 Conclusions

This chapter provided an overview of what is currently known about human HAT1, its implications in diseases that make it an important enzyme to investigate and target in drug discovery, as well as assays used to detect HAT activity. HAT1 behaves differently in yeast than it does in mammalian models; however, studies of HAT1 using mammalian models are very scarce. In addition, although HATs have been sought out as potential targets in drug discovery, to date there are no FDA approved therapies targeting these enzymes, much less HAT1. Here we will discuss some outstanding questions and the challenges that remain in this field.

To begin, HAT1 is the first HAT to be discovered however it is the most poorly studied in comparison to other HATs. More efforts should be made to fill in our gap in knowledge of HAT1. Currently, there are no inhibitors that target HAT1. There are assays available to screen for HAT inhibitors; however, we believe that the limitations of these assays discussed above make them less desirable to utilize. To combat these issues, an assay should be developed that addresses these concerns and provides reliable data. Discovering inhibitors that target HAT1 can be very beneficial because they can also be used as probes to investigate the binding mechanism and activity.

As previously mentioned, HAT1 has been implicated in various diseases; however, our understanding of the activity of this enzyme is limited. By expanding our knowledge about its activity, function, and mechanism, we can use that information to rationally design inhibitors to target HAT1 better. Various proteomics reports on novel PTMs such as crotonylation have noted HAT1 in their findings.[78-80] With HAT1 noted in these studies our outstanding questions are 1) What enzyme added the PTM on HAT1; 2) How is the activity of HAT1 affected by the addition of the PTM; and 3) Besides acetylation, does HAT1 also possess this novel PTM activity. Answers to these questions can enhance our understanding of not only HAT1 but also the role that the PTM plays.

In mammalian models when HAT1 is depleted there were severe implications to growth and viability.[25, 33] Due to these findings, we believe that HAT1 may be playing a more important role than what has been reported. To uncover its role, it is crucial to determine if HAT1 has any other substrates than the ones reported. Currently, there are only two known non-histone substrates of HAT1and it is possible that this enzyme possesses more.

1.9 The goal of this work

PTMs are essential for normal growth and development, however, when unregulated, can result in devastating and debilitating diseases. To combat these diseases, many laboratories have identified inhibitors, which target epigenetic writer enzymes, for therapeutic purpose. Unfortunately, HATs are not among the epigenetic enzymes that have FDA (Food and Drug Administration) approved therapeutic reagents. More specifically, when focusing on HAT1, lacking reports on this enzyme in comparison to other HATs result in huge gaps in knowledge on its function. Besides gap in knowledge, HAT1 has been correlated to many detrimental diseases such as various cancers and cardiovascular disease. Due to these reasons, it is crucial that we investigate HAT1; therefore, the goal of this work is to not only fill in the gaps in knowledge but to aid in the discovery of inhibitors targeting this enzyme. To accomplish this goal and to have a better comprehension of HAT1 and its functions, assays will be developed to enhance the detection of HAT activity, potent and selective inhibitors targeting HAT1 will be identified, novel acyl transferase activity will be discovered for, and HAT1biorthogonal probes will be rationally designed to aid in the identification of substrates.

CHAPTER 2

EFFECTIVE QUENCHERS ARE REQUIRED TO ELIMINATE THE INTERFERENCE OF SUBSTRATE—COFACTOR BINDING IN THE HAT SCINTILLATION PROXIMITY ASSAY

–

Ngo, L.; Wu, J.; Yang, C.; Zheng, Y. G., Assay Drug Dev. Technol. 2015, 13 (4), 210-220.

Reprinted here with permission of the publisher.

Abstract

Histone acetyltransferases (HATs) mediate the transfer of an acetyl group from the cofactor, acetyl-CoA, to the side chain amino group of specific lysines in diverse protein substrates, most notably nuclear histones. The deregulation of HATs is connected to a number of disease states. Reliable and rapid biochemical assays for HATs are critical for understanding biological functions of protein acetylation, as well as for screening small-molecule inhibitors of HAT enzymes. In this report, we present a scintillation proximity assay (SPA) for the measurement of HAT enzymatic activities. The acetyl donor was [^{3}H]-Ac-CoA, and a biotin-modified histone peptide served as the HAT substrate. After the HAT reaction, streptavidin-coated beads were added to induce proximity of acetylated substrate to the scintillant molecules. However, we observed strong nonspecific binding between the cofactor and the histone peptide substrates, which adversely complicated the SPA performance. To prevent this problem, a set of chemical agents were evaluated to eliminate the cofactor–substrate interaction, thus providing reliable SPA readings. With optimization, the SPA showed consistent and robust performance for HAT activity measurement and HAT inhibitor evaluation. Overall, this mix-and-measure assay does not require any washing procedure, can be utilized in the microplate format, and is well suited for high-throughput screening of HAT chemical modulators.

2.1 Introduction

Histone acetyltransferases (HATs) transfer the acetyl group from the cofactor, acetyl-Coenzyme A (, Ac-CoA), to the ε- amino group of specific lysines in histones and non-histone proteins. HATs are classified into several main families which include GCN5/PCAF, MYST, and CBP/p300.[17] Studies have shown that theses enzymes play critical roles in the regulation of chromatin restructuring, gene transcription, and signal transduction. Deregulation of HAT levels

and activities can result in the development and progression of various diseases such as cancers and cardiac hypertrophy.[81-83] Given that these diseases affect millions of lives, it is of great importance to discover inhibitors for these HAT enzymes. In this drug development journey, reliable and efficient biochemical methods that are able to screen numerous HAT inhibitor compounds are critically needed.

A few reported methods have been used to detect the acetyltransferase reaction mediated by HATs, which include radioactive filter binding assays, coupled fluorogenic assays, Flash plate assays, and fluorography assays.[48-49, 84] Among these assays, the radioactive filter binding method using negatively charged phosphocellulose paper discs is considered the gold standard because it has greater sensitivity over the other methods and it is not as time-consuming as the fluorography assays which require mixture separation by gel electrophoresis and radiographic film development. Despite these amenable attributes, the major limitation for the filter binding assay method is the requirement of repeated washing steps which are not only labor-intensive, but also cause a large accumulation of radioactive waste. This technical hindrance also poses a challenge for the filter binding method to be used for high-throughput screening of HAT inhibitors. Due to these problems, it is of interest to design a biochemical assay that would provide comparable data to the filter binding method yet would be more time efficient, environmentally friendly, and importantly, possess robustness and capability for high-throughput screening (HTS) of HAT inhibitors.

Of the HTS assays available, scintillation proximity assay (SPA) is known for being robust, reliable, sensitive and quick.[85] A common SPA protocol utilizes the strong interaction between biotin and streptavidin ($K_d = 10^{-15}$ M, ref. [86]) to bring the radiolabeled ligand close to the streptavidin-coated polyvinyl toluene (PVT) microbeads to emit light.[87-88] The emitted

photons can be detected by the photomultiplier of a scintillation counter. Generally, tritium (^{3}H) is used due to its strong yet short-path β-particle emission (1.5 μm) which ensures that only the bead-bound radiolabels can stimulate the polymer-immobilized scintillant molecules.[85, 88] The marked advantage of using SPA is the elimination of the laborious separation of product from unused radioactive cofactor, which greatly improves assay speed and allows for an efficient mix-and-measurement assay of the product. With these advantageous properties, the SPA method has been applied to study other posttranslational enzymes such as protein methyltransferases and kinases.[89-90]

We attempted to implement a biochemical assay for discovering HAT inhibitors based on the principle of SPA. In this strategy, biotin-labeled histone peptides were used as the HAT substrate and [^{3}H]Ac-CoA as the acetyl donor. Following the homogeneous acetyltransferase reaction, the [^{3}H]-labeled product would bind to the streptavidin-coated SPA beads and produce detectable photon signals. We initially posited that such a SPA protocol should work straightforwardly based on the great success of previously using an analogous SPA method for the study of histone methyltransferase activities.[89, 91] Unexpectedly, when applying the SPA to detect HAT reaction, we observed strong false-positive readings, especially in enzyme-negative controls. This acetylation-specific problem had to be illuminated and resolved in order to validate this SPA approach for HAT probe discovery. Herein, we found out that the cofactor-substrate interaction interfered with acetyltransferase SPA readings. Further, we tested chemical reagents that could remove the interference, characterized this SPA approach for quantitative analysis of HAT inhibitor potencies, and proved robustness and high potential of this method for use as a high-throughput assay for HAT inhibitor screening.

2.2 Materials and methods

2.2.1 Protein expression and purification

The expression of p300 HAT domain (1287-1666) was done following the method developed by Cole's lab.[92] Transformation was done with BL21(DE3)-RIL competent cells using heat-shock, spreading on plates containing both ampicillin and chloramphenicol antibiotics. Colonies were harvested and grown at 37 °C in 8 mL, then inoculated to 1L culture of 2XYT media containing both ampicillin and chloramphenicol. Protein expression was induced with isopropyl β-D-1-thiogalactopyranoside (IPTG) and shaken for 16 hours at 16°C. The cells were collected by centrifugation at 4000 rpm for 25 min and were resuspended in lysis buffer (25 mM Na-HEPES (pH 8), 500 mM NaCl, 1 mM $MgSO_4$, 10 % glycerol, and 2 mM phenylmethanesulfonyl fluoride (PMSF)).

The cells were lysed by passing through a microfluidizer (Microfluidics) at 17,000psi and, the supernatant was purified on chitin resins which were equilibrated with column buffer (25 mM Na-HEPES (pH 8), 250 mM NaCl, 1 mM EDTA, 0.1% Triton X-100 and 1 mM PMSF). The protein-loaded beads were thoroughly washed with the column buffer and wash buffer (25 mM Na-HEPES (pH 8), 500 mM NaCl, 1 mM EDTA, 0.1% Triton X-100 and 1 mM PMSF). Next, the CT14 peptide (CMLVELHTQSQDRF) was dissolved in the cleavage buffer (25 mM Na-HEPES (pH 8), 250 mM NaCl, 1 mM EDTA, and 200mM 2-Mercaptoethanesulfonic acid (MESNA)) and added to the column. The column was set out at room temperature for 16 hours before the protein was eluted from the column, and several volumes of cleavage buffer were added to ensure the complete protein elution. Further purification was done using the Bio-Rad NGC fast protein liquid chromatography (FPLC) system. p300 HAT domain protein band was verified with 12 % sodium dodecyl sulfate-polyacrylamide gel electrophoresis (SDS-PAGE).

Millipore centrifugal filter and Bradford assay were respectively used to concentrate and determine the protein's concentration. Lastly, the protein was aliquoted and stored at -80°C.

2.2.2 Peptide synthesis

The biotinylated peptide containing the N-terminal 20-amino acid sequence of histone H4, i.e. Ac-SGRGKGGKGLGKGGAKRHRK(Biotin)-NH_2 (abbreviated as H4(1-20)-BTN), and histone H3, i.e. Biotin-ARTKQTARKSTGGKAPRKQL-OH (abbreviated as H3(1-20)-BTN) were synthesized using Fmoc-based solid-phase peptide synthesis protocol according to Wu *et al.*.[89] The CT14 peptide for chemical ligation contained the residues 1653-1666 of p300 catalytic domain (CT14, i.e. CMLVELHTQSQDRF).

2.2.3 Measurement of histone acetylation with SPA

As a standard enzymology practice, we monitored the HAT-catalyzed reactions for a range of time and at different enzyme concentrations. Typically, the reaction time and enzyme concentration were controlled such that the reaction yield was kept to be under the linear, initial condition (see supplementary figures, **Figure S2.1** and **Figure S2.2**). The time of 6-min and enzyme concentration of 25-nM were chosen based on the fact these points were both in the linear range of rate—time and rate—[E] relationship. By keeping the reactions within the linear range we ensure that the enzymatic reaction occurred under a constant and maximal rate, and the product formation can be accurately quantitated using linear equation. When the reaction time becomes overly long or the enzyme concentration becomes too high, the reaction goes out of the linear range, and the reaction rate starts to decrease due to a number of factors such as substrate consumption, product feedback inhibition, and enzyme denaturing.

The SPA experiments were conducted in a 96-well plate (Isolate-96; Perkin Elmer) at 30°C using a reaction buffer containing 50 mM HEPES (pH 8), 1 mM EDTA and 0.5 mM

dithiothreitol (DTT). The cofactor used as an acetyl donor was [^{3}H]Ac-CoA (PerkinElmer) and the substrate was either H4(1-20)-BTN or H3(1-20)-BTN. The 30 µL reaction volume typically consisted of 2.5 µM of substrate, followed by 1 µM [^{3}H]Ac-CoA. After 5-10 minutes of incubation, 0.025 µM of p300 (final concentration) was added and samples were re-incubated for 6-10 min. The reaction was quenched with 30 µL of the tested quenchers or with varying volumes of quenchers. Lastly, 10 µL of suspended 20 mg/mL streptavidin-coated SPA beads (Perkin Elmer) in the reaction buffer were added to each well and thoroughly mixed. The plate was placed in the MicroBeta2 scintillation counter (Perkin Elmer) in total darkness for one minute before the wells containing sample were each scanned. Samples were performed in duplicate and were typically within 20% of each other.

2.2.4 Measurement of histone acetylation with SPA

Filter binding assay was done in the same buffer mentioned above. Radio-labeled Ac-CoA, was used to donate the acetyl group to either H4(1-20)-BTN or H3(1-20)-BTN. The total reaction volume was 30 µL. Peptide and cofactor were incubated for 5 minutes, followed by the addition of the enzyme. After another 6-10 minutes of incubation, the reaction was then quenched by spreading 20 µL of the reaction mixture over a Whatman P81 phosphocellulose filter disc (GE Healthcare Life Sciences). Once the filter discs were dried in air, they were washed three times with 50 mM $NaHCO_3$ (pH 9.0) and re-dried. Acetylated products were quantified with the addition of scintillation cocktail was scanned using the MicroBeta2 (Perkin Elmer). Assays were performed in duplicate with standard deviation within 20% of each other.

2.3 Design of the scintillation proximity assay for HATs

In order to design a fast and sensitive assay for HATs, we investigated the practicability of the scintillation proximity assay for HAT activity measurement. The SPA approach is built

upon the interaction between streptavidin-coated scintillation bead and biotin-labeled HAT substrate [93] (**Figure 2.1A**). In this protocol, a HAT enzyme catalyzes the transfer of [^{3}H]acetyl group from [^{3}H]Ac-CoA to a biotin-labeled substrate (e.g., H3 or H4 peptide). The HAT enzyme used in the assay was p300, which can effectively acetylate the N-terminal tails of both histone H3 and H4. The substrate was a biotinylated peptide containing the N-terminal 20-aa sequence of H3 or H4, namely H3(1-20)-BTN or H4(1-20)-BTN. After incubation of the enzyme, [^{3}H]Ac-CoA, and biotinylated substrate, the acetyltransferase reaction was stopped by adding a quenching reagent, such as isopropanol. Lastly, SPA scintillation beads were added and the acetylated product was counted. Through specific biotin-streptavidin interaction, the [^{3}H]-radiolabeled acetylated peptide product is brought into close proximity to the SPA bead. The beta-particle emission of [^{3}H] excites the scintillants immobilized in the SPA bead, generating luminescence that is detected by a microplate-compatible scintillation counter, e.g. the MicroBeta or TopCount. Any unbound [^{3}H]Ac-CoA is out of the scintillation proximity distance thus will not generate SPA signals.

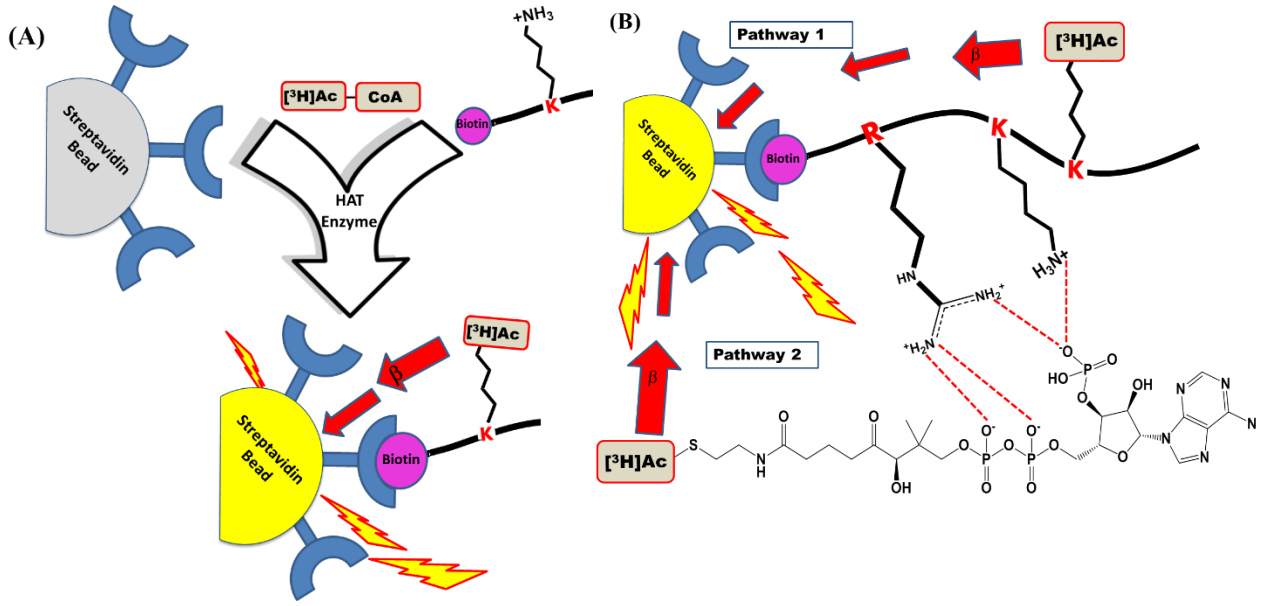

Figure 2.1: Scheme of the scintillation proximity assay (A) detecting HAT reaction (B) complicated by cofactor-substrate interaction. (A) The enzyme transfers the radioactive acetyl group to the biotinylated peptide, which is brought into proximity of the streptavidin-coated scintillation microsphere beads. (B) Pathway 1 produces signals as a result of the acetyltransferase reaction. Pathway 2 shows that the electrostatic interaction of acetyl-CoA and histone substrate leads to undesired SPA signals even in the absence of HAT enzymes. Pathway 2 must be removed in a reliable HAT SPA measurement.

2.4 Identifying effective quenchers and optimizing their concentrations for SPA measurements

To start, we first measured the SPA reading of [^{3}H]Ac-CoA in the reaction buffer. As expected, the sample showed only a background-level count (~100 cpm) (**Figure 2.2A**), supporting that the tritium atoms in the bulk Ac-CoA solution is not being brought into close enough proximity to the microsphere-coated scintillant molecules. Nevertheless, when the biotinylated histone H3 or H4 peptide was added, we observed strong SPA signals, which

increased proportionally with the increasing amount of the added peptide (**Figure 2.2A**). This result was quite unexpected because no HAT enzyme was present, and the 10-min incubation time could not have allowed for non-enzymatic acetylation to occur. Instead, the undesirable SPA signals were likely caused by nonspecific electrostatic interactions between the positively charged histone peptide and the negatively charged [^{3}H]Ac-CoA. Nevertheless, this interaction needed to be eliminated otherwise it would interfere with the signals from the HAT reaction.

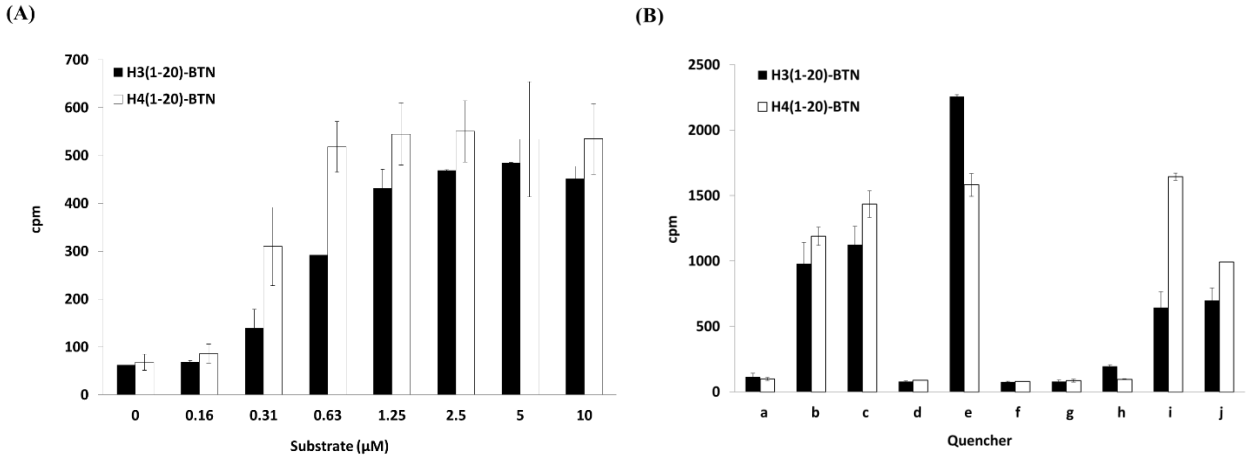

Figure 2.2.: Interaction of histone H3 and H4 substrates with [^{3}H]Ac-CoA measured by SPA(A) and the effects of various quenchers on the interaction between substrate and cofactor(B). Assays containing peptide (0-10 μM H3(1-20)-BTN or H4(1-20)-BTN peptide (A), or 2.5 μM H3(1-20)-BTN or H4(1-20)-BTN (B)) and 1 μM [^{3}H]Ac-CoA were incubated at 30°C for 6 min, before adding 30 μL of isopropanol (A) or various quenchers (B) and 10 μL of 20 mg/mL SPA beads. Quenchers in figure (B) are as follows: a. negative, b. positive, c. 50% isopropanol, d. 1% SDS, e. 1% Triton X-100, f. 4 M guan, g. 2 M guan, h. 50 mM $NaHCO_3$, i. 50% DMSO (Dimethyl sulfoxide), j. 50 mM AcOH. In the positive control, water was added as the quencher. Negative controls did not contain any peptide.

In end-point enzymatic assays, typically a quenching reagent is added to stop the enzymatic reaction so that the amount of products can be quantified at precise time points. In the previously reported HAT assays, the oft-used quencher is a water-miscible organic solvent, such as isopropanol and DMSO, which can stop the HAT reaction by disrupting the active enzyme folding structures.[50] In our previous SPA experiments for histone methylation, dilution of the reaction mixture with five-fold buffer was also found to be effective to diminish enzymatic activity.[89]

We reasoned that a different chemical quencher should be selected to remove the undesirable cofactor-substrate interaction in a HAT reaction. In this regard, several chemical quenching agents were tested, which included isopropanol, SDS, Triton-X100, guanidine HCl, $NaHCO_3$, DMSO, and acetic acid. In the first experiment, a reaction mixture containing biotinylated histone peptide and [^{3}H]Ac-CoA was incubated for 6 min. Then, an equal volume of individual quenchers was added to each reaction mixture. As seen in **Figure 2.2B**, several quenchers, including 1% SDS, 50 mM $NaHCO_3$, 2 M and 4 M guanidine HCl, gave low SPA signals that were comparable to the negative control, which was indicative of their effects on disrupting the interaction between the histone peptide (both biotinylated H3 and H4 peptides) and [^{3}H]Ac-CoA. Although 1% SDS showed promising results in this experiment, it was harder to work with because it is prone to generate air bubbles during the mixing process.

We are particularly interested in using guanidine HCl as the quenching reagent because it is a cheap agent and has been widely used in protein denaturing studies. The minimum guanidine HCl concentration that would produce reliable and accurate SPA readings by inhibiting the histone—Ac-CoA interaction was determined. Various concentrations of guanidine HCl were tested with samples containing 2.5 μM of H3(1-20)-BTN and 1 μM

[^{3}H]Ac-CoA. In the absence of enzyme, at least 0.125 M guanidine HCl was needed to keep the reading signal as low as the negative control and presumably block any interaction between H3 peptide and Ac-CoA (**Figure 2.3A**). Ideally, the quenching agent should also stop the enzymatic reaction as well, which is required for end-point enzymatic assays. So, a similar assay was performed with the presence of HAT enzyme, p300, and readings showed that a guanidine HCl concentration at 0.25 M was needed to keep the readings at the background level (**Figure 2.3A**). This suggests that under these experimental condition, to denature p300 required a higher concentration of guanidine HCl than to break down histone-Ac-CoA interaction. Together, 0.25 M of guanidine HCl was sufficient to both stop the HAT reaction and meanwhile eliminate histone-Ac-CoA interaction.

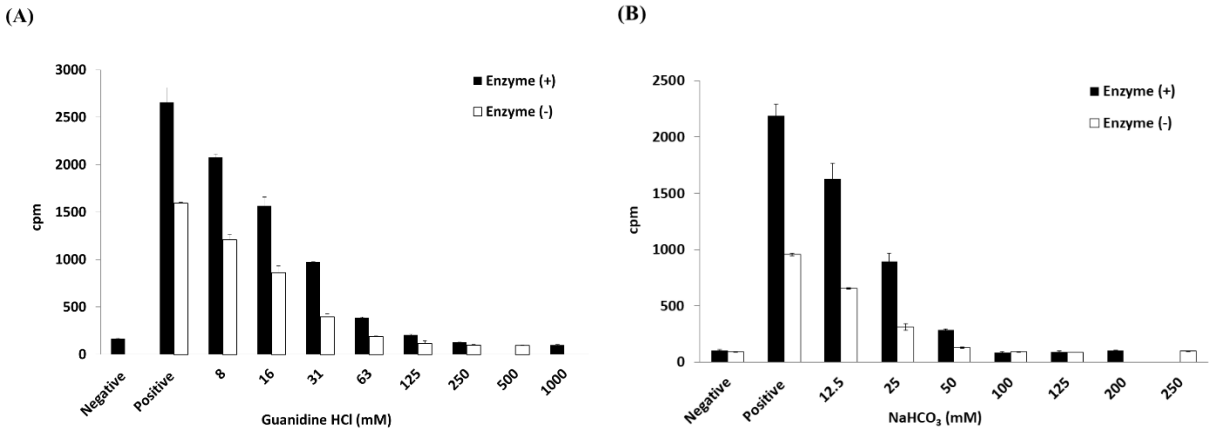

Figure 2.3. The dose response of SPA signals at different concentrations of guanidine HCl (A) and $NaHCO_3$ (B). All samples were incubated for 6 min at 30°C. Samples not containing enzyme had 2.5 µM H3(1-20)-BTN, 1 µM [^{3}H]Ac-CoA, and was quenched with 30 µL of guanidine HCl (A) or $NaHCO_3$ (B) at various concentrations. Samples with enzyme contained 6 µL of guanidine HCl (A) or $NaHCO_3$ (B) at various concentration in the reaction mixture of 2.5 µM H3(1-20)-BTN, 1 µM [^{3}H]Ac-CoA, and 0.025 µM p300. After the reaction, 30 µL of

isopropanol was added. Positive control did not contain any guanidine HCl or $NaHCO_3$. H3(1-20)-BTN was absent in the negative control samples.

Another quencher tested was $NaHCO_3$. This chemical is commonly used as the washing reagent in the filter-binding assay for HATs. The dose-dependent effect of $NaHCO_3$ on the histone—Ac-CoA interaction and p300 HAT activity was determined in the same way as the guanidine HCl experiment. As displayed in **Figure 2.3B**, 50 mM of $NaHCO_3$ was sufficient enough to break down the cofactor-substrate interaction and show low readings close to the background level. However, in the presence of p300, 100 mM of $NaHCO_3$ was needed to bring down the SPA readings in parallel to the negative control. This difference, again, suggests that inhibiting p300 activity needs a higher strength of quencher solution than does blocking the histone-Ac-CoA interaction.

2.5 Further comparison of guanidine quenching with the other quenching methods

We further evaluated and compared the quenching properties of different quenching reagents on substrate–cofactor interaction, and on the p300 enzymatic activity in the SPA measurement. As shown in **Figure 2.4A** (white column), the addition of isopropanol was unable to break histone—Ac-CoA interaction; even with 150 µL isopropanol (83% v/v), the SPA reading was still as high as 1251 cpm. Another often used quenching method is diluting the reaction mixture with buffer. By dilution, the enzyme will have a less access to its substrates, resulting in dramatic decrease of product formation. The results showed that even with a five-fold dilution using the reaction buffer, the SPA readings were not able to stay as low as the negative control (**Figure 2.4A**, square checkered column). This clearly suggests that the dilution

method is insufficient to break histone-Ac-CoA interaction. The addition of 90 µL DMSO (75% v/v) to the reaction mixture was able to get the readings down close to the background level. Guanidine HCl and $NaHCO_3$ were the only quenchers that were able to keep readings close to the background level with only one-volume addition (**Figure 2.4A**, grey and slanted line column).

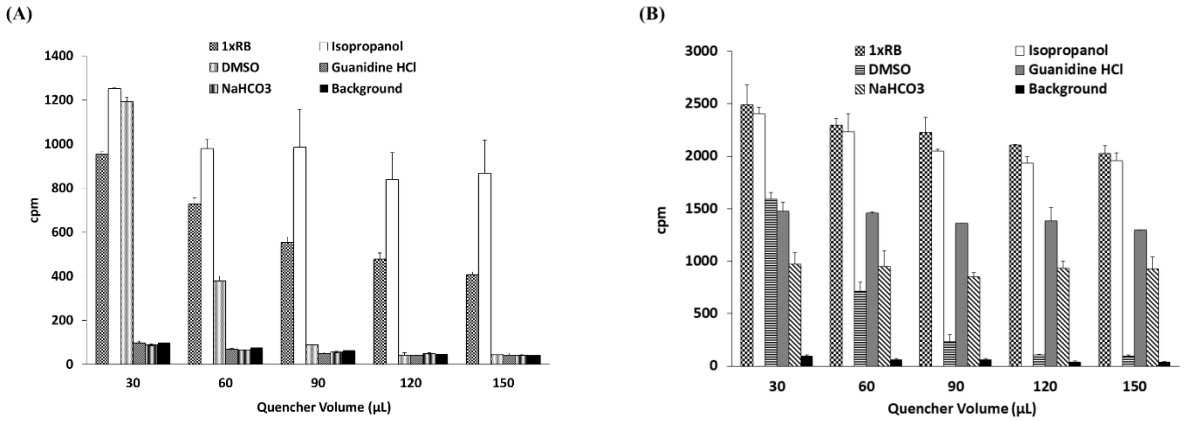

Figure 2.4. Quenching effects of 1xRB, isopropanol, DMSO, $NaHCO_3$, and guanidine HCl on samples (A) without HAT enzyme, and (B) with p300 enzyme. (A)Samples containing 2.5 µM H3(1-20)-BTN, and 1 µM [^{3}H]Ac-CoA was incubated for 6 min at 30°C before various volumes of the different quenchers were added. Lastly, 10 µL of 20 mg/mL SPA beads was added. Background did not contain any biotinylated peptide. (B) These samples followed the same conditions with the addition of 0.025 µM p300

This quenching effect was retested under the same conditions except that p300 enzyme was added to the reaction mixture (**Figure 2.4B**). Prior to the addition of any quenching agents, the reaction mixture was incubated for 6 minutes to allow histone acetylation to occur. Therefore, unlike the results in **Figure 2.4A**, we expected to observe a high SPA reading in every test due to the radiolabeling of the H3(1-20)-BTN substrate. Indeed, as displayed in **Figure 2.4B**, the SPA readings remained at high levels (> 900 cpm) for guanidine HCl,

$NaHCO_3$, isopropanol and 1XRB, independent of volume addition (**Figure 2.4B**). Comparing the data in **Figure 2.4A** and **2.4B**, we can conclude that: (1) quenching with isopropanol and extra volumes of buffer solution is not sufficient enough to block nonspecific histone-Ac-CoA interaction and thus cannot produce reliable data in SPA HAT assays. (2) Guanidine HCl and $NaHCO_3$ own the ability of inhibiting both HAT activity and histone—Ac-CoA interaction, thus providing reliable results with just a one-volume addition. (3) Surprisingly, as DMSO volumes increased, the readings gradually decreased close to the background level in both **Figure 2.4A** and **2.4B**. The observation of this trend for DMSO is very important for this assay; while the decrease of SPA signals in **Figure 2.4A** was because histone-Ac-CoA interaction was inhibited by DMSO, the diminished SPA readings in **Figure 2.4B** strongly indicate that high volumes of DMSO interfered with the interaction between biotin and streptavidin, which is detrimental to SPA efficiency.

To validate if DMSO was indeed disrupting the biotin-streptavidin interaction in the SPA procedure, an experiment using histone methylation was designed (**Figure 2.5**). In this methylation experiment, we used protein arginine methyltransferase 1 (PRMT1) enzyme, and [^{3}H]SAM as the methyl donor and H4(1-20)-BTN as the substrate. We had predetermined that there was no electrostatic interaction between [^{3}H]SAM and the histone substrate (data not shown). The histone methylation was first carried out prior to the addition of any quenching agent. Therefore, we would expect to observe strong SPA readings regardless of the type of added quenchers. Indeed, the samples showed high and relatively stable SPA signals in the presence of guanidine, $NaHCO_3$, isopropanol, and 150 µL reaction buffer (**Figure 2.5**). The reactions quenched with less than three-volume 1xRB had greater reading values likely because 1xRB did not denature the enzyme. Under a lower dilution of the reaction mixture, the enzyme

activity was still measurable by the continual substrate methylation. Importantly, again, it was observed that increasing DMSO volumes greatly reduced the SPA signals, which was similar to that observed in **Figure 2.4B**. From these experiments, it is clear that high volumes of DMSO interfered with the biotin-streptavidin interaction. Thus, using DMSO as a quencher in SPA experiments should be cautioned or avoided.

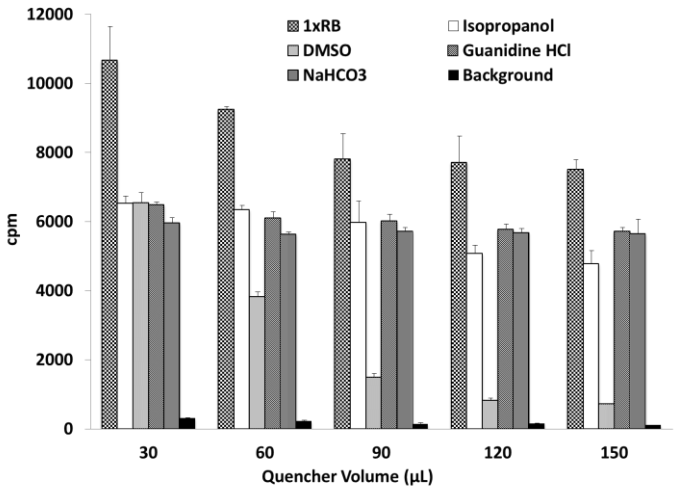

Figure 2.5. Effects of 1xRB, isopropanol, DMSO, $NaHCO_3$, and guanidine HCl on PRMT1-mediated H4 methylation. Samples containing 0.02 µM PRMT1, 1 µM H4(1-20)-BTN, and 0.5 µM [^{3}H]SAM was incubated for 7 min at room temperature. Reaction was quenched with 30 -150 µL of the different quenchers. Lastly, 10 µL of 20 mg/mL SPA beads was added. Background did not contain any biotinylated peptide.

2.6 Comparison between the SPA and the filter binding assay

The filter binding assay is considered the gold standard for measuring activities of HATs, both for enzyme mechanism studies and for inhibitor characterization studies. However, this method is laborious, creates a large amount of radioactive waste, and hinders HTS

application. The development of a more efficient and environmentally friendly method with results comparable to the filter binding assay would be highly valuable. We measured and compared the time-dependent reaction progression using both the SPA and the filter binding assay under identical reaction conditions. As shown in **Figure 2.6**, an excellent linear relationship (correlation coefficient (R) is 0.996) was observed between the data obtained from the SPA and the filter binding assay, demonstrating that these two methods are consistent and reliable.

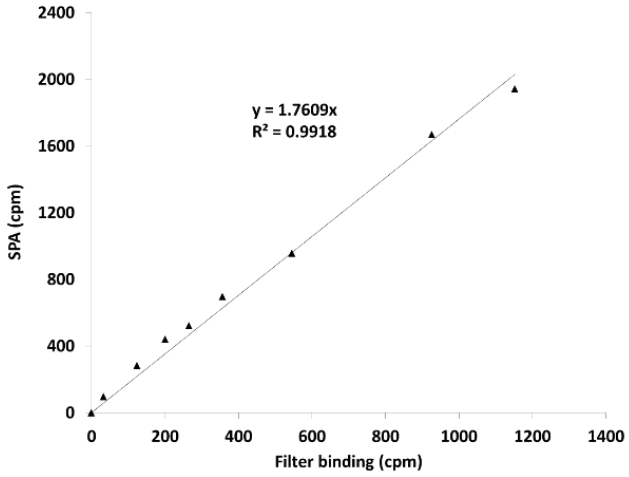

Figure 2.6. Linear correlation of the SPA with the filter binding assay. A time dependent assay was carried out using identical conditions for both assays. Samples containing 2.5 µM H3(1-20)-BTN, 1 µM [^{3}H]Ac-CoA and 0.025 µM p300 was incubated at 30°C before ending the reaction with 30 µL of 0.5 M (final) guanidine HCl, or by spreading 30 µL of the reaction mixture on P81 paper. Reaction times were 0, 1, 3, 5, 7, 10, 15, 30, and 60 min.

We also compared the two assay formats for HAT inhibitor characterization (**Figure 2.7**). C646 is a known inhibitor of p300 with submicromolar potency.[94] We measured the p300 inhibition by C646 at varying concentrations using both the filter binding assay and the

established SPA. Both assays contained 2.5 μM H3(1-20)-BTN and 1 μM [^{3}H]Ac-CoA and were reacted for a reaction time of 6 min at 30°C. The readings for the SPA measurements quenched with guanidine HCl followed the same trend as the readings for the filter binding. The IC_{50} value of the SPA measurement with guanidine HCl as quenching agent was calculated to be 3.4 ± 0.1 μM, which was very close to the value obtained from the filter binding assay (2.3 ± 0.01 μM). Therefore, the SPA showed the same-quality performance as the filter binding method for quantifying HAT activities both in the absence and presence of inhibitors. The SPA would be preferred because it is faster and does not require washing procedures. For comparison purpose, we also did the IC_{50} measurement using the SPA measurement using isopropanol as a quencher. An IC_{50} of 4.1 ± 0.6 μM was obtained from this assay. Although the value was similar to that of the filter binding assay and the guanidine-quenched SPA, it is seen clearly from **Figure 2.7** that even at 100 μM of the inhibitor where the p300 enzymatic activity was completely inhibited, the scintillation readings were still much higher than the background. This phenomenon of partial inhibition supports that the interaction between the substrate and cofactor led to false SPA readings and isopropanol was not able to disrupt the interaction between the substrate and cofactor. Therefore, the high SPA readings caused by the substrate-cofactor interaction reduced the signal dynamic window, making it more difficult to distinguish between positive and negative hits.

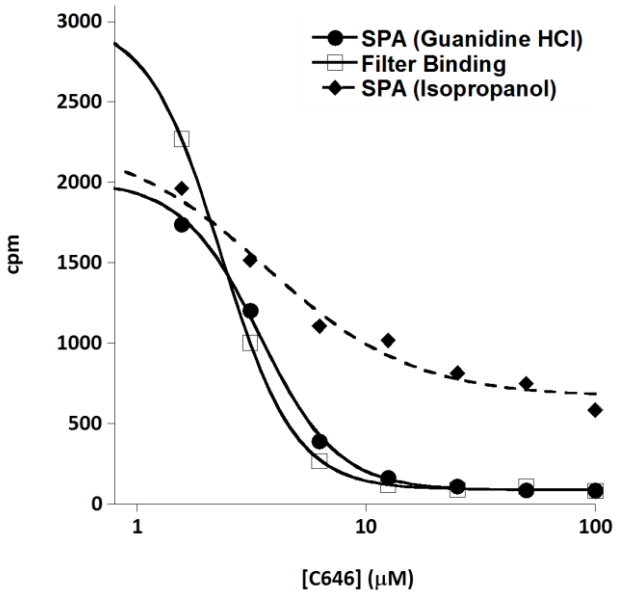

Figure 2.7. Dose-dependent inhibition of p300 activity by C646 measured using SPA and filter binding assay. Both the SPA and filter binding assays included 0.025 μM p300, 2.5 μM H3(1-20)-BTN, 1 μM [^{3}H]Ac-CoA and an incubation time of 6 min at 30°C. To quench the reaction, 30 μL of each reaction mixture was spread out on a Whatman filter binding paper or 30 μL of 100% isopropanol or 1 M guanidine HCl was added to the sample. IC_{50} was determined by fitting the data to the equation $\frac{y-y_{min}}{y_{max}-y_{min}} = \frac{1}{(1+\frac{[I]}{[IC_{50}]})^h}$, Where y_{max}, y_{min}, h and $[I]$ are maximum and minimum SPA signals on the y-axis, hill coefficient, and inhibitor concentration respectively.[95]

2.7 Evaluation of method for the use in HTS

Screening a large number of compounds represents a task that can become very laborious, so it is very valuable to have a HTS method which works efficiently and robustly and shows superior signal-to-background ratios. The Z' and Z factors are excellent parameters to evaluate effectiveness and robustness of a biochemical assay for HTS application.[96] The

theoretical Z' and Z values can range from zero to one, and a value greater than or equal to 0.5 is considered a preferable parameter for a stable HTS assay. We measured the Z' and Z factors of this HAT SPA. Three sets of samples each with 24 data points were tested in 96 well plate format. The first set was the enzyme-negative control (containing 2.5 µM H3(1-20)-BTN and 1 µM [^{3}H]Ac-CoA), the second set was the enzyme-positive control (containing 2.5 µM H3(1-20)-BTN, 1µM [^{3}H]Ac-CoA and 0.025 p300), and the third set included a HAT inhibitor in the enzymatic reaction (containing 2.5 µM H3(1-20)-BTN, 1 µM [^{3}H]Ac-CoA, 0.025 µM p300, and 10 µM C646). From the sampling data shown in **Figure 2.8**, the calculated Z and Z' factors for this HTS assay were found to be 0.68 and 0.69 respectively; therefore, supporting the robustness and effectiveness of this SPA protocol to screening HAT inhibitors in HTS format.

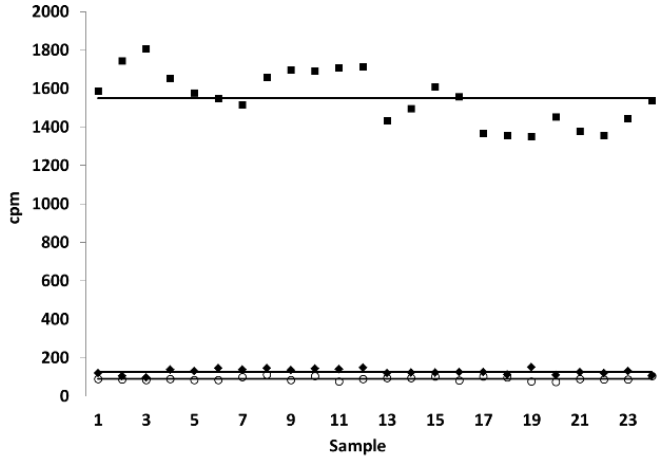

Figure 2.8. The scatter plot of the SPA signals comparing enzyme-positive, enzyme-negative, and inhibitor-containing samples. Squares (■): The enzyme-positive reaction samples contain 0.025 µM p300, 2.5 µM H3(1-20)-BTN, and 1 µM [^{3}H]Ac-CoA. Circles (○): The enzyme-negative samples contain 2.5 µM H3(1-20)-BTN, and 1 µM [^{3}H]Ac-CoA. Diamonds (♦): The inhibitor samples contain 0.025 µM p300, 2.5 µM H3(1-20)-BTN, 1 µM

[^{3}H]Ac-CoA, and 10 µM C646. All samples were incubated for 7 minutes at 30°C. Lastly, samples were all quenched with 30 µL of 0.5 M (final) guanidine HCl, and 10 µL of 20 mg/mL SPA beads was added before scintillation counting in MicroBeta2.

2.8 Conclusion

Lysine acetyltransferases have major physiological roles at the cellular level, yet in an unregulated state they contribute to various detrimental diseases. To develop new HAT-targeting therapies, it is crucial to have a reliable HTS method to quickly obtain chemical hits from a large library of compounds. With this task in mind, we set out to implement a scintillation proximity assay (SPA) for HATs. Using the SPA for biochemical assays of enzyme activities and protein-protein interactions is an appealing approach. SPA methods have been adopted to analyze several PTM enzyme activities, such as protein methyltransferases and kinases.[89-90] We reasoned that the SPA protocol could be analogously set up for HAT enzymes using [^{3}H]Ac-CoA as the acetyl donor and biotinylated histone peptide as the acetyl acceptor (**Figure 2.1.A**). Once the radioactive labeled acetyl group is transferred to the biotinylated peptide, it is brought to close proximity of streptavidin-coated scintillation beads by the specific binding of biotin with streptavidin. We want to mention that Ait-Si-Ali et al. [97] previously also performed radiometric HAT assays using biotinylated histone peptide. In their assay, the acetylated product was captured on streptavidin-modified agarose beads. Since it was not a SPA method, washing step was still needed to remove unreacted Ac-CoA before scintillation counting, which is similar to the standard filter binding assay. In our strategy, we attempt to devise the HAT assay in the SPA format, so that scintillation readings can be directly measured

following the HAT reaction without any washing, which would greatly improve the high throughput capacity.

When implementing the SPA method for HAT activity measurement, however, we observed that the enzyme-negative samples showed unexpectedly high SPA signals (e.g., **Figure 2.2A**). Also, using this assay to measure potency of HAT inhibitors yielded a pattern of incomplete inhibition (**Figure 2.7**). Through a series of comparative experiments, the issue was nailed down to the nonspecific electrostatic interaction between the cationic histone peptides and the anionic [^{3}H]Ac-CoA. The adverse histone-cofactor binding brought the tritium radiolabel in proximity to the SPA scintillation beads even in the absence of HAT enzyme, thus producing false readouts (**Figure 2.1B**). Apparently, this extra intermolecular interaction interfered with the true readings of HAT enzymatic assay and needed to be avoided in order to set up a reliable HAT SPA measurement.

To provide unbiased results for HAT activity measurement using the SPA, several chemical agents were studied that could eliminate the undesirable substrate-cofactor interaction. In selecting a quenching agent, we reasoned that the chemical quenchers must satisfy three basic requirements. Firstly, the quencher must disrupt the electrostatic interaction between histone peptide substrate and [^{3}H]Ac-CoA. Secondly, it must inhibit the HAT enzyme activity so that no further acetylation reaction proceeds after the quenching. Thirdly, the quencher must not interfere with the biotin and streptavidin interaction. We found that guanidine HCl and $NaHCO_3$ were excellent quenchers because they were able to satisfy all the three requirements. Isopropanol, 1% Triton-X100, and 50 mM AcOH were not strong enough to prevent cofactor-histone interaction. Excess DMSO disrupted biotin-streptavidin binding, so we recommend it not be used as a quencher in the HAT SPA experiments.

Previously, Turlais et al. [98] developed a radiometric assay utilizing the scintillating microplate (i.e. FlashPlate) to detect HAT activity. In their protocol, histone H3, [^{3}H]Ac-CoA, and HAT enzyme PCAF were incubated directly on the FlashPlate. In the HAT reaction, the tritium-labeled histone was captured by the walls of FlashPlate which contained immobilized scintillant molecules, generating a scintillation signal. That method apparently was also based on the principle of scintillation proximity. Interestingly, the authors did not show any interference from Ac-CoA-histone interaction. It was possible that 150 mM of NaCl present in their assay buffer somehow diminished the undesirable cofactor-histone interaction. Compared with the FlashPlate assay, our assay owns additional advantageous features. The previous FlashPlate assay was heterogeneous in nature because the histone substrate was adsorbed on the microplate surface throughout the enzymatic reaction. The solid surface may partially impact HAT-mediated histone acetylation. Further, the adsorption of histone H3 on FlashPlate was a nonspecific electrostatic interaction, so the efficiency of histone adsorption could be easily interfered by buffer compositions.[99] It was also difficult to assess the molecular stoichiometry of histone binding to the FlashPlate. The presence of a high salt concentration could be necessary to prevent cofactor-histone binding; however, it may also affect the efficiency of histone adsorption to the plate surface which is needed for SPA detection. Furthermore, high salt concentration has the pitfall of inhibiting enzymatic activity of HATs, and it has been recommended that strong ionic strength should be avoided in HAT reactions.[100-101] In this present study, we described a more clear scintillation proximity assay for HATs: The HAT reaction was conducted homogeneously in a buffer solution in regular 96-well plate. Following the HAT reaction, SPA beads were added so that the radiolabeled product was brought into proximity of the scintillant by the specific and potent biotin-streptavidin interaction.

Importantly, we showed that using chemical agents such as guanidine HCl and $NaHCO_3$ effectively quenched the HAT reaction and meanwhile removed any nonspecific interaction between acetyl-CoA and histone substrate. Using guanidine HCl or $NaHCO_3$ as a quencher is beneficial because of their intrinsic ionic properties as well as being readily available and cheap in price. Guanidine HCl is a strong electrolyte known to be a strong protein denaturant.[102-103] The chaotropic property of guanidine is very useful in this SPA for it assures that the HAT reaction ended once this reagent was added. The ability of guanidine HCl to break down the electrostatic substrate-cofactor interaction is critical to avoid false readings. At this point we are not sure why $NaHCO_3$ can stop the HAT reaction. Possibly, $NaHCO_3$ may interact with the positively charged histone peptide, which prevents the substrate from entering in the active site of the HAT. Nevertheless, $NaHCO_3$ is an effective quencher like guanidine HCl for this SPA experiment. Furthermore, in our studies, we found that 150 mM of sodium chloride or 30 mM of sodium phosphate (pH 8.0) fully eliminated the unwanted [^{3}H]Ac-CoA-histone interaction (supplementary **Figure S2.3** and **S2.4**). However, at those concentrations, neither sodium chloride nor sodium phosphate were capable of completely quenching the HAT activity (supplementary **Figure S2.5** and **S2.6**).

Taken together, we have developed and validated a scintillation proximity assay to measure the enzymatic activity of HATs. This mix-and-measure assay does not require any washing procedures and can be implemented in the microplate format. This SPA method is well suited for quantitative potency evaluation of HAT inhibitors and has the high-throughput capability to screen for new HAT chemical probes.

CHAPTER 3

BISUBSTRATE INHIBITORS TARGETING HISTONE ACETYLTRANSFERASE 1 (HAT1)

This work was submitted to Chemical Biology & Drug Design as Liza Ngo, Tyler Brown, Y. George Zheng. (2017) Bisubstrate Inhibitors Targeting Histone Acetyltransferase 1 (HAT1).

3.1 Introduction

Developing and identifying potent and selective inhibitors for enzymes allow scientists to expand molecular toolbox to investigate the role and activity of target enzymes. The histone acetyltransferase1 (HAT1) belongs to the GCN5-related N-acetyltransferase (GNAT) superfamily together with other canonical members such as GCN5 (general control nonderepressible 5) and PCAF (p300/CBP associated factor). Members of this family are conserved in organisms spanning from yeasts to humans and are known to share four distinct regions spanning around 100 residues.[16] HAT1 was among the first set of HAT enzymes that were discovered in the mid-1990s;[104] however, it is one of the most poorly studied enzymes in comparison to the other HAT members. This enzyme is categorized as a type B HAT based on its ability to acetylate newly synthesized histones, such as histone H4 at Lys5 and Lys12 as well as H2A at Lys5, but not the histones that are already incorporated into a nucleosome.[26-27]

Cancer formation and progression can occur due to the dysregulation of histone modifying enzymes that regulate gene transcription, cell differentiation, proliferation and apoptosis.[105-107] HAT1 has been linked not only to various diseases such as cardiovascular diseases,[37] colorectal cancer,[108] liver cancer,[41] lung cancer,[35] and human immunodeficiency virus (HIV),[109] but also to the regulation of immune responses.[26, 35] Besides the aberrant

expression, the localization of HAT1 can also aid in disease progression.[108] It has also been reported in an HIV study that HAT1 can be a biomarker of the disease state.[109] These disease studies shed light on the roles that HAT1 plays in pathology and suggest that HAT1 could be a potential molecular target in the design of new therapeutic treatment.

Reported inhibitors for HATs range from peptides to small molecules and include natural products as well as synthetic molecules.[110-112] Peptide bisubstrate inhibitors were first introduced to the HAT field by the Cole group with the p300-selective inhibitor Lys-CoA (IC_{50} 0.5 μM) and the PCAF-selective inhibitor, H3-CoA-20 (IC_{50} 0.3 μM).[113] These inhibitors were designed to mimic the ternary complex formation of the substrate and cofactor binding to the HAT enzyme. We have previously designed several bisubstrate peptide inhibitors on the MYST family of HATs.[55] In the search for inhibitors targeting Esa1 and Tip60, we tested and compared the potency of various bisubstrate peptide inhibitors, small molecules, as well as natural products on Esa1, Tip60, p300, and PCAF.[55] Of the inhibitors tested H4K16CoA was found to be the most potent against both Esa1 and Tip60 with IC_{50} of 5.51 μM and 17.59 μM respectively.[55] Furthermore, analysis with Esa1 demonstrated that the mode of inhibition was competitive against acetyl coenzyme A (AcCoA) and noncompetitive against H4-20 substrate.[55] Moreover, we rationally designed a set of multivalent peptide inhibitors containing methylated modifications in the peptide chain of the bisubstrate compound to inhibit Tip60, and found that the added methylated marks improved the potency of the bisubstrate inhibitors towards Tip60 by several folds.[114]

These substrate-based inhibitors are valuable chemical probes for mechanistic and structural studies of HAT activities. Several bisubstrate inhibitors have been applied to understand the substrate recognition mechanisms in HATs.[115-116] It is known that HAT1 prefers

to acetylate the N-terminal tail of histone H4 at Lys5 and Lys12.[104, 117] Thus, to develop inhibitors targeting HAT1 in this study, we rationally synthesized various histone H4 peptides containing the first 20 amino acids of histone H4 (H4-20) and the CoA moiety conjugated to different lysine residues. For the first time, inhibitors were identified that displayed potent inhibition activity towards HAT1. Two best inhibitors, H4K5CoA and H4K12CoA, had nanomolar inhibition potency towards HAT1 with IC_{50} values at 83 nM and 23 nM respectively. Inhibition analysis of the most potent inhibitor, H4K12CoA, indicated that the mode of inhibition was competitive towards both AcCoA and H4-20 peptide.

3.2 Materials and methods

3.2.1 Bisubstrate inhibitor synthesis

Various peptides containing the first N-terminal 20aa of histone H4 (i.e., ac-SGRGKGGKGLGKGGAKRHRK, H4-20) were synthesized using the Fmoc [N-(9-fluorenyl) methoxycarbonyl**]**-based solid-phase peptide synthesis protocol. The Fmoc-Lysine(Boc) preloaded Wang resin was used, and individual amino acids were coupled using activation reagents HBTU [2-(1H-Benzotriazole-1-yl)-1,1,3,3-tetramethyluronium hexafluorophosphate] and HOBt (N-Hydroxybenzotriazole). The Dde group (dimethyldioxocyclohexylidene) on either lysine 5, 8, 12, or 16 was deprotected using 65% hydrazine monohydrate. Next, bromoacetic acid was mixed with DIC (N, N'-diisopropylcarbodiimide) in DMF (dimethylformamide) to create a bromoacetyl linker which can be used to add CoA to the peptide. The peptide was cleaved off the resin using 95% trifluoroacetic acid (TFA), 2.5% H2O, and 2.5% triisopropylsilane (TIS) for 4 hr. The peptides were purified using a C-18 reverse phase column on a High-performance liquid chromatography (HPLC) instrument, and each sample analyzed by matrix assisted laser desorption/ionization mass spectrometry (MALDI-

MS). The bromo peptide was treated with five equivalence of CoA in sodium phosphate buffer (0.1 M, pH 8) the reaction mixture was shaken overnight in the dark at room temperature. The CoA-peptide compounds were purified and verified following the previous procedure. The concentrations of the CoA–peptide conjugates were determined by making serial dilutions of the compounds and measuring the absorbance at 260nm. Concentrated NaOH solution was used to neutralize the pH of the compound solutions prior to enzymatic assays.

3.2.2 HAT1 expression and purification

The expression and purification of catalytic domain HAT1 (20-341) was done following the method described by Wu et al. (Addgene plasmid # 25239).[34] Briefly, this protein was expressed in *Escherichia coli* and purified using the Ni-NTA resin. Transformation was done in *E coli* BL21-CodonPlus (DE3)-RIL competent cells using the heat-shock method, and then the cells were spread on agar plates containing antibiotics kanamycin and chloramphenicol. Protein expression was induced by the addition of 1 mM isopropyl β-D-1-thiogalactopyranoside (IPTG) and shaken for 16 hours at 16°C. The cells were collected and suspended in the lysis buffer (50 mM Na-phosphate (pH 7.4), 250 mM NaCl, 5 mM imidazole, 5% glycerol, 2 mM β-mercaptoethanol, and 1 mM phenylmethanesulfonyl fluoride (PMSF)) then disrupted using the Microfluidics cell disruptor. The supernatant was passed through a column containing Ni-NTA resin equilibrated with column washing buffer (20 mM HEPES pH8, 250 mM NaCl, 5% glycerol, 30 mM imidazole, 1 mM PMSF) and the resin was washed with column washing buffer. Next, the resin was washed with the buffer containing a higher concentration of imidazole (20mM HEPES pH 8, 250 mM NaCl, 5% glycerol, 50 mM imidazole, 1 mM PMSF). Lastly, HAT 1 was eluted with elution buffer (20 mM HEPES pH 8, 250 mM NaCl, 5% glycerol, 500 mM imidazole, 1 mM PMSF).

3.2.3 Determining K_i^{app}, K_i, and IC_{50} values of the bisubstrate inhibitors against HAT1

K_i^{app} values for all of the inhibitors (Lys-CoA, H4K5CoA, H4K8CoA, H4K12CoA, H4K16CoA, and CoA) were determined using the scintillation proximity assay (SPA) [118]. SPA experiments were conducted in a 96-well plate (Isolate-96; Perkin Elmer) at 30°C using a reaction buffer containing 50 mM HEPES (pH 8), and 0.1 mM EDTA. The cofactor used as an acetyl donor was [^{3}H]-Ac-CoA (PerkinElmer) and the substrate was a biotinylated H4-20 peptide (Ac-SGRGKGGKGLGKGGAKRHRK(Biotin)-NH2 (abbreviated as H4-20 BTN)). The 30 µL reaction volume typically consisted of various concentration of bisubstrate inhibitor, 2.5 µM of substrate, followed by 1 µM [^{3}H]-AcCoA. After 5 mins of incubation, 0.04 µM of HAT1 was added and samples were re-incubated for 20 mins. The reaction was quenched with 30 µL of guanidine HCl (0.5 M). Lastly, 10 µL of suspended 20 mg/mL streptavidin-coated SPA beads (Perkin Elmer) were added to each well and thoroughly mixed. The plate was placed in the MicroBeta2 scintillation counter (Perkin Elmer) in total darkness for one minute before the samples were quantified. Samples were performed in duplicate and were typically within 20% of each other. K_i^{app} was determined by fitting the data to the following Morrison equation

$$\frac{v_i}{v_0} = 1 - \frac{([E]+[I]+K_i^{app}) - \sqrt{([E]+[I]+K_i^{app})^2 - 4[E][I]}}{2[E]} \qquad \text{(Equation 1)}$$

Where v_i, v_0, $[E]$, $[I]$,and K_i^{app} are maximum and minimum SPA signals on the y-axis, enzyme concentration, inhibitor concentration, and apparent K_i respectively.[119] Next, the following equation was used to calculate the dissociation rate constant, K_i, from the K_i^{app} value:

$$K_{\mathrm{i}} = \frac{K_{\mathrm{i}}^{\mathrm{app}}}{1+\frac{[S]}{K_m}} \qquad \text{(Equation 2)}$$

Where $[S]$ is the concentration of AcCoA used in the assay, and K_m is the Michaelis-Menten constant of AcCoA.[119] Lastly, the following equation was used to calculate IC_{50} value from the $K_{\mathrm{i}}^{\mathrm{app}}$ value:

$$IC_{50} = K_{\mathrm{i}}^{\mathrm{app}} + \frac{1}{2}[E]_T \qquad \text{(Equation 3)}$$

Where $[E]_T$ is the total enzyme concentration used in the assay.[119]

3.2.4 Determining HAT1 kinetics and mode of inhibition

HAT1 kinetics and the mode of inhibition for the bisubstrate inhibitor, H4K12CoA, were measured using the radiometric filter binding assay.[120] The reaction time and enzyme concentration were controlled so that the reaction yield was kept less than 20%. H4K12CoA was added to the reaction at 0 nM, 20 nM and 100 nM. To determine the activity of HAT1 towards H4-20 peptide, various concentrations of H4-20 peptide (0-100 µM) was mixed with a reaction containing [^{14}C]-AcCoA (3 µM) and reaction buffer (50 mM HEPES (pH 8.0), 0.1 mM EDTA, and deionized water). This mixture was incubated for 5mins at 30°C. Next, HAT1 (0.02 µM) was added and the sample was re-incubated at 30°C for 9 mins. The mixture was spread onto the P81 filter paper to quench the reaction. Filter papers were left to dry for 45 mins before they were washed three times with 50 mM $NaHCO_3$ buffer (pH 9). Lastly, the papers were re-dried, put into vials, and quantified with the addition of scintillation cocktail on the Beckman Coulter LS 6500 multi-purpose scintillation counter.

To determine the activity of HAT1 as a function of AcCoA concentration, various concentrations of [^{14}C]-AcCoA (0-10 µM) was mixed with a reaction containing H4-20 peptide

(100 µM) and reaction buffer (25 mM HEPES (pH 8.0), 0.1 mM EDTA, and deionized water). Next, HAT1 (5 nM) was added and the sample was re-incubated at 30°C for 9 mins. The samples were quenched and the papers were prepared in the same way as mentioned above. All samples were performed in duplicate and were typically within 20% of each other. Data points were fitted to equation 4 to determine K_{is} and K_{ii} values.

$$v = \frac{V_{max}[S]}{K_m\left(1+\frac{[I]}{K_{is}}\right)+[S]\left(1+\frac{[I]}{K_{ii}}\right)} \qquad \text{(Equation 4)}$$

Variables: V_{max}, K_m, $[S]$, $[I]$, K_{is}, and K_{ii} represent the maximum velocity, the Michaelis-Menten constant, substrate concentration, inhibitor concentration, the inhibition constant for the inhibitor binding to the free enzyme, and the inhibition constant for the inhibitor binding to the ES complex respectively.[121]

3.3 Bisubstrate synthesis and purification

The type B histone acetyltransferase, HAT1, has been noted to acetylate newly synthesized histone H4 at Lys5 and Lys12 sites.[104, 117] We rationalized that bisubstrate inhibitors containing the CoA moiety at those respective lysine residues will possess strong inhibitory property towards HAT1. To initiate this project, we synthesized several H4-20 peptides with CoA motif conjugated at Lys5, Lys8, Lys12, and Lys16, respectively. Lys-CoA and CoA were used as control compounds. The Fmoc-based solid phase peptide synthesis methodology was applied to obtain each CoA-peptide bisubstrate inhibitor as previously reported.[55] The synthesis route is depicted in **Figure 3.1**. Briefly, the amino acids consecutively were conjugated to the Fmoc-Lysine(Boc) preloaded Wang resin. Lysine containing Dde group was used to conjugate with CoA at selected positions. A bromoacetyl linker was constructed on the targeted lysine residue which was then used to conjugate CoA to the peptide. After synthesis and purification

using C-18 reverse phase HPLC, the identity of each compound was confirmed by MALDI-MS. The MS results showed that the observed mass of each bisubstrate inhibitor matched the expected molecular weights (**Table 3.1**). Analytical HPLC confirmed the purity of the compounds (**Figure S3.1**).

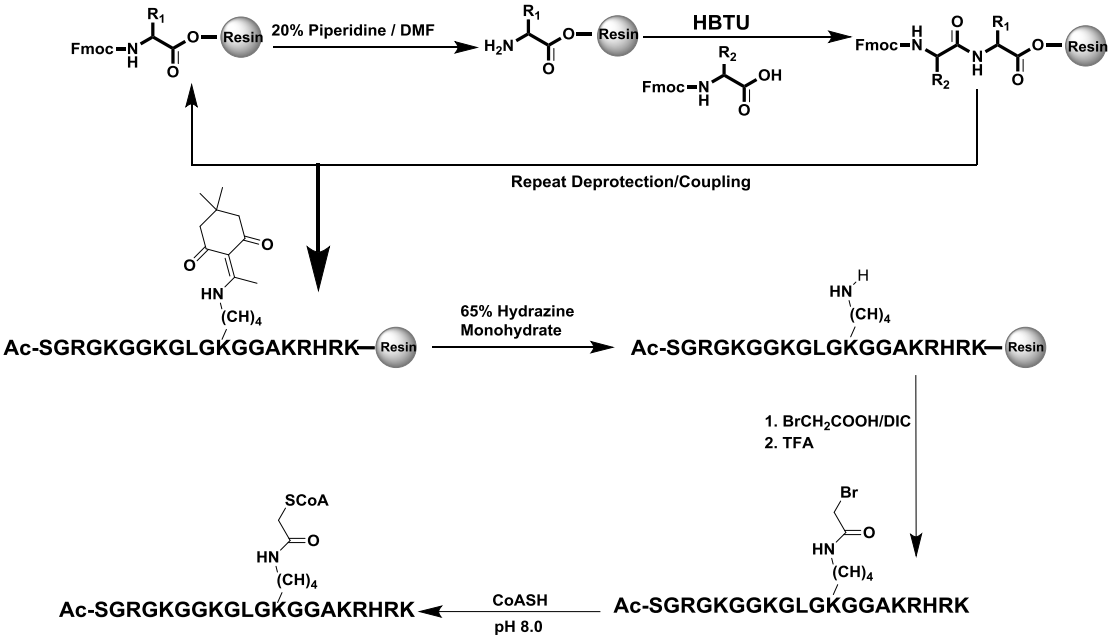

Figure 3.1: Peptide inhibitor synthesis scheme. These steps were used to synthesize the H4 peptide inhibitors.

Table 3.1: Inhibitor sequences and masses.

Inhibitor Name	Sequence	Expected Mass (Da)	Observe Mass (Da)
(**a**) Lys-CoA	Ac-Lys(CoA)-NH_2	998.2	995.1
(**b**) H4K5CoA	Ac-SGRGK(CoA)GGKGLGKGGAKRHRK	2840.9	2841.8
(**c**) H4K8CoA	Ac-SGRGKGGK(CoA)GLGKGGAKRHRK	2840.9	2841.8
(**d**) H4K12CoA	Ac-SGRGKGGKGLGK(CoA)GGAKRHRK	2840.9	2841.8
(**e**) H4K16CoA	Ac-SGRGKGGKGLGKGGAK(CoA)RHRK	2840.9	2841.6

The sequence of each peptide is provided along with the calculated molecular weight and the molecular weight obtained from the mass spectra.

3.4 IC_{50} measurements of bisubstrate inhibitors

Dose-dependent inhibition of HAT1 by each compound was determined using the scintillation proximity assay (SPA) with reactions containing 2.5 µM of biotinated H4-20 peptide (H4-20 BTN), 1 µM of [^{3}H]-AcCoA, and 40 nM of HAT1 incubated at 30°C for 20 min. Signals were read on the MicroBeta reader. Activity data points as a function of inhibitor concentration were fitted to the Morrison equation (Equation 1) (**Figure S3.2**). The observed K_i^{app} value was then used in equation 3 to calculate IC_{50} values for each compound. Control compounds, CoA and Lys-CoA had IC_{50} values at 41.51 µM and 74.85 µM, respectively, while all the H4-CoA bisubstrate inhibitors tested displayed IC_{50} values below 10 µM. This difference in potency is a suggestion of the innate ability of HAT1 to form a tighter binding by recognizing various moieties of CoA and the amino acids residues of the H4 substrate. Thus, placing the CoA moiety at Lys8 or Lys16 on the H4-20 peptide decreased the IC_{50} value to 2.63 µM (K_i

0.92 μM) and 7.17 μM (K_i 2.51 μM) respectively. These moderate IC_{50} values are likely because HAT1 does not demonstrate acetylation activity towards Lys8 or Lys16. Submicromolar potency of the bisubstrate inhibitor was observed when CoA was placed on Lys5 of the H4-20 peptide (IC_{50} 83 nM) (K_i 0.022 μM). Impressively, the lowest IC_{50} value of 23 nM (K_i 1.1 nM) was gained when CoA was positioned at Lys12 (**Table 3.2**). Such low IC_{50} values are most likely because HAT1 has its preferred acetylation positions at Lys5 and Lys12 on histone H4. In the previous study, Lys-CoA was a potent inhibitor that displayed submicromolar inhibition for p300 (IC_{50} 0.98 μM), and H4K12CoA had an IC_{50} of 4.35 μM for p300 which is several folds higher than the IC_{50} reported against HAT1 in this study.[55] This indicates that among the HATs, H4K12CoA is a highly specific inhibitor for HAT1.

Table 3.2: K_i^{app}, IC50 and K_i of each compounds tested with HAT1.

Inhibitor	K_i^{app}(μM)	IC_{50} (μM)	K_i (μM)
H4K5CoA	0.063 ± 0.006	0.083	0.022
H4K8CoA	2.61 ± 0.28	2.63	0.92
H4K12CoA	0.0030 ± 0.001	0.023	0.0011
H4K16CoA	7.15 ± 1.33	7.17	2.51
CoA	41.49 ± 2.55	41.51	14.55
Lys-CoA	74.83 ± 8.29	74.85	26.24

The SPA was used to measure the potency of each inhibitor against HAT1. Reactions containing 40 nM HAT1, 2.5 μM H4-20 BTN, and 1 μM [^{3}H]AcCoA were incubated at 30°C for 20 min. K_i^{app}, IC_{50}, and K_i values were determined using equation 1, 2 and 3 respectively.

3.5 Mode of bisubstrate inhibition

Further studies were carried out to determine the mode of inhibition of H4K12CoA given its high potency in HAT1 inhibition (**Figure 3.2**). The radiometric filter binding assay was used to measure the kinetics of HAT1 in the presence of varying H4-20 peptide and AcCoA concentrations and the data obtained were plotted in the Michaelis-Menten format. Steady state reaction conditions to determine the kinetic parameters of AcCoA included 100 μM of H4-20 peptide, 5 nM of HAT1, and 0-10 μM of [^{14}C]-AcCoA with a 9 min reaction time at 30°C. To determine the mode of inhibition with respect to AcCoA, H4K12CoA was added to the reaction mixture at 0 nM, 20 nM, and 100 nM. The velocity data as a function of substrate concentration were plotted in both Michaelis-Menten format (**Figure 3.3A**) and double reciprocal format (**Figure 3.3C**). On the double reciprocal plot, the three straight lines intersect on the y-axis and vary on the x-axis indicating that H4K12CoA behaves as a competitive inhibitor towards AcCoA (**Figure 3.3C**). To further verify the mode of inhibition, the Michaelis-Menten data points were fitted to the mixed inhibition rate equation (Equation 4) which provided K_{is} of 0.074 μM and K_{ii} of 0.73 μM. The fact that the K_{ii} is about 10-fold greater than K_{is} confirms that H4K12CoA is a primarily competitive inhibitor in respect to AcCoA (**Table 3.3**).[121]

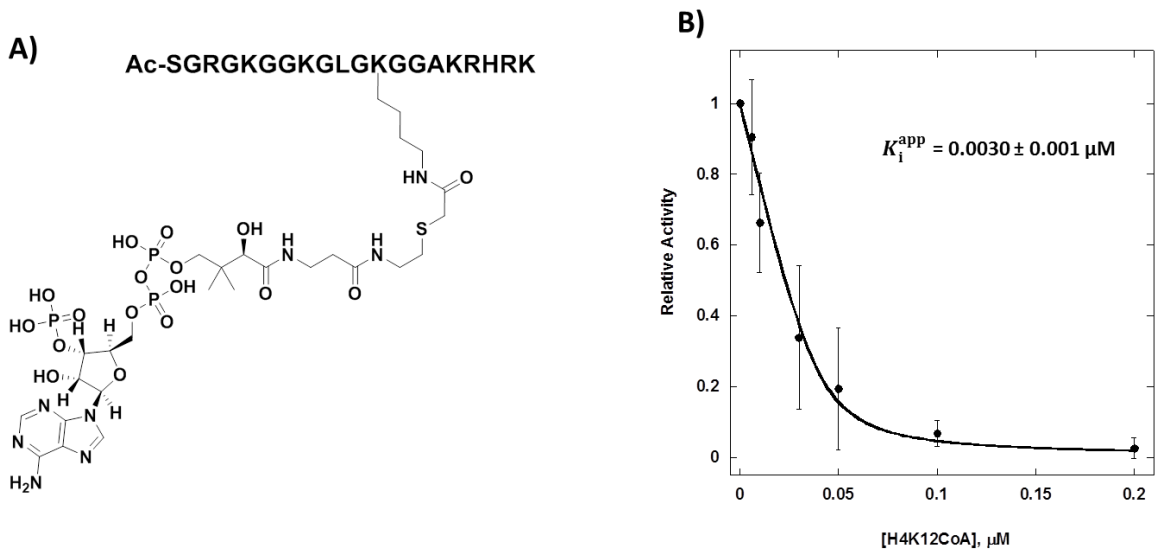

Figure 3.2: Potency of H4K12CoA towards HAT1. A) Structure of H4K12CoA. B) Dose dependent inhibition of HAT1 by H4K12CoA.

Next, we determined the mode of inhibition of H4K12CoA towards H4-20 peptide. The same steady state reaction conditions from above were used with some exception such as 3 µM [^{14}C]-AcCoA, 20 nM HAT1, and 0-100 µM of H4-20 peptide. When 0 nM, 20 nM or 100 nM of H4K12CoA was added to the samples, the double reciprocal graph shows a single intersection point on the y-axis and a change in the Km value; thus indicating that this bisubstrate inhibitor is also a competitive inhibitor towards H4-20 peptide (**Figure 3.3D**). Michaelis-Menten data points were fitted to Equation 4 to verify the mode of inhibition. The values obtained for K_{is} and K_{ii} were 0.022 µM and 1.28 µM respectively. Since K_{ii} is about 58-fold greater than K_{is} this confirms that H4K12CoA is a competitive inhibitor in respect to H4-20 (**Figure 3.3B; Table 3.3**).[121]

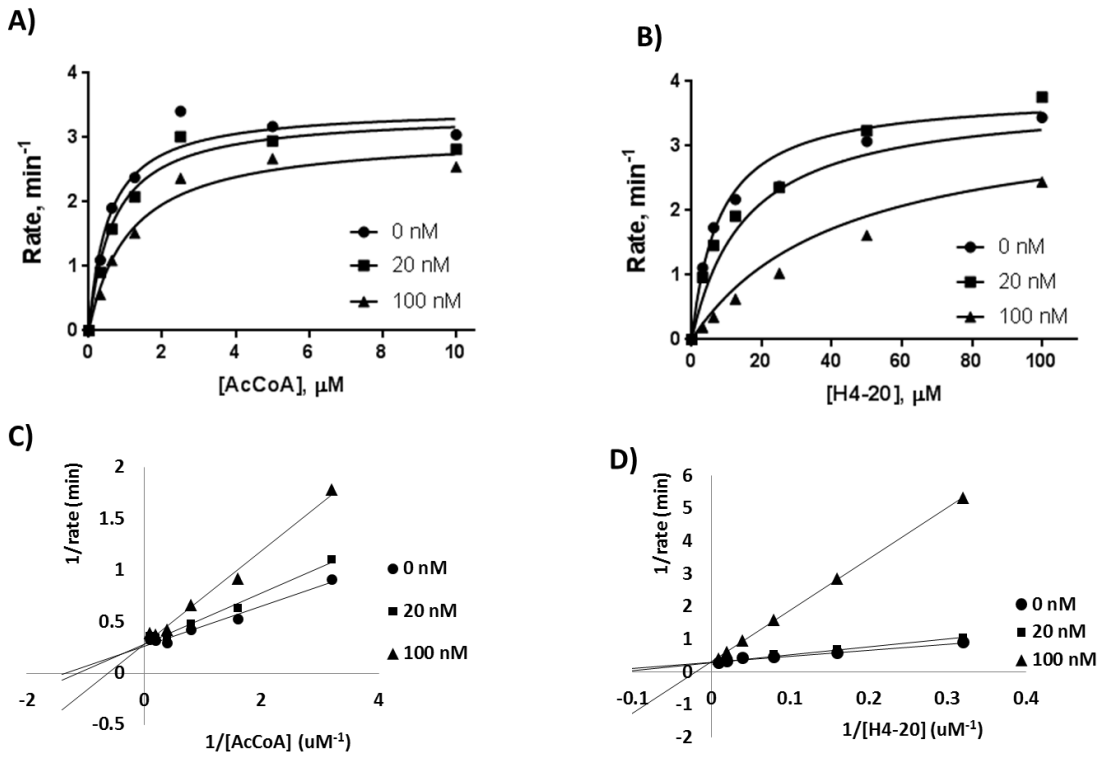

Figure 3.3: Michaelis-Menten data points fitted to the mixed inhibition rate equation and Double reciprocal plots. To determine the mode of inhibition in respect to AcCoA, H4K12CoA was added to the reaction mixture at 0 nM, 20 nM, and 100 nM. A) Reaction conditions to determine AcCoA kinetics include 100 µM H4-20 peptide, 5 nM HAT1, and 0-10 µM AcCoA, with a reaction time of 9 min. B) Reaction conditions to determine H4-20 peptide kinetics include 3 µM AcCoA, 20 nM HAT1, and 0-100 µM AcCoA, with a reaction time of 9 min. Double reciprocal plots of H4K12CoA against C) AcCoA; D) H4-20.

Table 3.3: Kinetics parameters of HAT1 with respect to H4-20 peptide and AcCoA when inhibited by H4K12CoA

	Varying [AcCoA]	Varying [H4-20]
V_{max}	3.47 min^{-1}	3.81 min^{-1}
K_m	0.54 µM	8.07 µM
K_{is}	0.074 µM	0.022 µM
K_{ii}	0.73 µM	1.28 µM

Kinetics in the presence of varying concentrations of H4K12CoA was obtained by fitting the Michaelis-Menten data points to the mixed inhibition rate equation.

Analysis of the mode of inhibition for H4K12CoA towards HAT1 demonstrated that it is a competitive inhibitor towards both the substrate H4-20, and cofactor AcCoA. This is an interesting finding because almost all of the previous bisubstrate inhibitors for acetyltransferases were shown to be competitive versus AcCoA but noncompetitive versus peptide substrate.[55, 122] Such a kinetic inhibition pattern is pertinent to the ordered Bi-Bi sequential kinetic mechanism of acetyltransferases such as RimI,[123] AANAT[124], and PCAF[122] in which AcCoA binds to the active site first followed by substrate binding. Herein, our data on the inhibition pattern of HAT1 bisubstrate inhibitor (i.e., competitive versus both AcCoA and H4 peptide substrate) indicates that HAT1 does not have a preferred order of AcCoA and H4 peptide. Such an inhibition pattern, most possibly, supports that HAT1 catalysis follows a random sequential kinetic mechanism.[123]

Although HAT1 is evolutionarily conserved from yeast to humans, the catalytic functions of human HAT1 in cells currently remains poorly studied.[23-24] The solved crystal structure of human HAT1 (PDB: 2P0W) does, however, provide hints on the catalytic

mechanism and possibly how these bisubstrate inhibitors are recognized and bound.[34] A ternary complex composed of HAT1-AcCoA-H4 peptide was depicted in the crystal structure. Residues such as Glu54, Asp62, and Glu64 of HAT1 are responsible for the specificity and anchoring of the substrate through the formation of hydrogen bonds. AcCoA binding requires various interactions with many different residues. Also, it is speculated that HAT1 catalysis requires a general catalytic base from residues Glu187 and Glu276 which aid Asp277 in deprotonating the ε-amino group of the lysine residue.[34] These combined interactions bring the amino moiety of Lys12 of H4 substrate close to the acetyl group of AcCoA. The distance between the sulfur atom of CoA and the epsilon nitrogen of Lys12 of H4 in the HAT1 complex structure is 4.8 Å (**Figure 3.4A**). On the other hand, we estimated the sulfur-nitrogen distance in the H4K12CoA bisubstrate inhibitor to be 3.3 Å based on the reported p300-Lys-CoA complex structure (PDB: 3BIY) (**Figure 3.4B**). Overall, both measurements are very close which may explain why the bisubstrate inhibitors can bind to HAT1 with strong potency, and it also supports H4K12CoA binding is located in the active site. Although Lys-CoA can bind to HAT1, its potency is very low even compared to CoA (IC_{50} 41.51 μM), indicating that the other amino acid residues of the H4 peptide significantly influence the potency to a great degree and are required for enzyme-substrate binding. In addition, the positioning of the CoA moiety at the proper lysine residue on the H4 peptide can also stimulate and further enhances potency. Further investigation of the interactions between HAT1 and these bisubstrate inhibitors can provide insight into the greater specificity that HAT1 has towards its substrates in comparison to other HATs such as p300 that have been reported to be more promiscuous.[57]

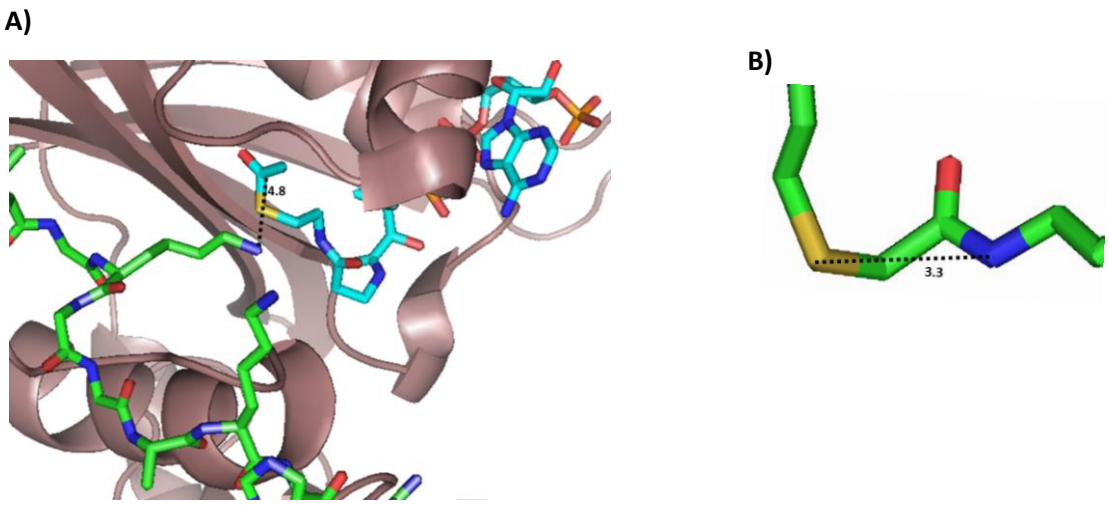

Figure 3.4: Distance between AcCoA and the lysine residue and measurements of bisubstrate inhibitor. A) Distance measurements between AcCoA and lysine residue. Using the crystal structure of HAT1 bound to AcCoA and H4-20 peptide (PDB:2P0W) measurements were done to determine the distance between the carbonyl carbon of AcCoA and the ε-amino group of the lysine residue. B) Distance between sulfur and amine of lysine residue of bisubstrate inhibitor, Lys-CoA. LysCoA was obtained from PDB: 3BIY.

3.6 Conclusion

To the best of our knowledge, we reported the first set of inhibitors that target HAT1 with submicromolar potency, thus offering a type of molecular tools to study HAT1 mechanism and function. As mentioned previously, HAT1 function is poorly studied, yet it has been linked to multiple diseases. To develop appropriate therapeutic agents to target HAT1, it is crucial to understand the preferential binding regions of the substrate and cofactor, as well as molecular cues to enhance the binding. These bisubstrate inhibitors and particularly H4K12CoA can be utilized as chemical probes to give mechanistic insight into the catalytic mechanism and structural biology of HAT1. We do acknowledge that these bisubstrate inhibitors may not have

ideal pharmacokinetic properties such as plasma membrane permeability issues caused by the charged CoA moiety, and metabolic instability.[125] Nevertheless, chemical modifications with membrane-penetrating motifs could generate membrane-permeable probes for both in vitro and in vivo applications. Further efforts could also be implemented to develop bisubstrate-based fluorescent probes for enzyme imaging and high throughput inhibitor screening. In all, this study lays a foundation for the discovery and development of new chemical probes targeting HAT1.

CHAPTER 4

HAT1 EXHIBITS CROTONYLATION ACTIVITY AND IS A NOVEL CROTONYLATED SUBSTRATE OF P300

4.1 Introduction

Post-translational modification (PTM) is a widely studied phenomenon which affects protein-protein interactions,[126] protein localization,[3] as well as its function,[3] and the deregulation of these modifications has been linked to various diseases.[42] An extensively studied PTM is acetylation, which is conducted by histone acetyltransferases (HATs). HATs catalyze the transfer of the acetyl group from acetyl coenzyme A (Ac-CoA) to the ε- amino group on specific lysine residues on histones and non-histone proteins, and the reversal of this reaction is carried out by histone deacetylases (HDACs). HATs are categorized into three main families which include GNAT, MYST, and CBP/p300.[17] Studies have shown that these enzymes have critical roles in regulating DNA damage repair, gene regulation, as well as protein localization and functions, therefore, their abnormal activity can result in the development and progression of various diseases such as cancers,[42, 127] heart disease,[128] and congenital developmental disorders.[42, 129]

Besides acetylation, certain HATs have demonstrated to have other acyltransferase activity such as succinylation, malonylation, propionylation, butyrylation, and crotonylation activity.[79, 130-132] The crotonylation modification was first identified on histones through mass spectrometry.[133] Just recently, the enzymes responsible for the crotonylation modification have been identified. HAT enzymes such as p300,[79] MOF,[134] and PCAF[135] have demonstrated

crotonylation activity while HDAC1,[135] HDAC3,[135] SIRT1,[136-137] SIRT2[136-137] and SIRT3[136-137] exhibited decrotonylation activity. In addition, proteomic studies have been carried out to identify histone as well as non-histone proteins tagged with this modification.[78-79, 135, 138] istone and non-histone substrates that are crotonylated are involved in various biological activities such as gene expression, RNA processing, and chromosome organization.[78, 139]

The typically active crotonylation mark has been noted to be enriched at transcription start sites as well as regulatory elements of activated genes and influences various cellular downstream effects.[79, 133] For example, in round spermatids and elongating spermatids, crotonylation has been found to aid in the reactivation of sex chromosome–linked genes and histone replacement respectively.[140] In acute kidney injury, lysine crotonylation on histones caused an increased expression in peroxisome-proliferator-activated receptor gamma coactivator-1α (PGC-1α) as well as sirtuin-3 and decrease the expression of CCL2 gene which has been shown to have a beneficial nephroprotective effect.[141] This modification has also been shown to have a higher activating transcriptional potency than acetylation.[79] The regulation of crotonyl modifications depend on the metabolic state of the cells, the cellular concentration levels of the crotonyl CoA, cell stress, and even the gut microbiota.[79, 132, 142-143]

HAT1, a member of the GNAT superfamily, was one of the first HATs identified; however, little is known about its functionality in comparison to other HATs. This HAT enzyme localized in both the cytoplasm and nucleus is evolutionary conserved from yeast to humans.[23] Some of the biological roles of HAT1 include DNA damage repair and chromatin assembly.[30, 144] The most well-known role of HAT1 in the cytoplasm is to acetylate newly synthesized histone H4 at lysine 5 and 12.[23] HAT1 has also been shown to acetylate histone H2A at lysine 5,[27] maintain the acetylation marks on histone H3 at lysine 9, 18, and 27 during replication-

coupled chromatin assembly,[25] as well as acetylate non-histone proteins such the promyelocytic leukemia zinc finger protein (PLZF)[38] and MVH.[145] Dysregulated HAT1 activity has also been correlated to several diseases such as cardiovascular diseases, colorectal cancer, liver cancer and lung cancer.[26, 35]

Deletion of the HAT1 gene in yeast, *S. cerevisiae*, or chicken DT40 cells did not show a change in acetylated lysine of histone H4 and resulted in no change in cell proliferation or viability.[26] On the other hand, HAT1 deletion in mammals, specifically in mice, causes neonatal lethality due to lung developmental issues.[25] That same study also showed that HAT1 deletion in embryonic fibroblast resulted growth defect, increase sensitivity to DNA damage and genome instability. These results suggest that HAT1 plays a major yet not fully understood role in mammalian biological systems.

Proteomic studies looking at protein crotonylation in mammalian cells have shown that HAT1 is crotonylated.[78-80] Due to the poor understanding of HAT1 activity, we wanted to determine how this enzyme is associated with crotonylation. The goal of this project is to reveal the enzyme responsible for crotonylating HAT1and to determine if HAT1 has crotonylation activity. This study was able to show that HAT1 has crotonylation activity toward histone substrates. The HAT enzyme responsible for crotonylating HAT1 was identified to be p300, and interestingly, the biochemical data showed that when HAT1 is crotonylated, it loses both acetylation and crotonylation activity.

4.2 Materials and methods

4.2.1 Protein expression and purification

The expression of p300 HAT domain (1287-1666) was done using the method developed by Phil Cole's lab.[146] Briefly this protein was expressed using *Escherichia coli* and

purified using chitin beads. The transformation was done using *E.coli* BL21(DE3)/ RIL competent cells through heat-shock and then spread on plates containing both ampicillin and chloramphenicol antibiotics. Colonies were harvested and grown at 37 °C in 8 mL then 1L cultures of 2xYT media containing both ampicillin and chloramphenicol. Protein expression was induced by the addition of isopropyl β-D-1-thiogalactopyranoside (IPTG) and shaken for 16 hours at 16 °C. The cells were collected by centrifugation at 4000 rpm for 25 min, suspended in lysis buffer (25 mM Na-HEPES (pH 8), 500 mM NaCl, 1 mM $MgSO_4$, 10 % glycerol, and 2 mM phenylmethanesulfonyl fluoride (PMSF)) and then ran through the cell disruptor.

Chitian resins were equilibrated with column buffer (25 mM Na-HEPES (pH 8), 250 mM NaCl, 1 mM EDTA, 0.1 % trition X-100 and 1 mM PMSF) before they were used to purify the supernatant. The column was thoroughly washed with column buffer and wash buffer (25 mM Na-HEPES (pH 8), 500 mM NaCl, 1 mM EDTA, 0.1 % trition X-100 and 1 mM PMSF) before the CT14 peptide was dissolved in cleavage buffer (25 mM Na-HEPES (pH 8), 250 mM NaCl, 1 mM EDTA, 200 mM 2-Mercaptoethanesulfonic acid (MESNA)) and added to the column. After the addition of the CT14 peptide in cleavage buffer, the column was set out at room temperature for 16 hours. The protein was then eluted from the column, and several volumes of cleavage buffer were added to ensure the complete elution of the protein. Further purification was done using the NGC fast protein liquid chromatography (FPLC) system by Biorad. The identification of p300 HAT domain was confirmed using a 12 % sodium dodecyl sulfate-polyacrylamide gel electrophoresis (SDS-PAGE). Millipore centrifugal filter and Bradford assay were respectively used to concentrate and determine the protein's concentration. Lastly, the protein was aliquoted and stored at -80°C.

The expression and purification of HAT1 (20-341) was done following the method described Hong Wu et al..[34] Briefly this protein was expressed using *Escherichia coli* and purified using NTA-ni resin. The transformation was done using BL21 (DE3)/ RIL competent cells through heat-shock and then spread on plates containing antibiotics, kanamycin, and chloramphenicol. Protein expression was induced by the addition of isopropyl β-D-1-thiogalactopyranoside (IPTG) and shaken for 16 hours at 16 °C. The cells were collected and suspended in lysis buffer (50 mM Na-phosphate (pH: 7.4), 250 mM NaCl, 5 mM imidazole, 5 % glycerol, 2 mM β-mercaptoethanol, and 1 mM phenylmethanesulfonyl fluoride (PMSF)) then disrupted using the cell disruptor. The supernatant was passed through a column containing NTA-ni resin equilibrated with column washing buffer (20 mM Hepes (pH: 8), 250 mM NaCl, 5% glycerol, 30 mM imidazole, 1 mM PMSF) and the resin was washed with column washing buffer. Next, the resin was washed with buffer containing a higher concentration of imidazole (20 mM HEPES (pH: 8), 250 mM NaCl, 5% glycerol, 50 mM imidazole, 1mM PMSF). The HAT1 was eluted with elution buffer (20 mM HEPES (pH: 8), 250 mM NaCl, 5% glycerol, 500 mM imidazole, 1 mM PMSF).

4.2.2 Western blot analysis

Recombinant HATs obtained from the methods described above was incubated with 70 µM crotonyl-CoA and in the presence or absence of 1µg of recombinant human H4-histone (NEB, cat# M2504S) in reaction buffer (50 mM HEPES (pH: 8); 1 mM EDTA). The reaction took place for 30 min to 1 hr before being separated on SDS-PAGE gels. Proteins were transferred to a 0.2 µm nitrocellulose membrane, stained with Ponceau S staining, then blocked with 5% non-fat milk prepared in a TBST buffer (Tris-buffered saline, 0.1% Tween) for 1 hr at

room temp. Membranes were incubated with primary antibodies overnight at 4°C with genital rocking. Next day, membranes were washed with TBST then incubated with secondary antibody for 1 hr at room temp with genital rocking. Membranes were rewashed with TBST buffer, and SuperSignal Chemiluminescent Substrates was added to the blot before imaging was conducted using Li-cor Odyssey.

4.2.3 Crotonyl-CoA synthesis

0.0065 mmol of CoA hydrate (5 mg) was dissolved in 1.5 mL of 0.5 M NaHCO3 (pH: 8.0) and cooled down on an ice bath. Crotonic anhydride (2 mg, 0.013 mmol) in 1 mL of CH3CN/Acetone (1:1 v/v) was added dropwise to the CoA solution. The reaction solution was stirred at 4 °C overnight and then quenched by adjusting the pH to 4 with 1 M HCl. The reaction mixture was subjected to reverse phase-HPLC purification with gradient 5—45% Acetonitrile over 30 min at a flow rate of 5 mL/min; UV detection wavelength was fixed at 214 and 254 nm. HPLC buffer was 0.05% TFA in water (solution A) and 0.05% TFA in acetonitrile (solution B). The fractions were collected and lyophilized after flash-freeze with liquid nitrogen to afford the desired product as a white solid (3.8 mg). Based on analytical HPLC the purity was 99.5% **(Supplemental figure S4.4).**

^{1}H NMR (400 MHz, Deuterium Oxide) δ 8.54 (s, 1H), 8.31 (s, 1H), 6.84 (dd, *J* = 15.5, 6.8 Hz, 1H), 6.17 – 6.03 (m, 2H), 4.76 (d, *J* = 5.8 Hz, 2H), 4.48 (s, 2H), 4.15 (s, 2H), 3.91 (s, 1H), 3.75 (d, *J* = 7.2 Hz, 1H), 3.49 (d, *J* = 7.1 Hz, 1H), 3.33 (t, *J* = 6.6 Hz, 2H), 3.23 (t, *J* = 6.4 Hz, 2H), 2.91 (t, *J* = 6.4 Hz, 2H), 2.31 (t, *J* = 6.5 Hz, 2H), 1.73 (dd, *J* = 6.9, 1.8 Hz, 3H), 0.82 (s, 3H), 0.69 (s, 3H).

4.2.4 H4-20 peptide synthesis

The first 20 amino acids the N-terminal of histone H4(Ac-SGRGKGGKGLGKGGAKRHRK) was synthesized on a peptide synthesizer using the Fmoc [N-(9-fluorenyl) methoxycarbonyl**]** -based solid-phase peptide synthesis protocols. The amino acids and Lys Wang resin were weighed out with an equivalence ratio four times greater than the amount of HCTU [O-(1H-6-Chlorobenzotriazole-1-yl)-1,1,3,3-tetramethyluronium hexafluorophosphate] coupling reagent. The resin was cleaved using trifluoroacetic acid (TFA). The peptides were purified using a C-18 reverse phase column on a HPLC (High-performance liquid chromatography) instrument, and each sample was sent off for mass spectrometry. Lastly, NaOH was used to neutralize the pH.

4.2.5 Measuring HAT1 activity using filter binding assay

HAT1 acetylation and crotonylation activity were measured using the filter binding assay. The same conditions were applied to all samples to give a clear comparison of HAT1 versus p300 crotonylation activity. 0.6 µM HAT1 or p300, H4-20 peptide (30 µM) and [^{14}C]Crotonyl-CoA (30 µM) or [^{14}C]Acetyl-CoA (30 µM) incubated in reaction buffer (50 mM HEPES (pH: 8.0), 0.1 mM EDTA, and deionized water (dH2O). Then at various time points ranging from 30 min to 240 min the reactions were quenched by spreading the mixture onto charged P81 filter paper. Filter papers were left to dry for 45 mins before they were washed three times with 50 mM $NaHCO_3$ buffer (pH: 9). Lastly, the papers were re-dried, put into vials, and quantified using the Beckman Coulter LS6500 scintillation counter after the addition of scintillation cocktail to each vial. The yield of each sample was determined and was used to obtain product formation.

4.2.6 Proteomics to locate histone H4 crotonylation site

To prep the sample, the protein mixture was first reduced in 20 mM DTT at 56 °C for 1 hr, and alkylated in 50 mM IAA at room temperature for 40 min in the dark. Then, trypsin was added at 1:30 (enzyme/substrate, m/m) and incubated at 37 °C for 16 h. After 2 μL FA was added to end the digestion, the digests were desalted by a C18 precolumn and finally dried down in a Speed Vac Concentrator (Thermo, Waltham, MA). All samples were stored at -80 °C pending further analysis.

For MS analysis and database search, the tryptic digests were analyzed on a Q-Exactive MS (Thermo Fisher Scientific, USA) equipped with an Easynano LC system (Thermo Fisher Scientific, USA). The mobile phases were 2% ACN with 0.1% FA (phase A) and 90% ACN with 0.1% FA (phase B). A C18 homemade capillary column (75 μm i.d. × 15 cm) was used for peptide separation. The Q-Exactive was operated in positive ion data dependent mode. The produced *.raw files were searched against the UniProtKB human database (release 2017_04) in MaxQuant (1.3.0.5). Mass tolerances for parent ions were set as 7 ppm and 20 ppm for fragments. Cysteine carbamidomethylation was searched as a fixed modification. Oxidation (M), acetylation (protein N-termini), acetylation (K), crotonylation (K), trimethylation (K), dimethylation (KR), methylation (KR) were searched as variable modifications. Reverse sequences were appended for FDR evaluation. Peptides were searched using tryptic cleavage constraints, and up to 4 missed cleavages. All the identified sites were filtered by localization probability > 0.75, score > 40 and further MS/MS manual confirmation.

4.2.7 Detecting crontylation activity of HAT1 in cells

HAT1 crotonylation activity was observed in HAT1 knockout and wt MEF cells as well as in HEK293T cells with HAT1 overexpressed. MEF cells and HEK293T cells were cultured

in Dulbecco's modified Eagle medium (DMEM- Corning) supplemented with 10% fetal bovine serum (FBS-Corning) and 1% antibiotics (Penn/Strep) at 37 °C in 5% CO_2. Transient transfections were carried out on cells at 90% confluency using Lipofectamine 3000 reagent. 2 ug of HAT1 plasmid was used to transfect HEK293T cells using instructions provided in Lipofectamine 3000 transfection kit. After 24 hrs 60 mM of sodium crotonate was added to the cells and the cells were collected at 8, 12 and 24 hrs time points. Cells were washed with PBS buffer three times before being resuspended in M-PER buffer containing a protease inhibitor cocktail and 30 µM suberoylanilide hydroxamic acid (SAHA). Next, the cells incubated on ice for 20 min before being sonicated and centrifuged to remove cell debris. Protein concentration was determined using the Bradford assay and protein crotonylation was visualized by western blot using pan anti-crotonyllysine antibody (cat# PTM-502). Sodium crotonate (NaCro) was prepared by dissolving crotonic acid with deionized H_2O and adjusting the pH to 7.4. The final product was verified using mass spectrometry. MEF cells were cultured to 80-90% confluency. Next, 20 mM of NaCro was fed to the cells and the cells were collected 24 hrs later.

4.3 Screening HATs for crotonylation activity towards HAT1

HATs have been noted for acyltransferase activity either by auto-acylation[92] or acylation of other proteins.[147] To date, the HATs that have been identified to have crotonylation activity toward other proteins include p300,[79] CBP,[135] MOF,[134] and PCAF[135]. Proteomic studies looking at protein crotonylation in mammalian cells have reported HAT1as a crotonylated substrate.[78-80] Therefore, we first wanted to identify the HAT enzyme responsible for crotonylating HAT1. Also, because HAT1 is part of the histone acetyltransferase family we also wanted to reveal if this enzyme possessed any novel crotonylation activity towards its known substrate histone H4. The pan anti-butyryllysine antibody was used, as it was available to us at the time, to visualize

HAT crotonylation activity. The crotonyl and butyryl moieties are very similar in structure, and it has been noted that pan anti-crotonyllysine antibody can identify butyryl modifications on lysine residues; therefore, we were interested to see if the opposite was true.[78] Indeed, under our testing conditions, the pan anti-butyryllysine antibody could detect crotonylation but not acetylation activity (**Figure 4.1A and B**). In addition, crotonylation activity cannot be detected when using pan anti-acetyllysine antibody (**Figure 4.1C**).

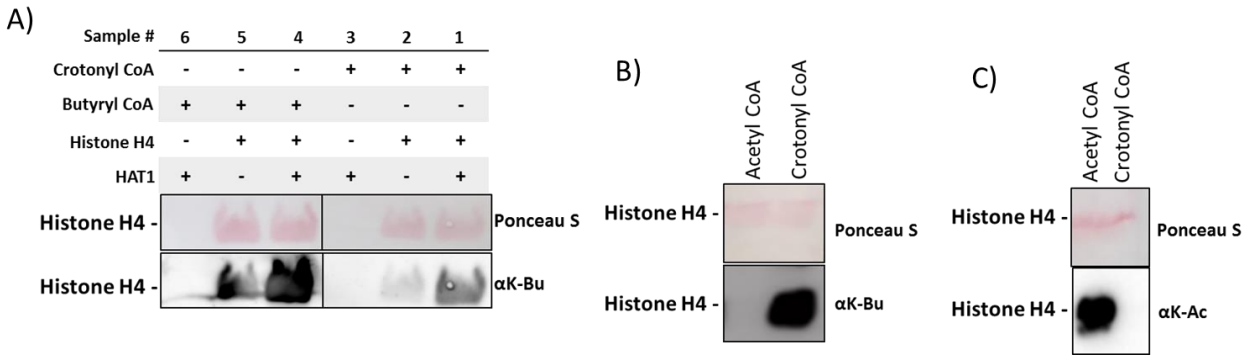

Figure 4.1: Verifying Anti-butyryllysine antibody. A) Anti-butyryllysine antibody can detect both butyryl and crotonyl modifications. Samples contain crotonyl CoA (70 µM), H4-protein (1µg**)** and HAT1 (0.5 µM) and was incubated for 1hr at 30°C **B)** Anti-butyryllysine antibody cannot detect acetylation. **C)** Anti-acetyllysine antibody cannot detect crotonylation. Samples in B and C contain crotonyl or acetyl CoA (70 µM), H4-protein (1µg**)** and HAT1 (0.5 µM) and was incubated for 1hr at 30°C. H4 protein modifications were detected by pan-antibutyryllysine antibody or pan-antiacetyllysine antibody.

Various HATs were screened using the pan anti-butyryllysine antibody to detect crotonylation activity towards HAT1 and histone H4. Histone H4 is observed to be crotonylated by TIP60, p300, MOF and HAT1 (**Figure 4.2,** sample 1, 6, 7, and 18 respectively). These results reconfirm previous studies showing p300[79] and MOF[134] crotonylation activity, as well as

revealing TIP60 and HAT1 as novel enzymes that display crotonylation activity towards histone H4.[79, 148] MORF and HBO1 did not exhibit any crotonylation towards histone H4 or HAT1. Of the tested HATs, p300 was the only enzyme able to crotonylate HAT1 (**Figure4.2,** sample 5; bottom band). The top band in sample 5 is indicative of p300 autocrotonylation activity because it lines up well with the band in sample 4 which contains p300 and Crotonyl-CoA. None of the other HATs displayed autocrotonylation activity (**Figure 4.2**).

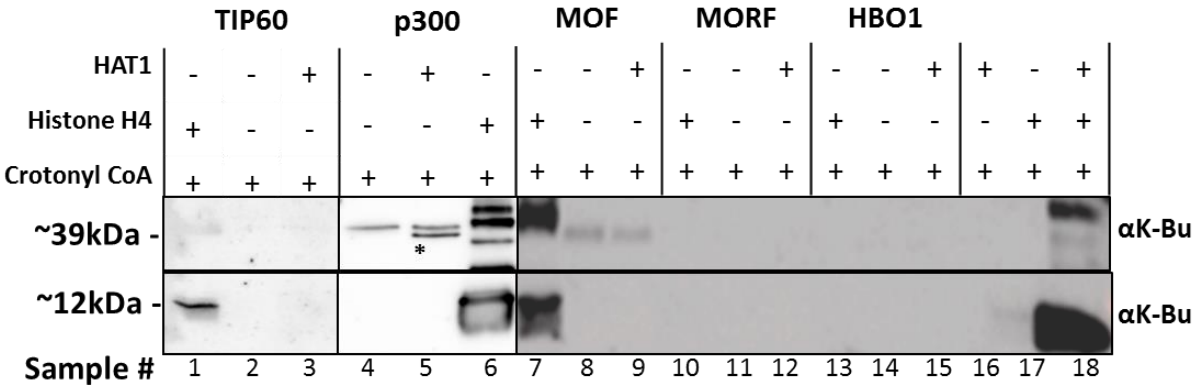

Figure 4.2: Screening for HATs that can crotonylate HAT1 and histone H4. Crotonyl CoA (70 µM) was incubated for 1hr at 30°C with various HAT enzymes (0.5 µM), with or without histone H4 (1 µg), and HAT1 (0.5 µM). Crotonylation activity was detected using pan-antibutyryllysine antibody. *Band directly above asterisk denotes position of HAT1.

4.4 Detecting crotonylation activity of HAT1 using mass spectrometry

The previous experiments showed that HAT1 has crotonylation activity towards histone H4 and that p300 was responsible for the crotonylation of HAT1. Attempts were made to locate the crotonylation site in HAT1; however, it was unsuccessful and could be due to low stoichiometry, or the modification is in un-identified peptide portion. To verify the crotonylation activity of HAT1 mass spectrometry was used with H4-20 peptide and histone

H4. H4-20 peptide was crotonylated by HAT1, and this was confirmed by MALDI (**figure S4.1**).

Next, proteomics was used to determine the crotonylation sites on histone H4 by HAT1. Three crotonylation sites were detected on histone H4 with high confidence. The crotonylation sites identified are at Lys12, Lys16 and Lys31. As mentioned previously, Lys12 and Lys5 are widely accepted and known as acetylation sites of HAT1; therefore, the crotonylation of Lys12 was anticipated due to the fact that it is the preferred substrate.[30] There has been a report of HAT1 also acetylating histone H4 at Lys8 and Lys91; however, for the crotonylation at Lys16 and Lys31, to our knowledge, there has not been any reports of modification at those sites by HAT1(**Table 4.1**).[33]

Table4.1: Mass spectrometry analysis of HAT1 crotonylation sites on histone H4.

			Crotonoyl (K)Sites			
Proteins	**Protein names**	**Gene names**	**Score**	**Modified sequence**	**Position in peptide**	**Positions within proteins**
P62805	Histone H4	HIST1H4A	53.967	_DNIQGITK(cr)PAIR_	8	32
P62805	Histone H4	HIST1H4A	147.37	_GLGK(cr)GGAK(cr)R_	4	13
P62805	Histone H4	HIST1H4A	71.501	_GLGK(cr)GGAK(cr)R_	8	17

Reaction contained crotonyl CoA (100 µM), histone H4 (3.12 µM) and HAT1 (0.5 µM) incubated for 1hr at 30°C.

4.5 HAT1 and p300 Crotonylation vs. Acetylation Products

As mentioned previously, p300 has been reported to have crotonylation activity,[79] and we have shown that HAT1 can crotonylate histone H4. To compare the acetylation versus crotonylation activity of HAT1 and p300, the same conditions were applied to all samples. The radioactive filter binding assay was done with 0.6 µM HAT1 or p300, H4-20 peptide (30 µM) and [^{14}C]Crotonyl-CoA (30 µM) or [^{14}C]Acetyl-CoA (30 µM) with various reaction times.

Under the listed conditions, HAT1 and p300 both have high yields for acetylated products. HAT1 and p300 crotonylation activity are several folds less than the acetylation activity at every time point. Although p300 produced more acetylated product than HAT1 at each time point, there was less crotonylaed H4-20 peptide in comparison to HAT1 (**Figure 4.3**).

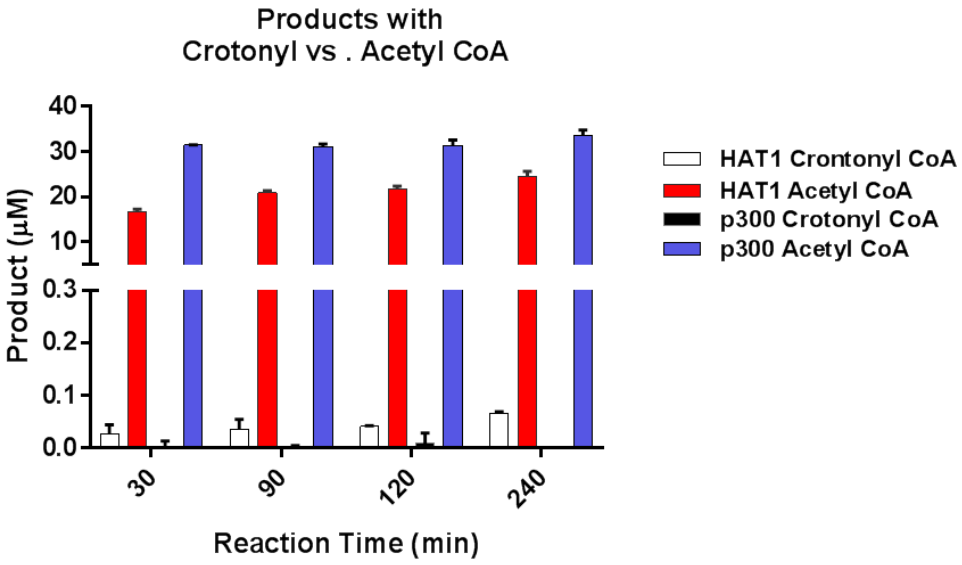

Figure 4.3: HAT1 crontylation vs. acetylation activity. Filter binding assay was used to compare the crotonylation and acetylation activity of HAT1. Reaction conditions include HAT1 or p300 (0.6 µM) incubated with [^{14}C]crotonyl-CoA or [^{14}C]acetyl-CoA (30 µM) and H4-20 peptide (30 µM). At the respective times the product was separated with P81 paper and quantified using a scintillation counter. The yield of each sample was determine and used to obtain product formation.

4.6 HAT1 crotonylation activity in cells

Next, we wanted to visualize HAT1 crotonylation activity of histone H4 in mammalian cells. Immortalized MEF cells containing endogenous levels or knockout of HAT1 were obtained from the Parthun lab.[25] These cells were treated with 20 mM sodium crotonate and

incubated for 24 hrs. HAT1 crotonylation activity was observed in MEF cells containing endogenous levels of HAT1 and in cells that had a knockout of HAT1. Crotonylation of histone H4 was observed by western blot using a pan anti-crotonyllysine antibody which showed that in the absence of HAT1 histone H4 was not crotonylated; however, with HAT1 a band could be observed indicating histone H4 was crotonylated. The histone H4 crotonylation band was faint which could be due low abundance of free histone H4 (**Figure 4.4A**).

Next, HAT1 was overexpressed to obtain a clearer image of HAT1 crotonylating histone H4. HAT1 was overexpressed in HEK293T cells using Lipofectamine 3000 reagent following the instructions provided in the kit, and the cells were fed with 60 mM of sodium crotonate with varying incubation times (0-24 hrs). Without the treatment of sodium crotonate crotonylation of histone H4 was not observed (**Figure 4.4B,** sample 1 and 5); however, with sodium crotonate the crotonylation of histone H4 increases with increasing incubation time. In **figure 4B** sample 6-8 do not have an overexpression of HAT1 yet crotonylation of histone H4 can still be observed. This crotonylation activity could be due to the endogenous level of HAT1 or from other HAT enzymes present in these cells. When HAT1 is overexpressed, the crotonylation levels of histone H4 at 12 and 24 hrs incubation period is higher in comparison to samples containing endogenous levels of HAT1 (**Figure 4.4B and C**).

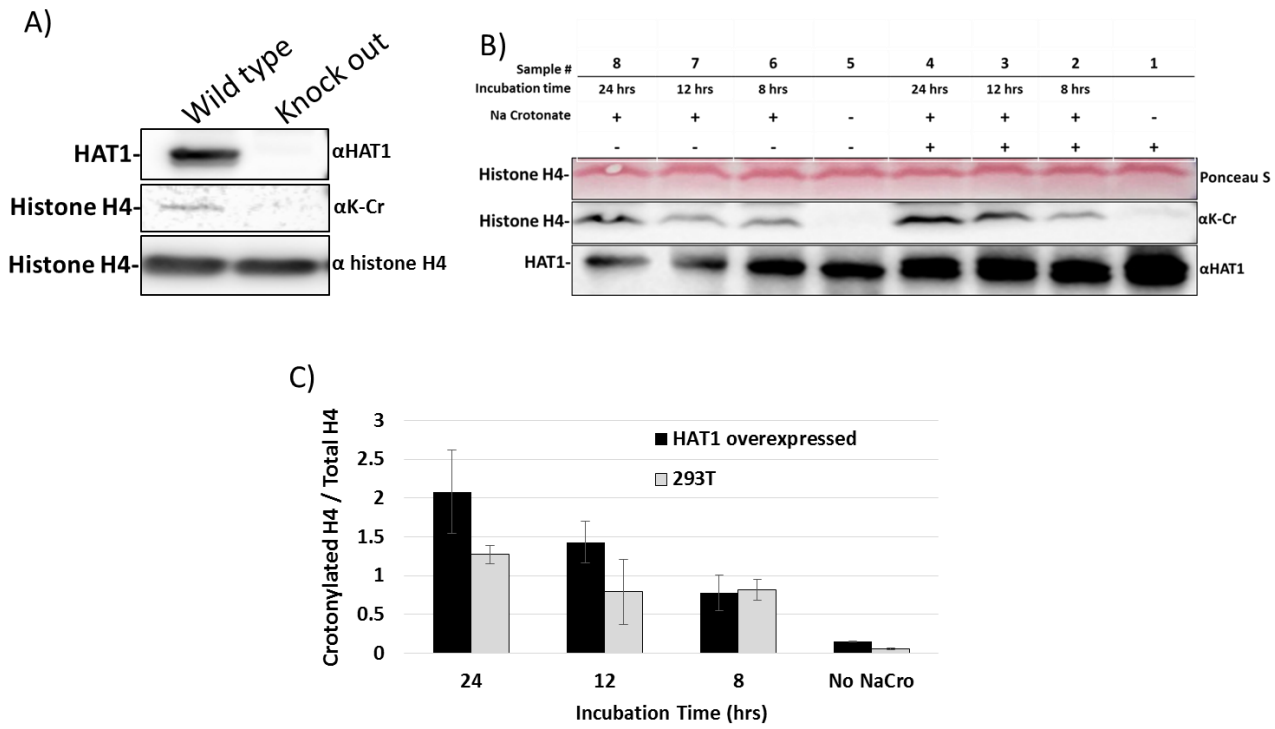

Figure 4.4: HAT1 crotonylation activity in cells. A) Crotonylation of histone H4 can be observed with endogenous levels of HAT1 in wild type MEF cells. Wild type and HAT1 knock out MEF cells were fed with 20 mM sodium crotonate and incubated for 24 hrs. **B)** Overexpressed HAT1 had increase histone H4 crotonylation levels as incubation time increase. HAT1 was overexpressed in 293T cells and 60 mM of sodium crotonate was added and the cells incubated for 8, 12 or 24 hrs. **C)** Quantified band density of bands in **B**.

4.7 Histone H4 forms higher molecular weight structures in the presence of crotonyl CoA

The western blot from **figure 4.2** displayed bands at higher molecular weights when HAT enzymes were in the presence of crotonyl-CoA and histone-H4. These higher molecular bands can be observed very clearly in **figure 4.2** (sample 6) with the sample containing p300, histone H4 and crotonyl CoA. We wondered if these bands were higher order structures of histone H4 and if this phenomenon was acyl-CoA dependent. Propionyl-, butyryl, acetyl-, and

crotonyl-CoA were tested with histone H4 in the presence or absence of HAT1 and histone H4. Western blot probing for histone H4 confirmed that the higher order molecular weight structure was indeed histone H4 and this phenomenon occurred only in the presence of crotonyl-CoA (**Figure 4.5A**)

The blot was then stripped and re-probed with monoclonal pan-anti crotonyllysine antibody. This antibody was able to detect HAT1 butyrylation, propionylation as well as crotonylation activity but not acetylation activity. Higher molecular weight bands can be detected clearly when histone H4 is crotonylated by HAT1 (**Figure 4.5A**, sample 4). Spontaneous histone H4 crotonylation labeling can be observed from the faint bands from the sample containing just histone H4 and crotonyl-CoA (**Figure 4.5A**, sample 5). Non-enzymatic labeling is caused by the high energy bond of the thioester moiety of acyl-CoA which has been noted to be reactive.[132] There are no higher molecular weight bands of histone H4 detected when propionyl-, butyryl-, or acetyl-CoA was present (sample 6-11). It should also be noted that the higher order molecular weight structures were not specific to histone H4. The HAT1 mutant, HAT1M222G, contains a mutation in the cofactor binding pocket abolishing its acetylation activity (data not shown). When this mutant is added at the same concentration as histone H4 there are no higher order structures of histone H4 detected (**Figure 4.5A**, sample 3); however, if the mutant is added after histone H4 and crotonyl CoA has incubated for 30 min, then higher order structures of histone H4 can be observed (**Figure 4.5A**, sample 1).

We suspect that the alkene from the crotonyl group is reacting with nucleophiles such as a free amine or thiol moiety from cysteine residues. To test this hypothesis, we incubated histone H4 and crotonyl CoA in buffers at pH: 5, 7, 8, and 10. Spontaneous crotonylation can be observed at pH: 8, and 10. At a lower pH of 5, there was neither crotonylation nor

oligomerization of histone H4 observed. At pH: 7 there is a very faint band representing the crotonylation of histone H4 and a slight dimerization band. However, at pH: 8 and 10, there are clear indications of histone H4 forming higher molecular weight structures (**Figure 4.5B**). These results are as expected because at higher pH nucleophiles generally become more nucleophilic aiding in the attack of the crotonyl moiety at the double bond.

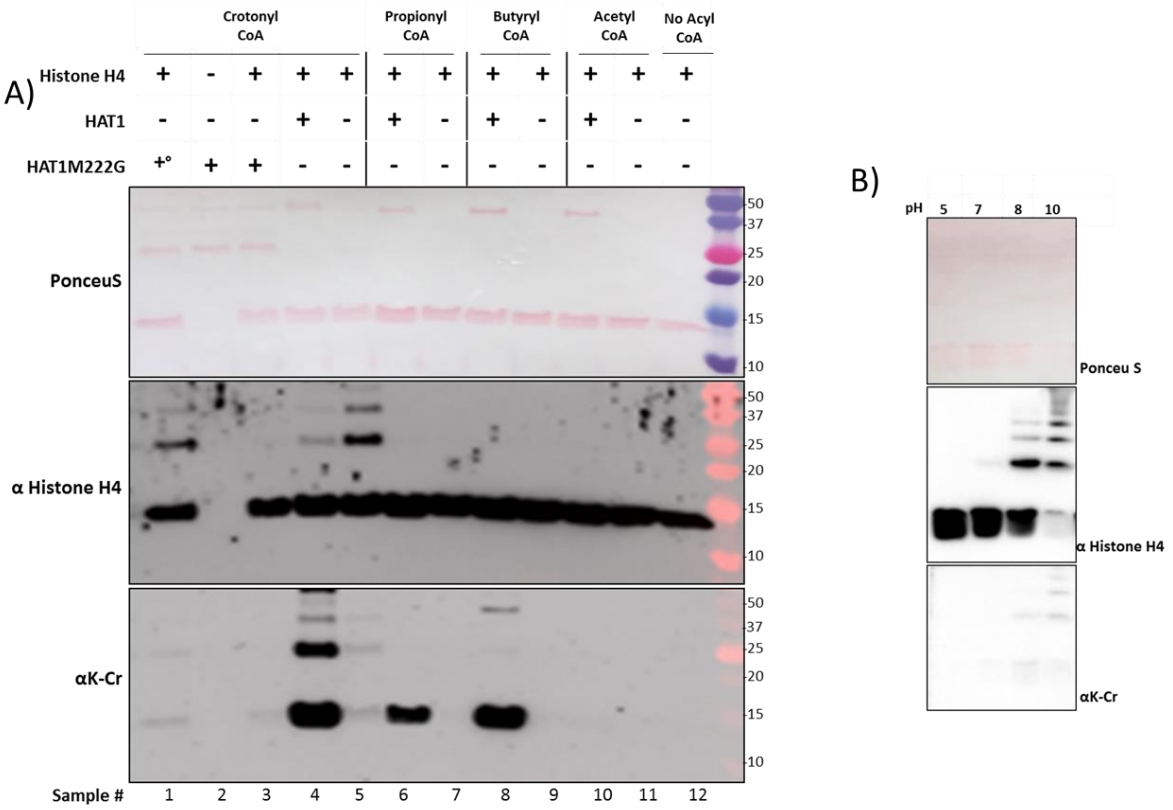

Figure 4.5: Histone H4 forms higher molecular weight structures in the presence of crotonyl CoA. A) Acyl CoA (70 µM) and histone H4 (1µg) was incubated for 1hr at 30°C with and without HAT1 (0.5 µM) and HAT1M222G (4.45 µM). (+°) M222G was added after Crotonyl-CoA and histone H4 incubated for 30min. Crotonylation activity was detected using Pan-anticrotonyllysine antibody. **B)** The higher molecular weight structures of histone H4 formation is pH dependent. Reactions conditions included histone H4 (1µg) and crotonyl CoA (70 µM) incubated at pH 5, 7, 8, and 10.

4.8 The abolished acetylation and crotonylated activity of crotonylated HAT1

So far, our experimental data showed that HAT1 has crotonylation activity towards histone H4 and itself is a substrate of p300 that becomes crotonylated. Next, we wanted to determine if the crotonyl modification on HAT1 affects its enzymatic activity. A reaction mixture containing p300, HAT1 and crotonyl CoA was incubated first to allow for HAT1 crotonylation to occur. Then, the potent p300 inhibitor, C646[72] (20 µM), was added to inhibit p300. Lastly, histone H4 and AcCoA were added to determine the crotonylated HAT1 acetylation and crotonylation activity. HAT1 activity was tested at various concentrations of C646, and it was determined that with 20 µM of C646 HAT1 crotonylation activity was negligibility affected while its acetylation activity decreased to about 20% (**Figure S4.2A**). It is known that this inhibitor is a potent submicromolar inhibitor towards p300 so at 20 µM we are confident that p300 would be adequately inhibited.[72] Indeed, there is a missing band in sample 9 of **figure 4.6** indicating that p300 acetylation activity is fully inhibited with 20 µM of C646; however, HAT1 still retains some acetylation activity (sample 5). Sample 1-3 show that p300 and HAT1 indeed became crotonylated. In the absence of C646, there is a strong acetylation band of histone H4 which is due to p300 activity, because in the presence of C646 (sample 3) there is no H4-protein acetylation band present which indicates that crotonylated HAT1 has lost its acetylation activity (**Figure 4.6**).

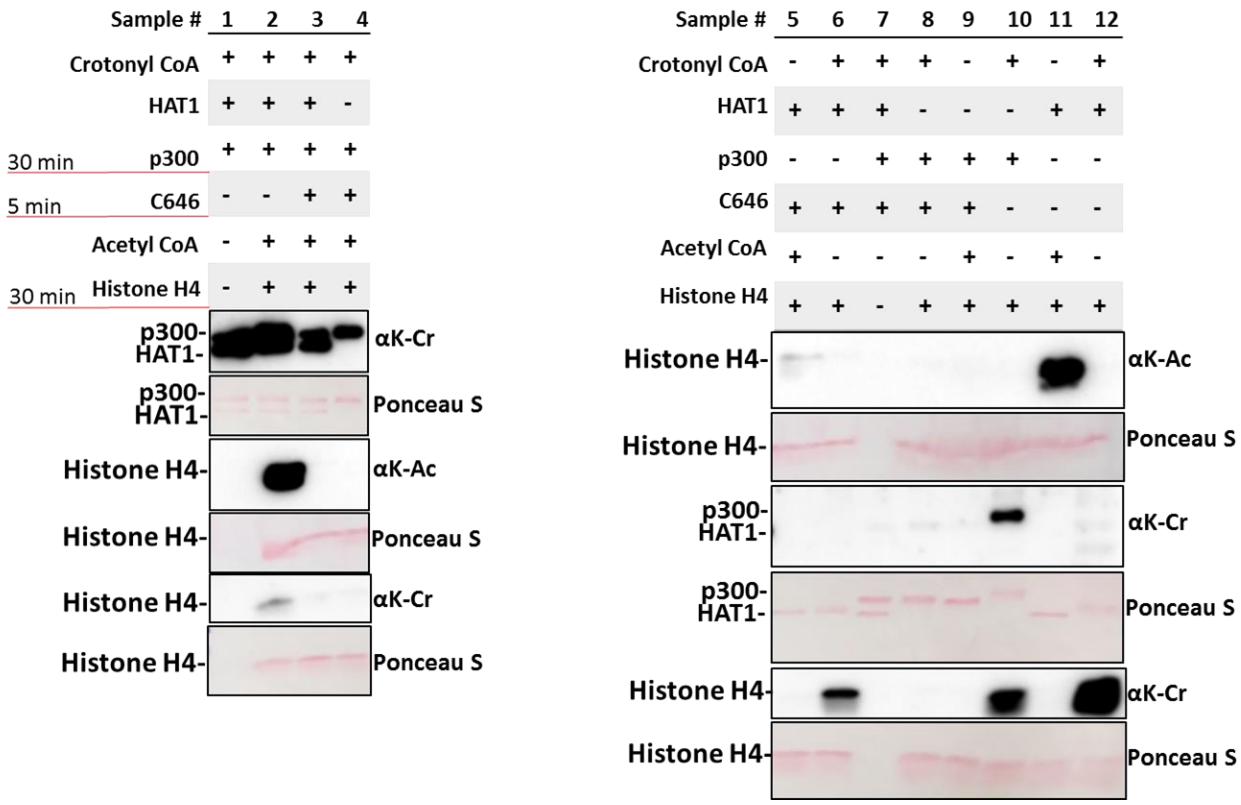

Figure 4.6: Acetyltransferase and crotonyltransferase activity of HAT1 acetylation when crotonylated by p300. Samples 1-4 was incubated with crotonyl-CoA (70 µM), HAT1 (0.5 µM) and p300 (0.5 µM) for 30min at 30°C. Then, C646 (20 µM) was added and the sample was incubated again for 5 min. Next, acetyl CoA (70 µM), and H4 protein was added and the sample was further incubated for 30min at 30°C. Control samples 5-12 incubated for 30min at 30°C with the respective components. Modification was identified using pan-antiacetyllysine antibody or pan-anticrotonyllysine.

Crotonylation activity of crotonylated HAT1 was determined next (**Figure 4.6**). As shown previously, when HAT1 was in the presence of C646 crotonylation activity is still observed (sample 6 and **Figure S4.2B**); however, there was no crotonylation band present when

p300 is incubated with C646 (sample 7, 8 & 4). There are clear bands indicating the auto crotonylation of p300 and the crotonylation of HAT1 (sample 1-4 and 10). In the absence of C646, there is crotonylation of histone H4 observed which is owed to p300 activity (sample 2). When C646 is present there is no crotonylation of histone H4 detected suggesting that crotonylated HAT1 lost its crotonylation abilities (sample 3).

4.9 Conclusion

As more light is being shed on crotonylation and the gaps in knowledge are filled, a better picture of its biological relevance is revealed. Using mass spectrometry, several research reports have shown that HAT1 is crotonylated.[78-80] These data inspired us to further investigate which enzyme is responsible for crotonylating HAT1 and the role HAT1 plays in crotonylation. Our biochemical results showed that HAT1 displayed crotonylation activity and when tested under the same conditions as the known crotonyltransferase, p300, HAT1 had higher crotonylation activity than p300 towards H4-20 peptide (**Figure 4.3**). HAT1 crotonyltransferase activity was further verified using mass spectrometry and cellular studies (**Table 4.1 and Figure 4.5**). While some of the other HAT enzymes did display crotonylation activity towards histone H4, p300 was the only one tested that was able to crotonylate histone H4 and HAT1 (**Figure 4.2**). Furthermore, when crotonylated HAT1 activity was tested, there was no acetylation or crotonylation activity detected (**Figure 4.6**).

Previous studies by Kaczmerska et al. compared the activity of p300 with various acyl-CoA including crotonyl-CoA.[131] The authors showed that p300 had a 62-fold decrease in crotonylation activity in comparison to acetylation. The authors correlated this decrease in p300 activity to the longer chain length of the acyl-CoA which is buried in the lysine substrate-binding tunnel, and they also hypothesized that there needs to be a ~180° rotation of the

carbonyl carbon of the acetyl moiety before the nucleophilic attack can occur. In addition, the crotonyl moiety has a more elongated planar conformation due to its rigid unsaturated Cα-Cβ bond.[131] Perhaps this is the reason why we observed low crotonylation activity in comparison to acetylation activity of HAT1.

Discover Studio software was used to dock crotonyl CoA into the HAT1 binding site, and its orientation was compared to that of acetyl-CoA (PDB: 2P0W). Next, the docked structure was overlapped with the reported HAT1 structure containing AcCoA in the cofactor pocket. In general, crotonyl CoA is secured by most of the same residues in the active site that was reported to anchor AcCoA.[149] Our focus was more on analyzing the binding of the crotonyl moiety in the pocket. Analysis of the docked structure shows that the crotonyl moiety is secured through van der Waals interactions by residues Y282, F185, E276, and A275 (**Figure S4.3**).

As mentioned previously, the crotonyl moiety is bigger and more rigid than AcCoA; therefore, it may be more difficult for this moiety to get properly localized and positioned in the binding pocket. The docking model not only shows the more extended crotonyl group having to insert 2.511 Å further into the HAT1 active site, but the carbonyl carbon of the crotonyl moiety is pushed further away from the ε-amino group of the lysine residue perhaps making it more difficult for the transfer to occur (**Figure 4.7A and 4.7B**). Measurements from the ε-amino group of the lysine residue to the carbonyl moiety of AcCoA and crotonyl CoA is 4.31 Å and 5.68 Å respectively (**Figure 4.7B**). Additionally, acetyl-CoA does not insert in a straight linear manner, due to the kink in the cofactor binding pocket of HAT1.[34] This kink may hinder the ridged crotonyl moiety from inserting and snaking its way to the acyl transfer site (**Figure 4.7C**).

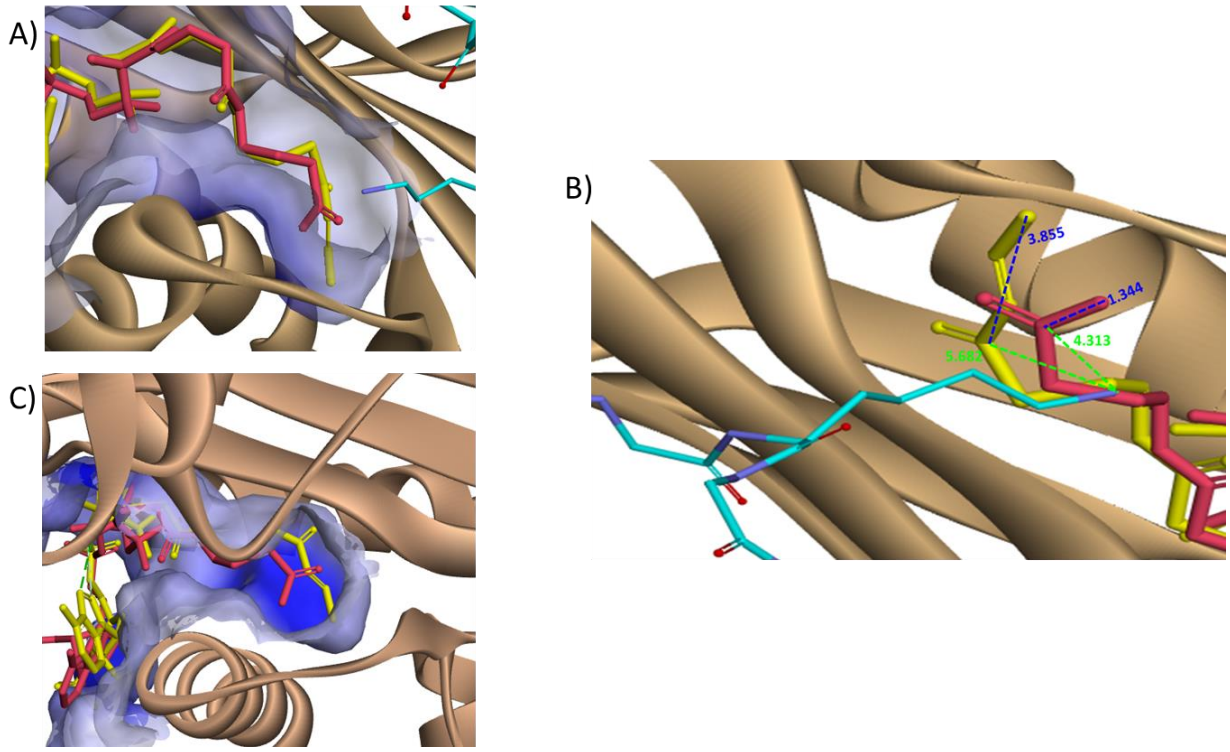

Figure 4.7: Crotonyl-CoA docked into the active site of HAT1 (PDB: 2P0W). Crotonyl-CoA (yellow) was docked into the active site of HAT1 then, the docked structure was overlaid with the original crystal structure containing HAT1 bound to acetyl-CoA (pink) and H4-20 peptide (cyan). A) Docking was done using Discover Studio software which shows that crotonyl-CoA has to reach further in the binding pocket. B) Measurements of the crotonyl and acetyl moieties are shown in blue. Distances from the carbonyl group of crotonyl-CoA (5.68 Å) and acetyl-CoA (4.31 Å) to ε-amino group of lysine residue are depicted in green. C) Kink in HAT1.

It is interesting that HAT1 and crotonylation have been suggested in overlapping studies, yet a direct link has not been made between the two, and this study aims at providing that link. HAT1 has been shown to be overexpressed at the mRNA level as well as the protein level in colorectal cancer.[108] Seiden-Long et al. studied the transcriptional changes that occurred

due to Ki-*ras* oncogene and hepatocyte growth factor (HGF)/Met signaling in colon cancer. Among the transcripts identified in the microarray was HAT1, and the in vitro and in vivo expression profiling showed significant HAT1 gene expression changes. When comparing the distribution of HAT1, array immunohistochemistry showed HAT1 in normal tissues to be more localized in the nucleus at the crypt base; however, in primary and metastatic tumors there was a drastic increase in cytoplasmic HAT1.[39] Just recently, Fellows and coworkers correlated histone crotonylation in the colon to short chain fatty acids derived from the gut microbiota.[142] This study tested several tissues for lysine crotonylation activity and of the tissues tested; the brain and the colon had the highest levels. In the immunofluorescence microscopy of the colon, the proliferative crypt base section was highlighted to be an area of intense crotonylation activity. The same area that was depicted in the HAT1 colon cancer study was shown by Fellows et al. to have crotonylation activity. Based on these studies and our findings, it may be possible that the crotonylation activity found in the colon crypt base is due to HAT1. Future study will be warranted to investigate these possibilities.

CHAPTER 5

BIORTHOGONAL PROBE TO IDENTIFY NOVEL SUBSTRATES OF HAT1

5.1 Introduction

Post-translational modifications (PTMs) conducted by the evolutionarily conserve histone acetyltransferases (HATs) is a widely studied phenomenon that has significant impacts on protein-protein interactions,[126] protein localization,[3] as well as its function in eukaryotic organisms,[3] and the deregulation of these modifications have been linked to various diseases.[42] HATs are categorized into three main families which include GNAT, MYST, and CBP/p300.[17] The canonical function of HATs is to transfer the acetyl moiety from acetyl CoA to the ε- amino group on specific lysines on histones and non-histone proteins and the removal of the acyl moiety from lysine residues is carried out by histone deacetylases (HDACs).

HAT1, a member of the GNAT superfamily, was one of the first HATs identified; however, little is known about its functionality in comparison to other HATs. This HAT enzyme localized in both the cytoplasm and nucleus is evolutionarily conserved from yeast to humans.[23] Some of the biological roles of HAT1 include DNA damage repair and chromatin assembly.[30, 144] The most well-known role of HAT1 in the cytoplasm is to acetylate newly synthesized histone H4 at lysine 5 and 12.[23] HAT1 has also been shown to acetylate histone H2A at lysine 5,[27] and maintain the acetylation marks on histone H3 at lysine 9, 18, and 27 during replication-coupled chromatin assembly.[25] Other than histone substrates there are two non-histone proteins, the promyelocytic leukemia zinc finger protein (PLZF)[38] and MVH (mouse Vasa homologue),[145] that have been reported to be acetylated by HAT1.

Deletion of the HAT1 gene in yeast, *S. cerevisiae*, or chicken DT40 cells did not show a change in acetylated lysine of histone H4 and resulted in no change in cell proliferation or viability.[26] On the other hand, HAT1 deletion in mammals, specifically in mice, causes neonatal lethality due to lung developmental issues.[25] That same study also showed that HAT1 deletion in embryonic fibroblast resulted in growth defect, increase sensitivity to DNA damage and genome instability. In addition, several studies have shown that HAT1 is upregulated and is correlated to several diseases such as cardiovascular diseases, colorectal cancer, liver cancer and lung cancer.[26, 35] These results suggest that HAT1 plays a major yet not fully understood role in mammalian biological systems.

To have a better understanding of the roles that HAT1 plays in cells and to reveal its novel substrates we will utilize a bioorthogonal probe approach. Previously our lab has developed bioorthogonal AcCoA analog probes containing reactive alkyne or azide moieties and engineered HATs to have an enlarged active site which were capable of transferring larger acyl groups to its substrates.[150] Next, this proof of concept was tested with p300 as well as GCN5, and by using the copper-catalyzed reactive moieties transferred to the substrates pull down was then proteomics was conducted. Of the more than four hundred substrates identified, two substrates, IQGAP1 and SMC1, were further confirmed as novel substrates of GCN5.[151]

The goal of this project is to rationally design and demonstrate that the bioorthogonal probe approach can be used to label substrates of HAT1. First, various mutations were made to augment the cofactor binding site. The various AcCoA analog probes were screened against the HAT1 mutants to reveal which one had specificity towards the probes containing the warheads and not for AcCoA. HAT1Y282A had the greatest specificity and favorable kinetic results toward the acyl CoA analog, 3-AZ, 4-AZ, and 6-HY. As a proof of concept, we were able to

confirm that HAT1 Y282A was able to transfer the warhead from 3-AZ to known H4-20 peptide substrates. Next, by overexpressing HAT1Y282A in mammalian cell successfully labeling of substrates was obtained.

5.2 Materials and methods

5.2.1 Synthesis of peptide and CoA analogs

The first 20 amino acids the N-terminal of histone H4(Ac-SGRGKGGKGLGKGGAKRHRK) (H4-20) were synthesized on a peptide synthesizer using the Fmoc [N-(9-fluorenyl) methoxycarbonyl**]** -based solid-phase peptide synthesis protocols. The amino acids and Fmoc-Lysine(Boc) preloaded Wang resin was weighed out with an equivalence ratio four times greater than the amount of HCTU [O-(1H-6-Chlorobenzotriazole-1-yl)-1,1,3,3-tetramethyluronium hexafluorophosphate] coupling reagent. The peptides were purified using a C-18 reverse phase column on a HPLC (High-performance liquid chromatography) instrument, and each sample was sent off for mass spectrometry. Lastly, NaOH was used to neutralize the pH.

5.2.2 Obtaining HAT1 wt and HAT1 mutants

HAT1 mutants were produced using the QuikChange procedure (Stratagene). DNA sequencing confirmed all mutations. The expression and purification of HAT 1 (20-341) was done following the method described Hong Wu et al..[34] Briefly this protein was expressed using *Escherichia coli* and purified using NTA-ni resin. The transformation was done using BL21 (DE3)/ RIL competent cells through heat-shock and then spread on plates containing antibiotics, kanamycin and chloramphenicol. Protein expression was induced by the addition of isopropyl β-D-1-thiogalactopyranoside (IPTG) and shaken for 16 hours at 16 °C. The cells were collected and suspended in lysis buffer (50 mM Na-phosphate (pH 7.4), 250 mM NaCl, 5 mM imidazole,

5% glycerol, 2mM β-mercaptoethanol, and 1 mM phenylmethanesulfonyl fluoride (PMSF)) then disrupted using the cell disruptor. The supernatant was passed through a column containing NTA-ni resin equilibrated with column washing buffer (20 mM Hepes pH8, 250 mM NaCl, 5% glycerol, 30 mM imidazole,1 mM PMSF) and the resin was washed with column washing buffer. Next, the resin was washed with buffer containing a higher concentration of imidazole (20 mM Hepes pH8, 250 mM NaCl, 5% glycerol, 50 mM imidazole, 1mM PMSF). The HAT 1 was eluted with elution buffer (20 mM Hepes pH8, 250 mM NaCl, 5% glycerol, 500 mM imidazole, 1 mM PMSF).

5.2.3 Acylation fluorescence assay

The acylation activity of HAT1 and HAT1 mutants was analyzed using the CPM assay. To screen the various HAT1 mutants against the CoA analogs, reactions contained 0.04 µM enzyme, H4(1-20) peptide (40 µM), and Acyl-CoA (20 µM). Samples were incubated for 1hr at 30°C. Evaluation of HAT1 Y282A kinetics was also done using the CPM assay with reactions carried out at 30°C for 15min and sample conditions were as follows: 0.04 µM enzyme, H4(1-20) peptide (200 µM), and Acyl-CoA (0-200 µM). All reactions were quenched by the addition of CPM dissolved in DMSO then incubated in total darkness for 20 min at room temperature. Fluorescence was measured at an excitation and emission wavelength of 392 nm and 482 nm respectively.

5.2.4 Labeling substrates in vitro

Cells were grown to 90% confluency before transient transfection with HAT1Y282A plasmid was performed. Transient transfection was done according to the Lipofectamine 3000 manufactures protocol. Next, 20 mM of 3-AZ sodium salt (Na 3-AZ) or 4-AZ sodium salt (Na

4-AZ) was added to the cells. After 12 hrs the cells were collected and lysed using M-PER Mammalian Protein Extraction Reagent (ThermoFisher, cat: 78501) containing a protease cocktail. Copper click cocktail (40 uM Ak-BTN, 5 mM sodium ascorbate, 0.5 mM BTTAA (2-[4-((bis[(1-tert-butyl-1H-1,2,3-triazol-4-yl)methyl]amino)methyl)-1H-1,2,3-triazol-1-yl]acetic acid), 0.5 mM copper sulfate and DMSO)was added to the cell lysate and reacted for 1 hr at room temperature. Loading dye was added to the sample and sample was boiled before running the sample on a gradient SDS gel. The proteins were transferred to a membrane, and labeled substrates were probed using Streptavidin-Horseradish Peroxidase (HRP) Conjugate (cat: 21130)

5.3 Screening CoA Analogs with HAT1 Mutants

Bulky residues in the HAT1 CoA binding pocket were mutated to smaller residues to allow for CoA analogs containing larger acyl moieties to bind and be transferred to substrates. Residues: Met222, Val238, Met241, Ala275, Phe278, Ser279, and Tyr282 were mutated to smaller residues such as Ala or Gly (**Figure 5.1A**). HAT1 mutants were obtained through QuikChange site directed mutagenesis and the plasmids were sequenced before transformation. To screen all the enzymes against various CoA analogs (**Figure 5.1B**), the CPM assay was utilized with reactions containing 40 nM of enzyme, 40 µM of H4-20 peptide, and 20 µM of various acyl CoA analogs incubated at 30°C for 1hr. All activity readings were normalized to the CPM reading obtained from the reaction containing HAT1wt with Ac-CoA. As expected, HAT1 wt had the highest activity with Ac-CoA, 8% activity with 3-AZCoA and less than 5% activity for all the other cofactors. According to the crystal structure, residues Ile186, Pro278 and Tyr282 aid in stabilizing the acyl moiety of AcCoA in the cofactor binding pocket of HAT1.[34] When Pro278 was mutated to Gly there was only10% activity for AcCoA and none for

the other cofactors. However, when replaced with an Ala the activity for AcCoA increased to 40% and there was 10% activity for 3-AZ CoA. This suggests that a residue with a side chain is needed at this position to aid in the stabilization of the cofactor. The same phenomenon observed with the HAT1P278 mutant was seen with the HAT1Y282. Again, methyl side chain of Ala in HAT1Y282A was observed to increase the acyltransferase activity greatly in comparison to the HAT1Y282G mutant. HAT1 Y282G had 1% activity with Ac-CoA, less than 17% activity with 4-PY, 5-HY, as well as 3-AZ, about 20% activity with 4-AZ, and the highest activity at 50% with 6-HY CoA. HAT1Y282A had about 6% activity with Ac-CoA, 3% activity with biotin CoA, and 61% activity with 4-Py. Activity greater than 80% was observed with most of the CoA variants, such as 5-HY, 6-HY, 3-AZ, and 4-AZ **(Figure 5.1C**). The activity of HAT1Y282A towards the CoA analogs was further verified by mass spectrometry (**Figure S5.1**). Due to the drastic difference of HAT1Y282A activity with Ac-CoA versus the CoA analogs, this mutant was chosen to be further tested in substrate labeling tests.

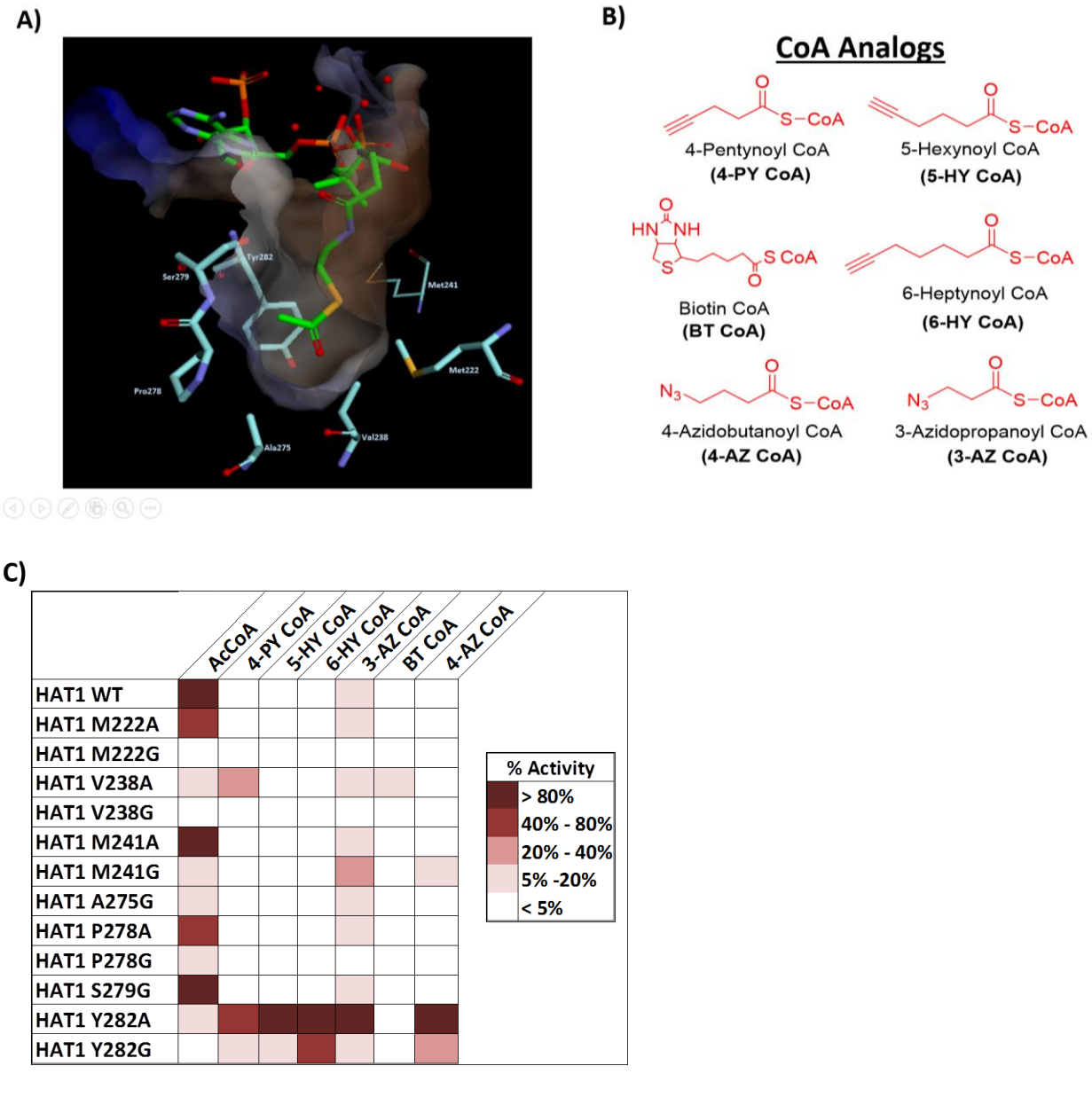

Figure 5.1: Screening CoA Analogs with HAT1 Mutants. A) Bulky residues surrounding HAT1 cofactor binding site that was mutated to smaller residues (PDB: 2P0W). B) Structure of CoA analogs. C) Heat map of the activity of various HAT1 screened against CoA analogs using the CPM single point assay. Reactions conditions included 40 nM of enzyme, 40 µM H4-20 peptide, and 20 µM of various acyl CoA with an incubation time of 1hr at 30°C.

5.4 Kinetics of HAT1 Y282A with CoA Analogs

To compare HAT1Y282A acylation activity against the various CoA analogs, kinetic analysis was carried out using the CPM assay. Reaction conditions for this assay included 40 nM of HAT1Y282A, 0.2 mM H4-20 peptide, and 0-0.2 mM of varying acyl CoA. K_m values were the lowest for 3-AZ CoA (10.3 µM) and 5-HY CoA (11.7 µM). 4-PY CoA had the highest km value at 85.9 µM. The activity of HAT1 Y282A towards AcCoA is very low and the kinetic parameters could not be accurately obtained. 6-HY CoA and 4-PY CoA had the highest turnover rate at 33.2 min^{-1} and 25.4 min^{-1}. However, the catalytic efficiency of 6-HY CoA (1.4 min^{-1}•μM^{-1}) was the highest with 3-AZ CoA (1.08 min^{-1}•$\mu M^{-}1$) coming in next (**Table 5.1; Figure 5.2**).

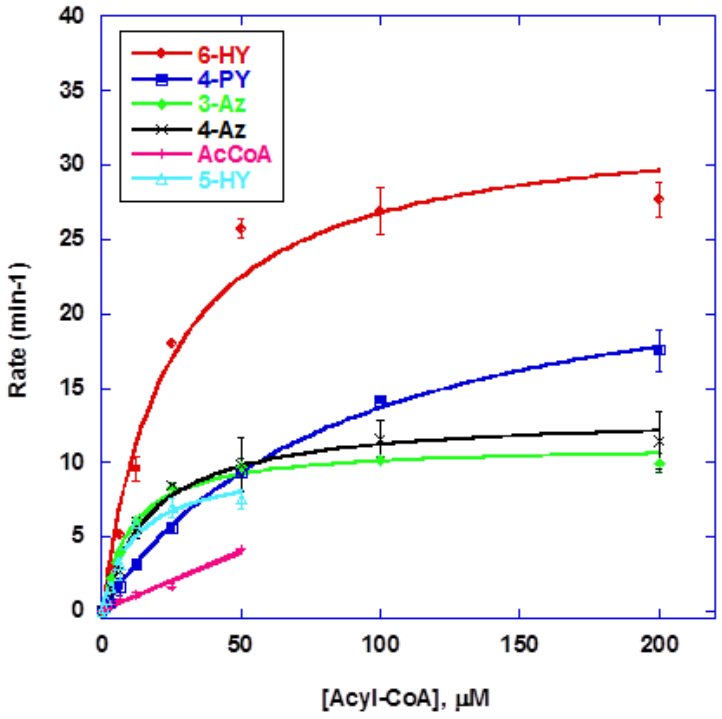

Figure 5.2: Kinetics of HAT1 Y282A with CoA Analogs. Graphical representation of HAT1Y282A activity fitted to the Michaelis–Menten equation. To determine the kinetics of

HAT1Y282A against various CoA analogs, reactions containing 40 nM of HAT1Y282A, 200 µM H4-20 peptide, and 0–200 µM of various acyl CoA were incubated for 15 min at 30°C.

Table 5.1: Kinetics analysis of HAT1Y282A activity against various CoA analogs.

Cofactor	kcat (min^{-1})	Km (µM)	kcat/Km (min^{-1}*µM^{-1})
3-AZ CoA	**11.1 ± 0.3**	**10.3 ± 1.2**	**1.08**
6-HY CoA	**33.2 ± 2.3**	**23.7 ± 5.2**	**1.40**
5-HY CoA	**9.8 ± 0.8**	**11.7 ± 2.6**	**0.84**
4-AZ CoA	**13.15 ± 0.6**	**17.4 ± 2.6**	**0.76**
4-PY CoA	**25.4 ± 0.8**	**85.9 ± 5.9**	**0.30**
AcCoA	**NA**	**> 200**	**0.08^**

Kinetics in the presence of varying concentrations of CoA analogs was obtained by fitting data points to the Michaelis-Menten equation. ^This kcat/Km value was determined by its slope.

5.5 HAT1Y282A Labeling vs. Spontaneous Labeling

The thiol moiety of acyl-CoA has an intrinsic reactive nature and has been reported to spontaneously transfer the acyl moiety.[152-153] We wanted to determine how much of the acyl labeling was spontaneous versus being promoted by the enzyme. Due to the favorable kinetics results of 6-HY CoA, 3-AZ CoA, and 4-AZ CoA towards HAT1Y282A, the spontaneous vs. enzymatic transfer of these CoA analogs was tested. With enzyme, 3-AZ and 4-AZ had the highest observed labeling of histone H4 while 6-HY had the lowest (**Figure 5.3**, sample 1-3). Without HAT1Y282A, the labeling of histone H4 did occur for all three CoA analogs. The

labeling intensity of 6-HY and 4-AZ CoA with and without enzyme were very similar (**Figure 5.3**, sample 4 and 6). However, for 3-AZ-CoA the labeling intensity was greater with HAT1Y282A in comparison to the spontaneous labeling; therefore, this CoA analog will be further tested (**Figure 5.3**, sample 5). Spontaneous labeling from reagents used in the click chemistry was also tested. Slight labeling of histone H4 was observed with alkyne-tetramethylrhodamine (sample 7) but not with alkyne-tetramethylrhodamine (sample 8) (**Figure 5.3**).

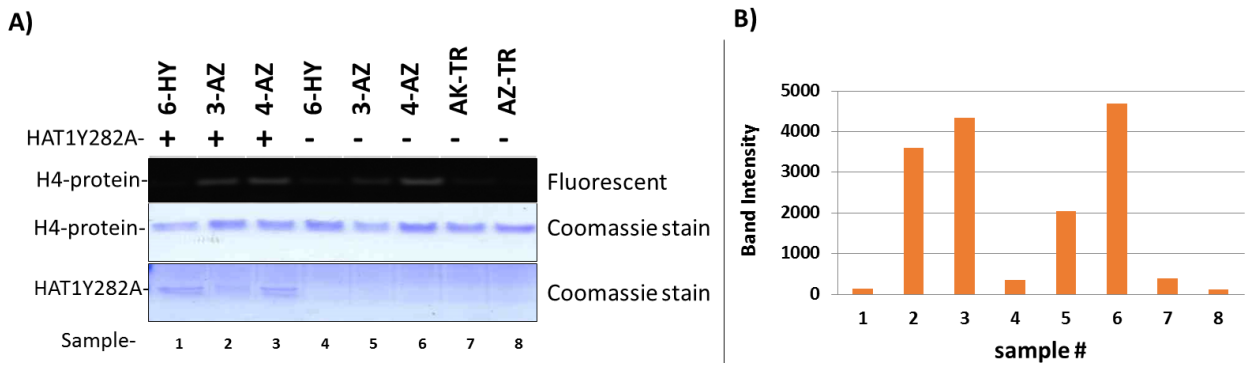

Figure 5.3: HAT1Y282A Labeling vs. Spontaneous Labeling. A) All reactions were carried out at 30°C for 1hr before click cocktail was added. Reactions in samples 1-3 contained 2 µM HAT1Y282A with 1.5 µg histone H4 and 20 µM of 6-HY, 3-AZ CoA, and 4-AZ CoA respectively. Samples in lane 4-6 contained the same components except HAT1Y282A was not added. Sample 7 contained histone H4 and alkyne-tetramethylrhodamine while sample 8 contained histone H4 and azide-tetramethylrhodamine. B) Quantification of the fluorescent histone H4 bands.

5.6 HAT1Y282A Labeling H4-peptides

The CoA analog, 3-AZ-CoA, was used to verify HAT1Y282A labeling of various H4-peptides. Reactions containing 20 µM 3-AZ CoA, with or without 0.2 µM HAT1Y282A, and 40

μM of various H4- peptide was incubated at 30°C for 1hr before click cocktail was added. As mentioned previously, HAT1 acetylates histone H4 at K5 and K12. Expectedly in **Figure 5.4**, labeling was detected with samples containing enzyme and H4 (1-20) (sample 1) or H4(1-22) (sample 2) peptide and not with the sample containing enzyme and H4(15-38) (sample 3) peptide. In the gel as well as the graph of the band intensity, there was minor spontaneous labeling in the samples with no enzyme (**Figure 5.4 A and B**, sample 4-6).

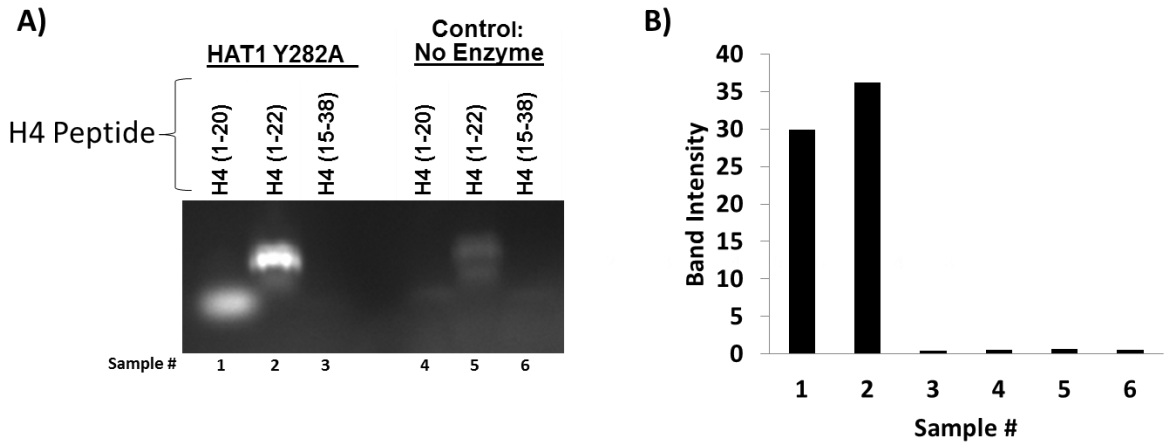

Figure 5.4: Labeling various H4-peptides using HAT1Y282A. A) Reactions containing 20 μM 3-AZ CoA, with or without 0.2 μM HAT1Y282A, and 40 μM H4- peptide was incubated at 30°C for 1hr before click cocktail was added and gel was de-stained overnight. Gel was imaged at excitation of 532nm and emission of 580nm. B) Quantification of the fluorescent histone H4 peptide bands.

5.7 Labeling substrates in cells

Next, we wanted to show that this bioorthogonal probe system could work in cells. HEK293T cells were transiently transfected with HAT1Y282A plasmid following the Lipofectamine 3000 manufactures protocol and were fed with 20mM Na 3-AZ or Na 4-AZ.

After 12 hrs of incubation, the cells were collected, lysed, reacted with a copper click cocktail containing alkyne biotin and labeled substrates were probed by western blot using Streptavidin-Horseradish Peroxidase (HRP) Conjugate. The controls show that there was little labeling for samples that did not have an overexpression of HAT1Y282A or was not fed with the probe (**Figure 5.5**, sample 1 and 4-6). Sample 3 had the overexpression of HAT1Y282A and was fed with Na 4-AZ. This sample did have slightly more substrates labeled than the control (**Figure 5.5**, sample 6); however, a greater number of substrates was labeled when the samples were fed with Na 3-AZ (**Figure 5.5**, sample 2).

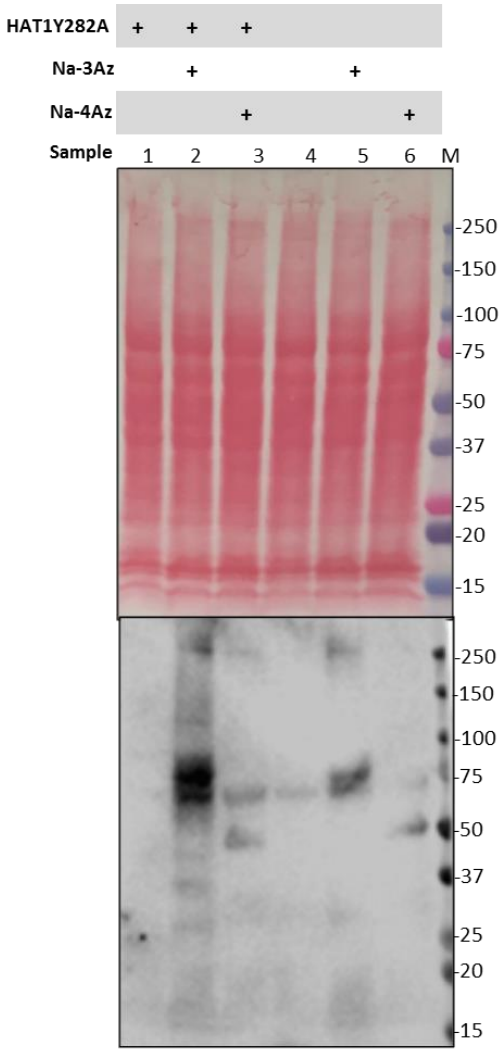

Figure 5.5: Labeling substrates in cells using HAT1Y282A. HAT1Y282A was transiently transfected in HEK293T cells following the Lipofectamine 3000 manufactures protocol. Cells were fed with 20 mM of 20mM Na-3AZ or Na-4AZ then incubated for 12 hrs. Cell lysate was reacted with a copper click cocktail containing alkyne biotin and probed by western blot using Streptavidin-Horseradish Peroxidase (HRP) Conjugate.

5.8 Conclusion

The histone code is comprised of three important components writers, readers, and erasers. Of the writers, lysine acetylation plays one of the most prominent roles in protein

modification because this modification can determine normal or disease development.[154-155] HAT1 is the first histone acetyltransferase identified and is conserved yeast to mammalians; however, it is poorly studied in comparison to other HATs.[23] Although deletion of the HAT1 gene in yeast, *S. cerevisiae*, or chicken DT40 cells did not show a change in acetylated lysine of histone H4 and resulted in no change in cell proliferation or viability; deletion in mammals did cause notable developmental issues.[26] More specifically, the deletion in mammals was done in mice and it was observed that it caused neonatal lethality due to lung developmental issues.[25] That same study also showed that HAT1 deletion in embryonic fibroblast resulted in growth defect, increase sensitivity to DNA damage and genome instability. These results suggest that HAT1 plays a major yet not fully understood role in mammalian biological systems.

Some of the biological roles of HAT1 include DNA damage repair and chromatin assembly.[30, 144] The most well-known role of HAT1 in the cytoplasm is to acetylate newly synthesized histone H4 at lysine 5 and 12.[23] HAT1 has also been shown to acetylate histone H2A at lysine 5,[27] maintain the acetylation marks on histone H3 at lysine 9, 18, and 27 during replication-coupled chromatin assembly,[25] as well as acetylate non-histone proteins such the promyelocytic leukemia zinc finger protein (PLZF)[38] and MVH.[145] Dysregulated HAT1 activity has also been correlated to several diseases such as cardiovascular diseases, colorectal cancer, liver cancer and lung cancer.[26, 35] Due to the diseases that have been correlated to HAT1 activity and the gap in knowledge we have about its substrates, we think that it is important to further investigate and reveal unknown substrates of this enzyme.

To tackle this challenge and reveal novel substrates of HAT1, we utilized and implemented the bioorthogonal probe approach that was previously developed in our lab.[150] This bioorthogonal probe approach exploits AcCoA analog probes containing reactive alkyne or

azide moieties and engineered HATs that have augmented active site and is capable of transferring larger acyl groups to its substrates.[150] Of the engineered HAT1 enzymes, HAT1Y282A had the highest activity with the modified CoA analogs and very little activity with AcCoA, thus it will recognize and label substrates with the cofactor containing the reactive warhead. 3-AZ was tested to have the most desirable labeling with HAT1Y282A. The kinetics of 3-AZ was favorable and there was less spontaneous labeling observed. In addition, when labeling substrates in cells 3-AZ was able to label more substrates with low background levels. The evidence provided here demonstrates that perhaps HAT1 plays a more prominent role in cells and that it has many unknown substrates that should be further investigated.

CHAPTER 6

SUMMARY AND FUTURE DIRECTIONS

Summary and future directions

HATs have become a sought-after target due to its link to many diseases including cancer and inflammatory disease to cardiovascular disease.[58, 156] Many inhibitors ranging from small molecules to natural product derivatives and bi-substrate inhibitors have been identified for HATs; however, due to the unfavorable properties such as poor cell permeability, metabolic instability, low potency, little selectivity, or being Pan Assay INterference compoundS (PAINS) they could not further advance to therapeutic agents.[77] These issues have not only hindered our efforts towards a therapeutic discovery targeting HATs, but some of the PAINS compounds which have not undergone a counter screen have cast doubts in the published HAT inhibitors. Therefore, the challenge in the HAT field is to identify other inhibitors that do not possess PAINS moieties and have better pharmacokinetic properties. The challenges not only lie there but also in the disadvantages of the existing assays used to detect HAT activity.

As mentioned previously, many disadvantages lie in the current assays used in high throughput screenings to detect HAT activity. The reported methods to detect HAT activity fall into two major categories: radiometric and fluorescence. Some of the radiometric assays include the gold standard filter binding assay, and the flash plate assay. The major disadvantages of the filter binding assay are that it is very time consuming and it generates large amounts of radioactive waste. For the flash plate assay, it was shown that the histones have the intrinsic

ability to bind to the surface of the wells, thus causing the homogeneity of the mixture to be questioned.

High throughput fluorescence assays developed include the CPM and the cell-based ELISA assay. The CPM assay has been reported to react with reducing agents such as DTT in reaction mixtures and to compounds that have free thiols.[51] These non-specific reactions result in false positive leads which can be costly and time-consuming. In the cell-based ELISA assay, whole cells instead of recombinant enzymes are used which makes the identification of the target more challenging. Also, since this assay utilizes antibodies there can be nonspecific binding as well as variability from batch to batch.

Due to those challenges that exist in the reported assays used to detect HAT activity, we have developed the scintillation proximity assay (SPA) that serves as a solution to all of those issues. During the development of this assay, it was noticed that electrostatic interaction exist between the histone peptide and AcCoA; therefore, to provide unbiased results for HAT activity measurement using the SPA, several chemical agents were studied to determine the best quencher (**Figure 2.3**). The ideal quencher had to disrupt the substrate-cofactor electrostatic interaction, stop the reaction, and not interfere with the biotin and streptavidin interaction. Of the reagents tested, guanidine HCl and $NaHCO_3$ were determined to be the most suitable quencher that satisfied all the requirements. The development of the SPA provides a simple mix and measure assay which can be implemented in a 96-well format as well as offers high sensitivity, efficiency and is qualified to be used in a HTS fashion.

In addition to assay development, this project also had a specific focus on HAT1. HAT1 was targeted because among the HATs it is considered to be poorly studied, and has been linked to various detrimental diseases such as cardiovascular disease, immunological disease, and

many cancers. To fill in the knowledge gaps and to aid in the discovery of inhibitors targeting HAT1, the SPA was used to identify the first potent inhibitors of HAT1. This inhibitor provided insight into the catalytic mechanism of this enzyme. Next, we wanted to explore novel cofactors and substrates for HAT1. In our search, not only did we reveal that p300 was the enzyme responsible for crotonylating HAT1, but HAT1 was also discovered to have crotonylation activity towards histone H4. The crotonylation of HAT1 exposed that this modification disabled the acetylation and crotonylation activity of this enzyme. Lastly, the biorthogonal approach was rationally taken and designed to identify novel substrates of HAT1. As a proof of concept, we were able to show that the biorthogonal approach was effective in labeling substrates of HAT1.

In conclusion, this project not only allowed for the development of SPA, an improved assay to detect HAT activity, but the use of this assay was identify new HAT inhibitors and shed more light on the catalytic mechanism of HAT1. In addition, this work also revealed a novel crotonylation activity on and by HAT1 and that a biorthogonal proof of concept of the approach could be utilized to label substrates of HAT1. With our improved comprehension of HAT1 and its functions, the following future studies shall be conducted to strengthen the foundation of this enzyme further:

(1) Extracting the information obtained from the identified potent bisubstrate inhibitors to discover improved inhibitors targeting HAT1.

Not a lot is known about the catalytic mechanism of HAT1, and from the solved crystal structure some speculations have been made, but confirmation has not been entirely made.[24, 149] In this instance, inhibitors can be a handy molecular tool because they can be used as probes to dissect the catalytic mechanism of an enzyme further. The development and use of the SPA allowed us to identify the very potent bisubstrate inhibitor, H4K12CoA. This discovery was not

only the first reported inhibitor which specifically targeted HAT1, but also exposed information about the catalytic mechanism of the enzyme. Interesting kinetic analysis of this enzyme and inhibitor with respect to cofactor as well as substrate showed that it was competitive towards both (**Figure 3.2 and Table 3.3**). These results suggested that unlike most other HAT members, HAT1 does not have a preferred binding order for AcCoA and H4 peptide, thus likely follows a random sequential kinetic mechanism. From testing the different inhibitors in this study, it was also shown that the placement of CoA, as well as the length of the peptide, effected on the potency of the inhibitor. A limitation of H4K12CoA is the charged CoA moiety that causes cell permeability issues. In the future more, efforts could be made to improve this inhibitor by adding chemical modifications that introduce membrane-penetrating motifs. Furthermore, by using the information obtained in this study structure activity relationship (SAR) studies could be conducted to rationally design and fine-tune new inhibitors with the desired pharmacokinetic properties. The work from this study provided some insights on the catalytic mechanism of HAT1; however, further investigation perhaps by solving a crystal structure of HAT1 and the bisubstrate inhibitor, or mutational studies on HAT1 could be carried out to obtain a full understanding of this mechanism.

In all, this work presented the first bisubstrate inhibitor, H4K12CoA, which is both potent and selective towards HAT1. The identification of H4K12CoA provides a foundation and guidance for the discovery of other inhibitors targeting. Although this compound may have cell permeability issue, it has not reported as a PAINS, therefore, can still serve as a probe. As a probe, this inhibitor can allow us to understand the catalytic mechanism and interactions of various residues better, thus aiding in the rational design of an inhibitor with improved

properties. Besides, modifications to this compound can be carried out to address the permeability challenge.

(2) Determining if HAT1 is involved in any other acyl activity may aid in the discovery of inhibitors targeting HAT1.

Proteomic studies looking at protein crotonylation in mammalian cells by several other groups showed that HAT1 was among the identified substrates that were crotonylated.[78-80] These studies captivated our interest to investigate what enzyme is responsible for modifying HAT1 with the crotonyl moiety. To our surprise, not only were we able to identify p300 as the HAT enzyme responsible for crotonylating HAT1 but also discovered the novel crotonylation activity of HAT1 towards the substrate, histone H4 **(Figure 4.2).** In addition, this study was able to show that when HAT1 is crotonylated, it loses its acetylation and crotonylation abilities **(Figure 4.6).**

HAT1 and crotonylation have been suggested in overlapping studies such as when looking at the colon. In one study, HAT1 was shown to be overexpressed at the mRNA level as well as the protein level in colorectal cancer.[108] Then when comparing the distribution of HAT1, array immunohistochemistry showed HAT1 in normal tissues to be more localized in the nucleus at the crypt base; however, in primary and metastatic tumors there was a drastic increase in cytoplasmic HAT1.[39] Just recently, Fellows and coworkers tested several types of tissues and was able to correlated histone crotonylation in the colon to short chain fatty acids derived from the gut microbiota.[142] It is interesting to note that in the immunofluorescence microscopy of the colon, the proliferative crypt base section was highlighted to be an area of intense crotonylation activity. This was the same area depicted in the HAT1 colon cancer study

that was shown by Fellows et al. to have crotonylation activity. Our study was able to provide a link between HAT1 and crotonylation; however, further studies should be conducted to confirm if HAT1 plays a role in modifying proteins in the proliferative crypt base section of the colon with the crotonyl moiety.

When looking into the acylation activity of HAT1. We also tested the activity of HAT1 with propionyl CoA and butyryl CoA which showed that it also had activity with these cofactors (**Figure 4.5**). The identification of HAT1 crotonylation is the first report of HAT1 displaying activity other than acetylation. In the future, the activity of HAT1 with these various acyl CoAs should be further explored. Also, since p300 has been reported to have propionylation and butyrylation activity, it would be interesting to see if p300 could add these modifications onto HAT1.[130]

Currently, it has been reported that the HAT enzymes: p300,[79] MOF,[134] and PCAF[135] have crotonylation activity. Besides HAT1 crotonylation activity, the results from our study also revealed that TIP60 displayed crotonylation activity towards histone H4 which to our knowledge has not been reported (**Figure 4.2**). In the future, we would like to investigate this further to provide a full understanding of the impact TIP60 crotonylation activity has.

Overall, not a lot is known about HAT1 or the newly discovered crotonylation modification; however, this study was able to shed more light on these two topics. This work was able to reveal the novel crotonylation activity of HAT1 and TIP60, demonstrate the effect that the crotonyl modification had on HAT1, and reveal another substrate of p300. These findings have not only expanded our knowledge of HAT1 activity, but also provided possible links to correlate numerous studies which should be further verified.

(3) Identify and confirm the novel substrates of HAT1 obtained using the bioorthogonal probe design.

Our understanding of HAT1 activity is insufficient. To date, reports have shown that HAT1 only has two histone substrates and two non-histone substrates. Rationally identifying or designing an inhibitor for an enzyme requires a great understanding of its substrates because it will offer clues on how the enzyme binds to molecules. To expose other substrates of HAT1, we explored the bioorthogonal approach. In this approach, mutations were introduced to the cofactor binding pocket to augment it, thus allowing slightly larger analogs of acyl CoA containing a reactive warhead to enter and be transferred to substrates. Through copper-catalyzed alkyne-azide cycloaddition click chemistry, the reactive warhead be would conjugated to a fluorophore or biotin allowing for further analysis. This work served as a proof of concept to show that this approach could be implemented on HAT1. After generating various HAT1 mutants and undergoing the screening with the various CoA analogs, it was determined that HAT1Y282A was the most promising mutant. HAT1Y282A was active towards the warhead containing cofactors and had little activity towards Ac-CoA (**Figure 5.1**). Using this mutant, we were able to conduct kinetic studies and show that that labeling of the known histone H4 could be done. Lastly, HAT1Y282A was overexpressed in HEK293T cells, and the labeling of substrates was observed (**Figure 5.5**).

Overall, the evidence in this work demonstrates that perhaps HAT1 plays a more prominent role in cells and that it has many unknown substrates that should be further investigated. This study can be used as a guide to identify novel substrates of HAT1 and fill in the knowledge gap. In the future, using this rationally designed bioorthogonal approach, we

would like to do pulldowns of the substrates labeled by the engineered HAT1. The proteins obtained through the pulldown would then be submitted for proteomics to identify substrates of HAT1. Information from this can be used to aid in fully understanding biological functions of HAT1 in normal physiology and in diseased conditions.

APPENDICES

A Supporting information for Chapter 2

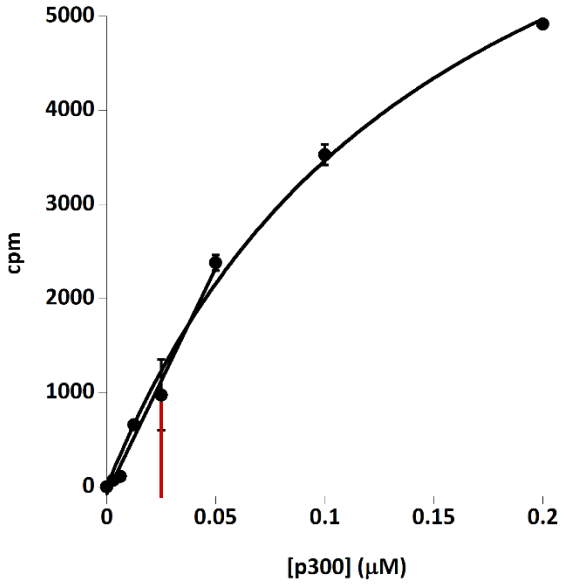

Figure S2.1. Concentration-dependent activity of p300. Experimental conditions include 0-0.05 μM p300, 2.5 μM H3-20 BTN, 1 μM [^{3}H]-AcCoA, reaction time 6 min at 30°C. Red line indicates 0.025 μM of p300

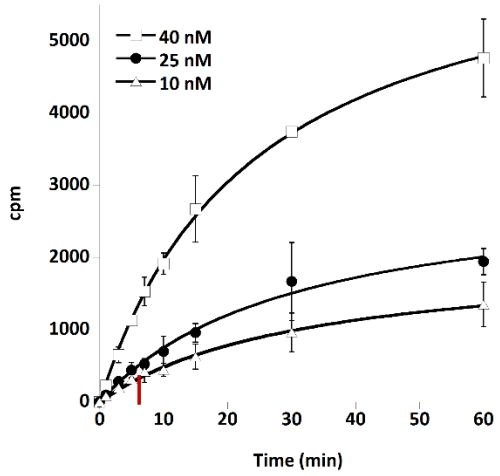

Figure S2.2. The time course of p300 activity. Experimental conditions include 10 nM, 25 nM, or 40 nM p300, 2.5 μM H3-20 BTN, 1 μM [^{3}H]-AcCoA, reaction time 0-15 min at 30°C. Red line indicates 6 min of reaction time.

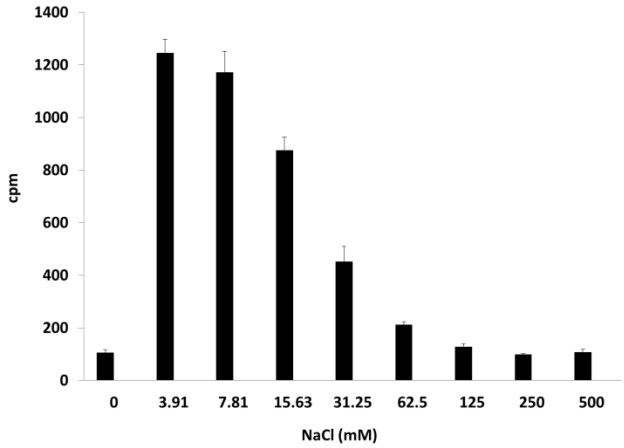

Figure S2.3. Effect of various concentrations of NaCl on the interaction of H3(1-20)-Biotin with ^{3}[H]Ac-CoA. Conditions include: 2.5 μM H3(1-20)-BTN, 1 μM [^{3}H]Ac-CoA with an incubation time of 6 min at 30°C. To quench reaction 30 μL of NaCl at various concentrations was added. Negative control samples were quenched with 0.5 M guanidine HCl.

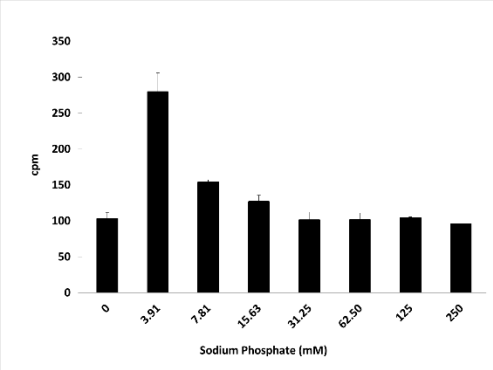

Figure S2.4. Effect of various concentrations of sodium phosphate (pH 8.0) on the interaction of H3(1-20)-Biotin with ^{3}[H]Ac-CoA. Conditions include: 2.5 µM H3(1-20)-BTN, 1 µM [^{3}H]Ac-CoA with an incubation time of 6 min at room temperature. To quench reaction 30 µL of sodium phosphate at various concentrations was added. Negative control samples were quenched with 0.5 M guanidine HCl.

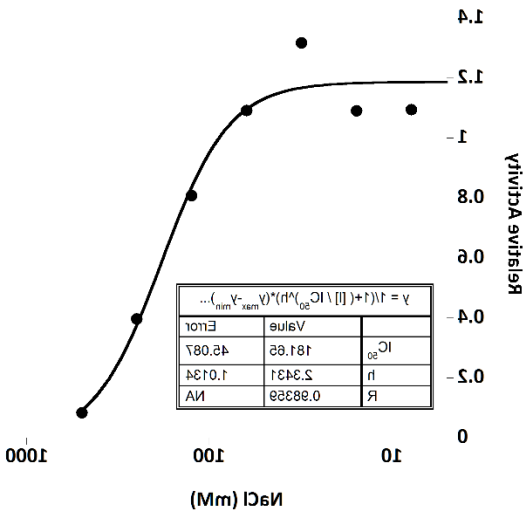

Figure S2.5. Effect of NaCl on p300 activity. Conditions for filter binding assay included 0.025 µM p300, 100 µM H3(1-20), 1 µM [^{14}C]Ac-CoA, 0-500 mM NaCl, and an incubation time of 6 min at 30°C. To quench the reaction, 20 µL of each reaction mixture was spread out on a Whatman filter binding paper. IC_{50} was determined by fitting the data to the equation

$\frac{y-y_{min}}{y_{max}-y_{min}} = \frac{1}{(1+\frac{[I]}{[IC_{50}]})^h}$, Where $\boldsymbol{y_{max}}$, $\boldsymbol{y_{min}}$, *h* and $[\boldsymbol{I}]$ are maximum and minimum SPA signals on the y-axis, hill coefficient, and inhibitor concentration respectively.[95]

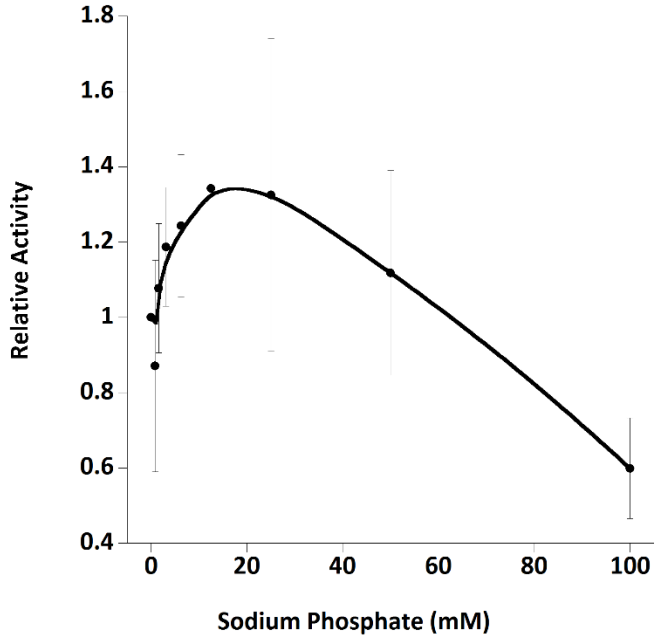

Figure S2.6. p300 activity was partially inhibited by sodium phosphate (pH 8.0). Conditions for filter binding assay included 0.025 µM p300, 100 µM H3(1-20), 1 µM [^{14}C]Ac-CoA, 0-100 mM sodium phosphate, and an incubation time of 6 min at 30°C. To quench the reaction, 20 µL of each reaction mixture was spread out on a Whatman filter binding paper.

B Supporting information for Chapter 3

Figure S3.1: Analytical spectrum of bisubstrate inhibitors. The purity of all peptides was determined via reverse phase chromatography along a gradient of 3-30% acetonitrile over 13 minutes. The samples were analyzed using a UV detector at 214nm, and the intensities of the signals were quantified to calculate the percent composition of the sample. Purity >89% (based on HPLC).

H4K5CoA

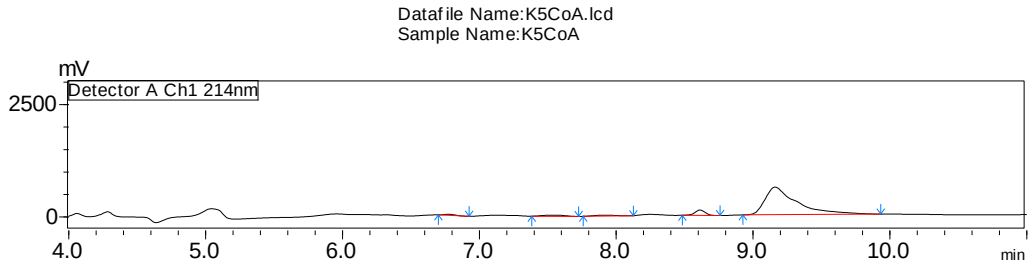

H4K8CoA

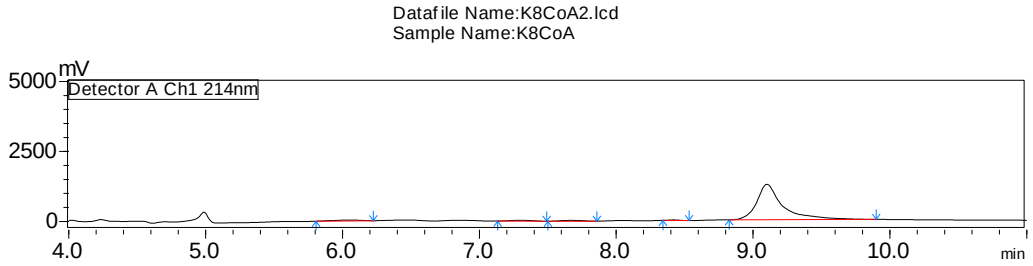

H4K12CoA

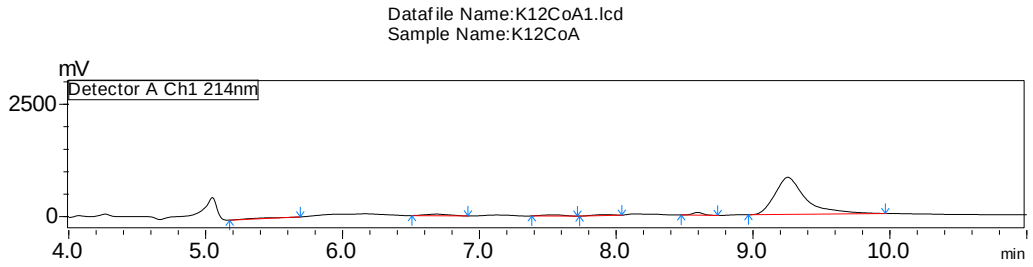

H4K16CoA

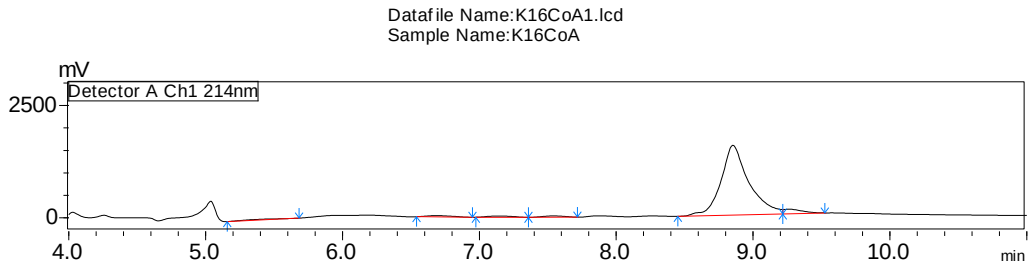

Lys-CoA

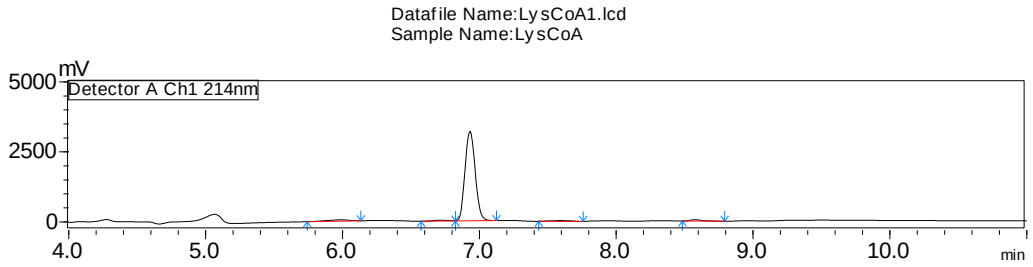

Figure S3.2: Fitting data to Morrison equation to obtain K_i^{app} values of each compounds tested with HAT1. The SPA was used to measure the potency of each inhibitor against HAT1. Reactions containing 40 nM HAT1, 2.5 µM H4-20 BTN, and 1 µM [^{3}H]AcCoA were incubated at 30°C for 20 min.

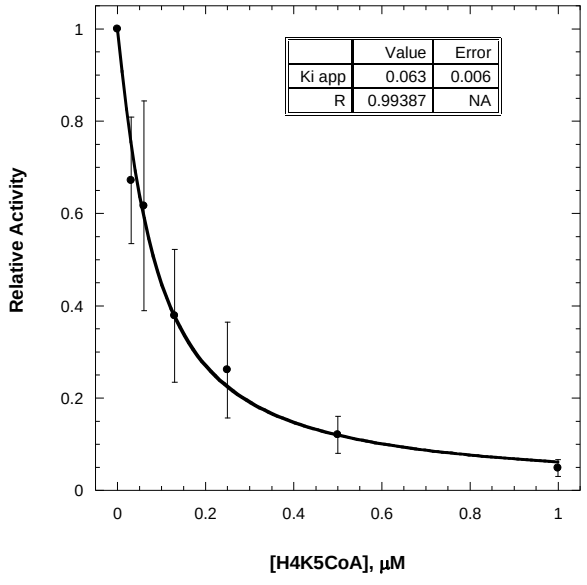

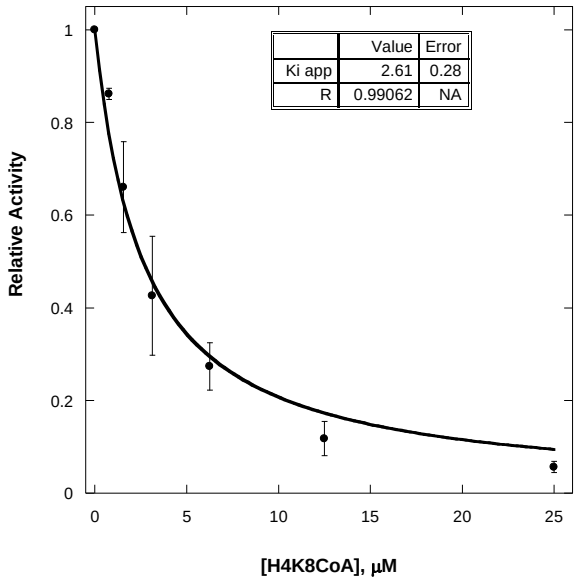

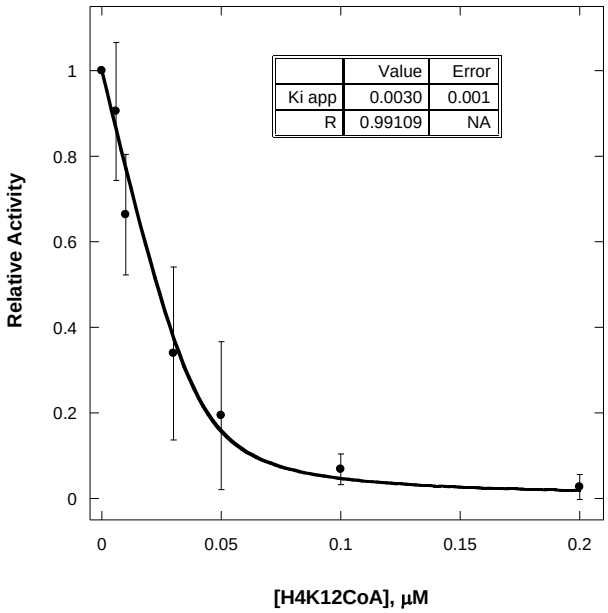
Value Error
Ki app 0.0030 0.001
R 0.99109 NA
Relative Activity
[H4K12CoA], µM

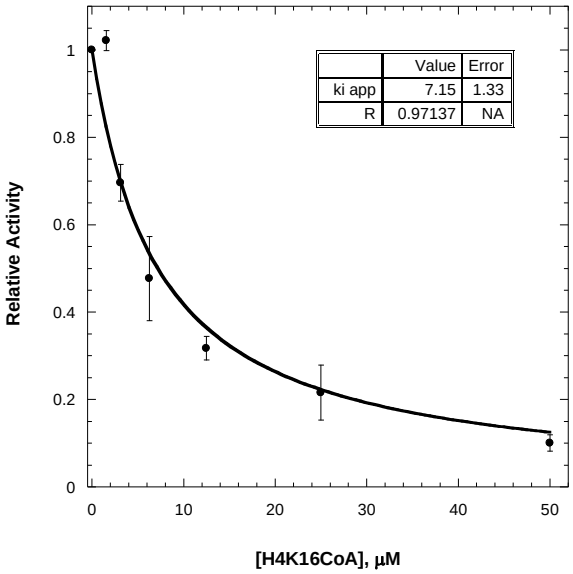
Value Error
ki app 7.15 1.33
R 0.97137 NA
Relative Activity
[H4K16CoA], µM

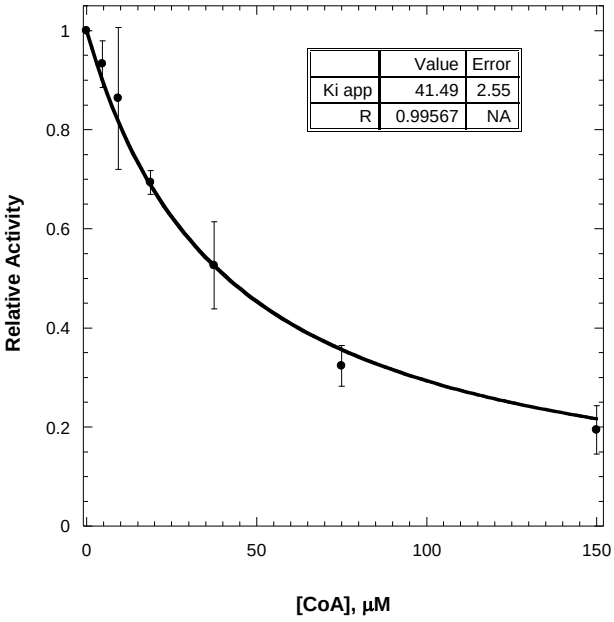
Value Error
Ki app 41.49 2.55
R 0.99567 NA
Relative Activity
[CoA], µM

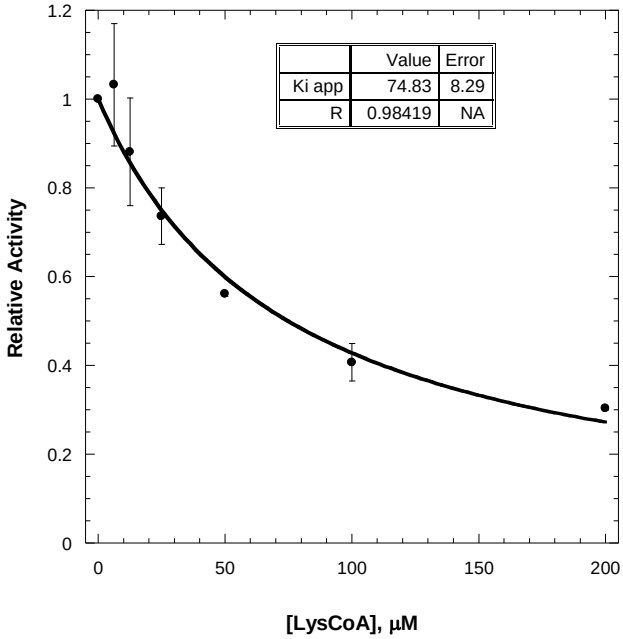
Value Error
Ki app 74.83 8.29
R 0.98419 NA
Relative Activity
[LysCoA], µM

C Supporting information for Chapter 4

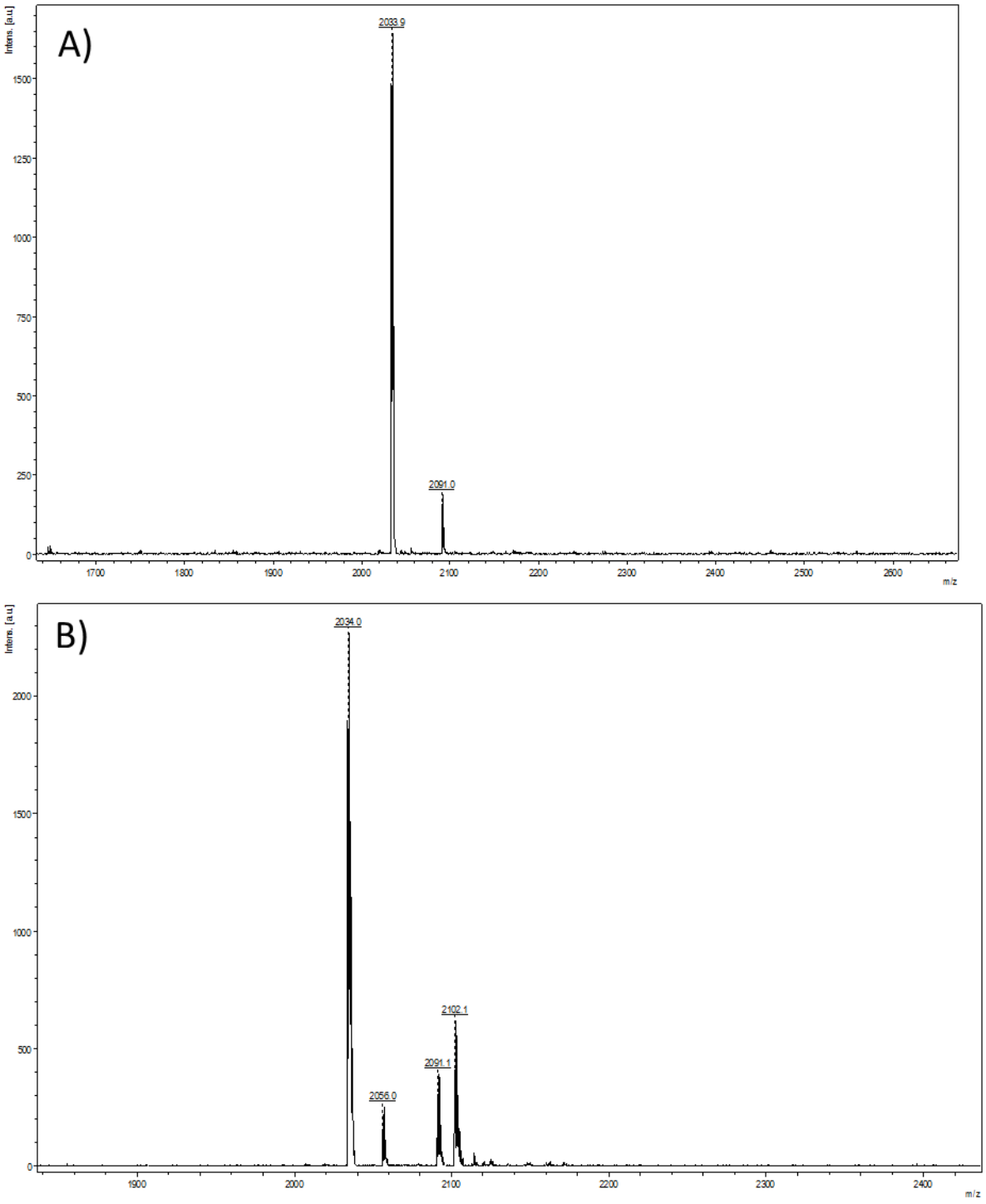

Supplemental figure S4.1: **A)** MALDI of control sample containing just H4-20 peptide (20 µM) and crotonyl CoA (20 µM)

B) MALDI of crotonylated H4-20 peptide. Sample contained HAT1 (0.8 µM), H4-20 peptide (20 µM)and crotonyl CoA (20 µM).

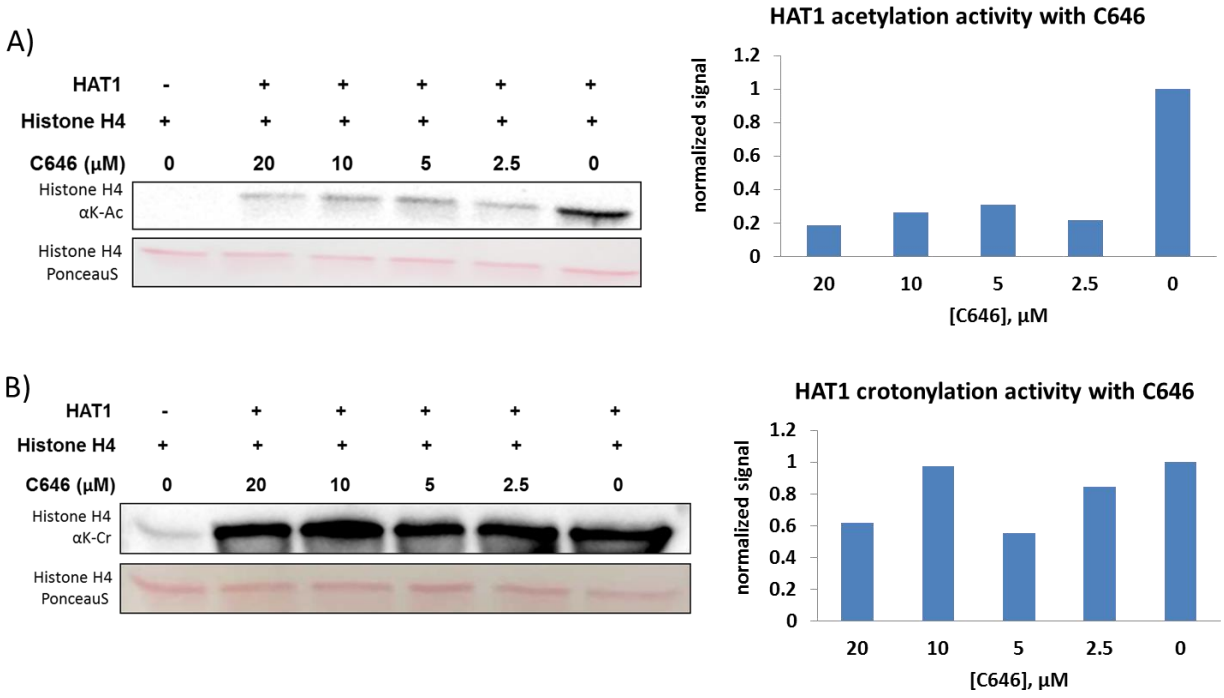

Supplemental figure S4.2: A) The affects of inhibitor C646 on the acetylation and crotonylation activity of HAT1. A) HAT1 acetylation activity in the presence of C646. B) HAT1 crotonylation activity in the presence of C646. Acyl CoA (70 µM) and H4-protein (1µg**)** was incubated for 1hr at 30°C with and without HAT1 (0.5 µM) and varying concentrations of C646 (0-20 µM). H4 protein modifications were detected by pan-anticrotonyllysine antibody or pan-antiacetyllysine antibody. Bar graphs represent the quantified band detected on the western blot.

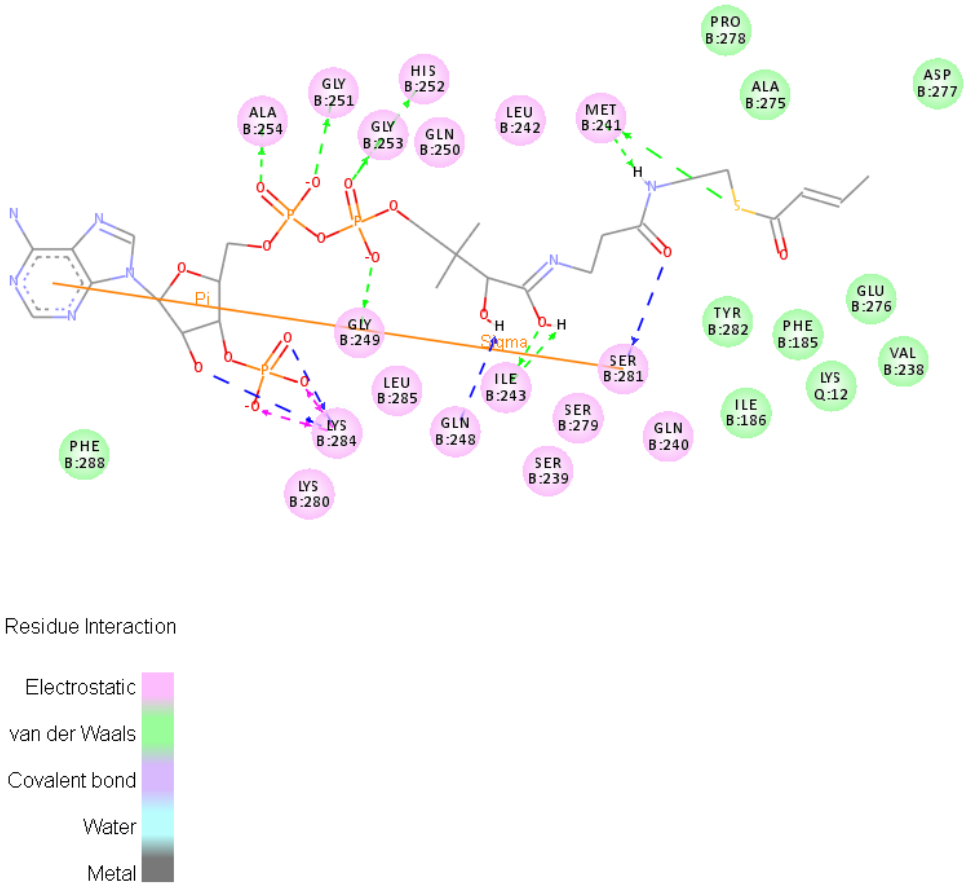

Supplemental figure S4.3: Docking crotonyl CoA into cofactor pocket of HAT1. Residues of HAT1 that anchor Crotonyl CoA into the cofactor binding site.

A)

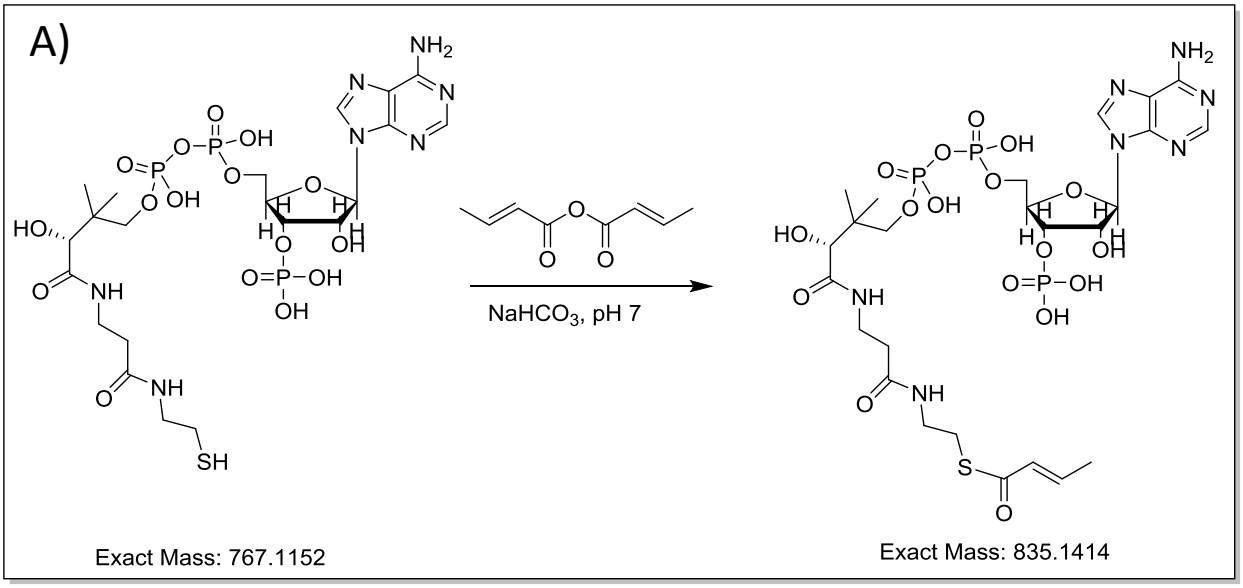
NaHCO3, pH 7
Exact Mass: 767.1152
Exact Mass: 835.1414

B)

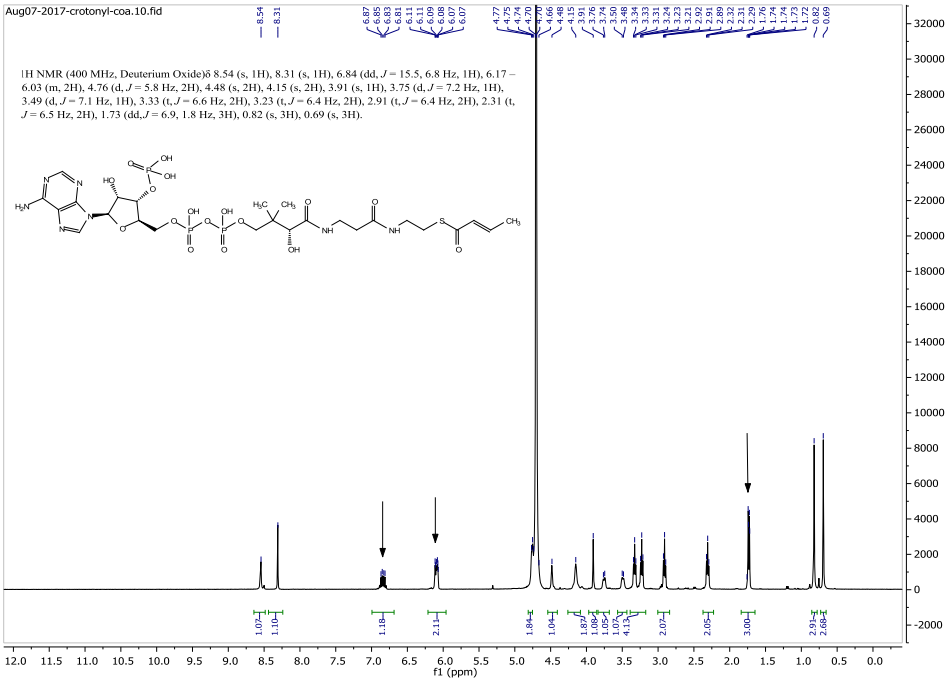
Aug07-2017-crotonyl-coa.10.fid
1H NMR (400 MHz, Deuterium Oxide)δ 8.54 (s, 1H), 8.31 (s, 1H), 6.84 (dd, J = 15.5, 6.8 Hz, 1H), 6.17 – 6.03 (m, 2H), 4.76 (d, J = 5.8 Hz, 2H), 4.48 (s, 2H), 4.15 (s, 2H), 3.91 (s, 1H), 3.75 (d, J = 7.2 Hz, 1H), 3.49 (d, J = 7.1 Hz, 1H), 3.33 (t, J = 6.6 Hz, 2H), 3.23 (t, J = 6.4 Hz, 2H), 2.91 (t, J = 6.4 Hz, 2H), 2.31 (t, J = 6.5 Hz, 2H), 1.73 (dd, J = 6.9, 1.8 Hz, 3H), 0.82 (s, 3H), 0.69 (s, 3H).
f1 (ppm)

C)

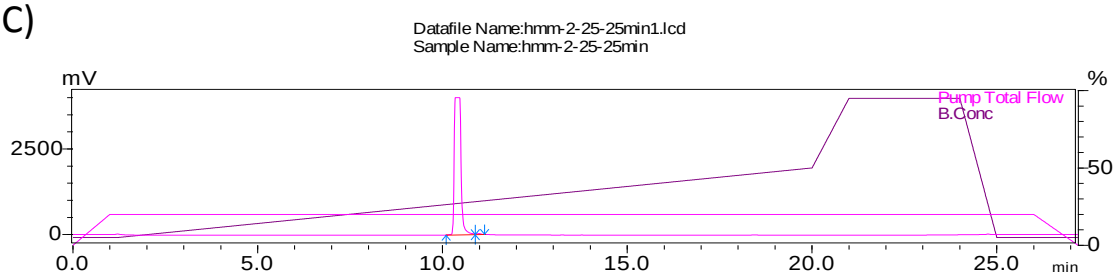

D)

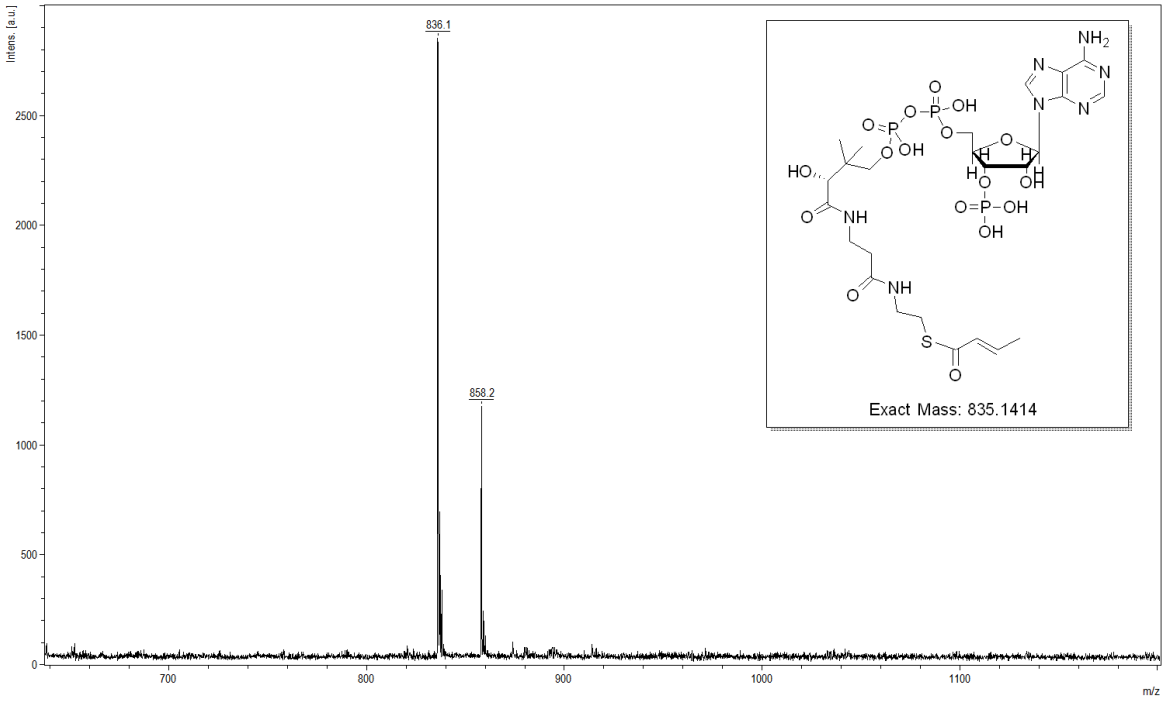

Supplemental figure S4.4: Synthesis of crotonyl CoA. A) Synthetic scheme of crotonyl CoA synthesis. B) NMR spectrum of crotonyl CoA. C) Purity analysis using HPLC. D) MALDI spectrum of crotonyl CoA.

D Supporting information for Chapter 5

Figure 5.1S: MALDI of HAT1wt and HAT1Y282A with CoA analogs

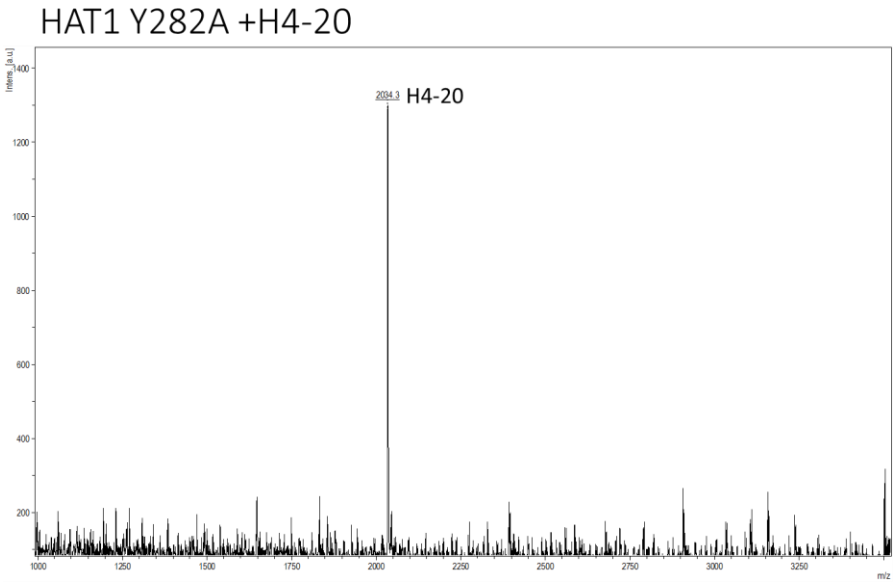

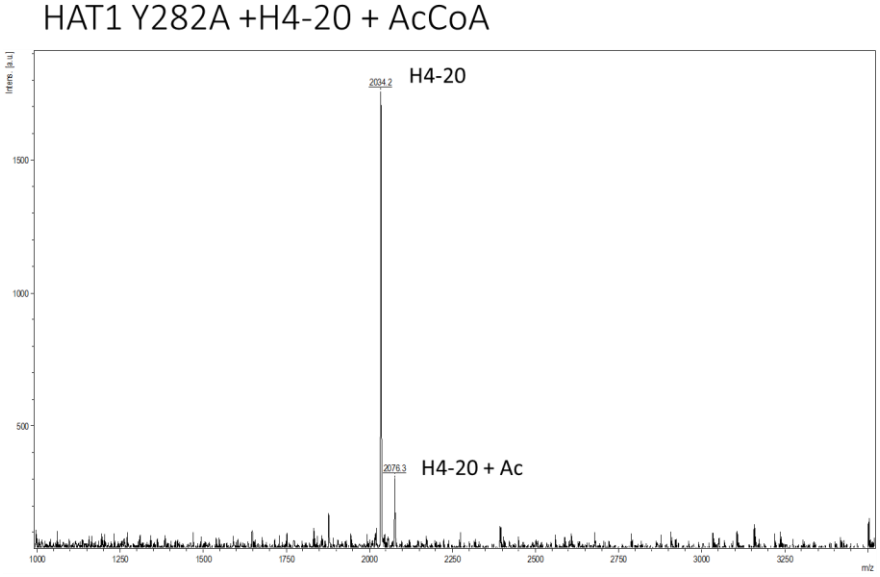

HAT1 Y282A +H4-20 + 4-Pentynoyl CoA

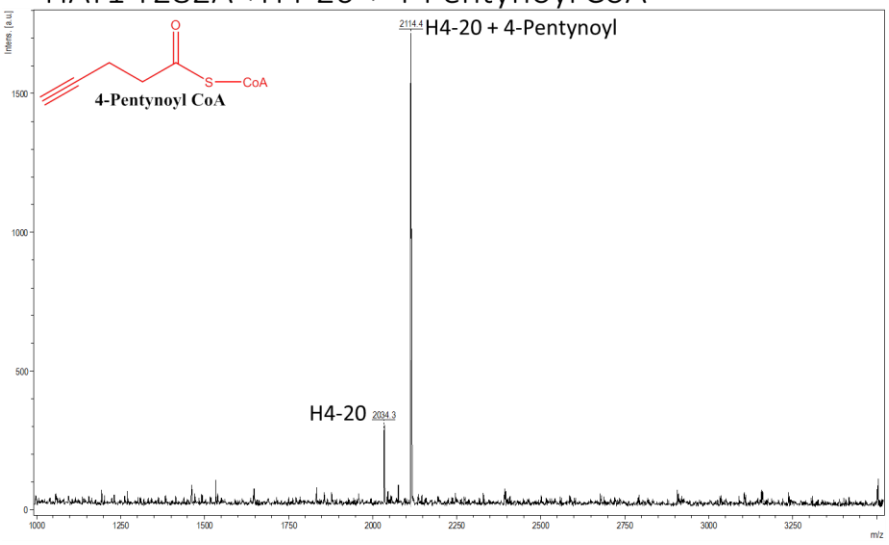

HAT1 Y282A +H4-20 + 5-Hexynoyl CoA

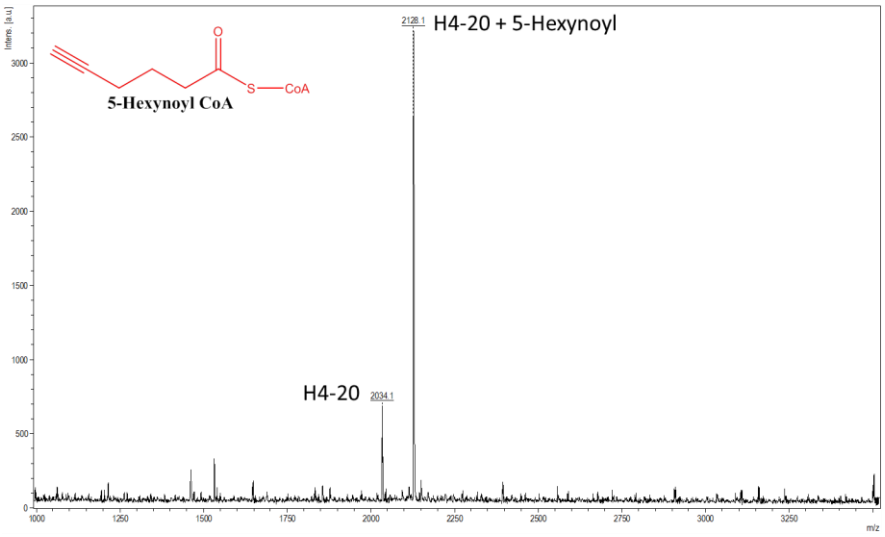

HAT1 Y282A +H4-20 + 6-Heptynoyl CoA

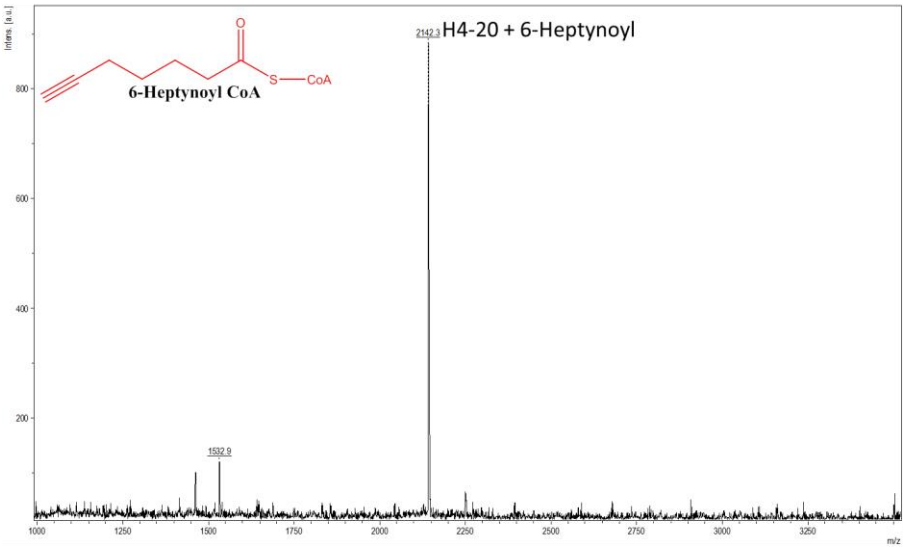

HAT1 Y282A +H4-20 + 3-Azidopropanoyl CoA

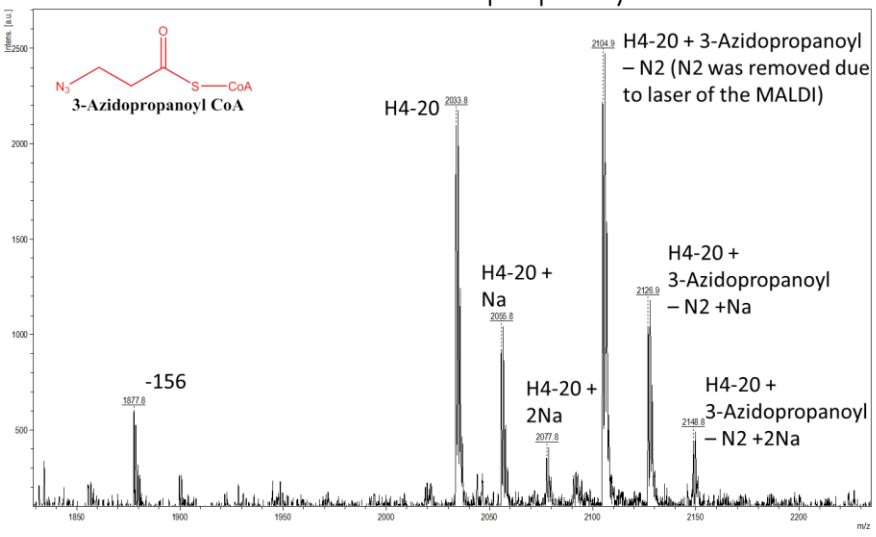

HAT1 Y282A +H4-20 + Biotin CoA

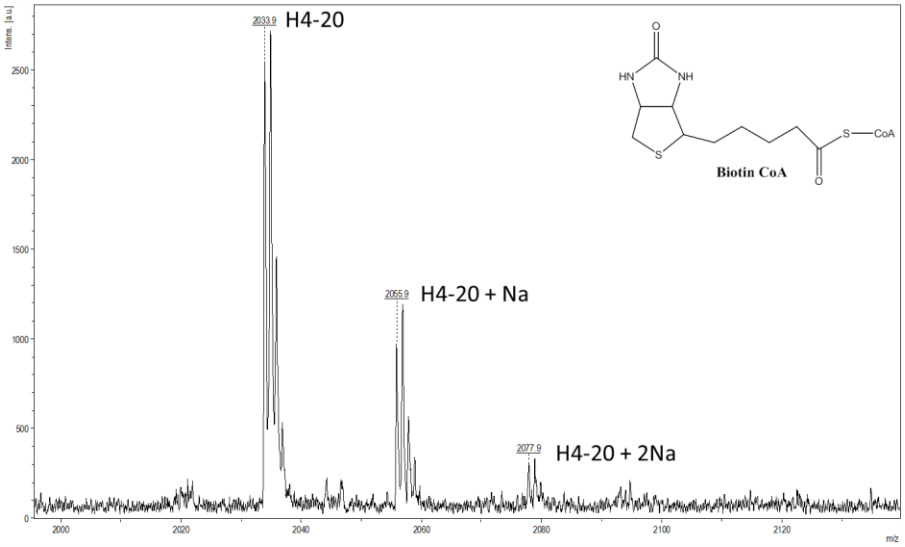

REFERENCES

1. Luger, K.; Mader, A. W.; Richmond, R. K.; Sargent, D. F.; Richmond, T. J., Crystal structure of the nucleosome core particle at 2.8[thinsp]A resolution. *Nature* **1997,** *389* (6648), 251-260.

2. Cole, P. A., Chemical probes for histone-modifying enzymes. *Nat. Chem. Biol.* **2008,** *4* (10), 590-597.

3. Drazic, A.; Myklebust, L. M.; Ree, R.; Arnesen, T., The world of protein acetylation. *Biochimica et Biophysica Acta (BBA) - Proteins and Proteomics* **2016,** *1864* (10), 1372-1401.

4. Khan, S. N.; Khan, A. U., Role of histone acetylation in cell physiology and diseases: An update. *Clinica Chimica Acta* **2010,** *411* (19), 1401-1411.

5. Allfrey, V. G.; Faulkner, R.; Mirsky, A. E., Acetylation and Methylation of Histones and Their Possible Role in the Regulation of Rna Synthesis. *Proceedings of the National Academy of Sciences* **1964,** *51* (5), 786-794.

6. Kleff, S.; Andrulis, E. D.; Anderson, C. W.; Sternglanz, R., Identification of a Gene Encoding a Yeast Histone H4 Acetyltransferase. *Journal of Biological Chemistry* **1995,** *270* (42), 24674-24677.

7. Brownell, J. E.; Zhou, J.; Ranalli, T.; Kobayashi, R.; Edmondson, D. G.; Roth, S. Y.; Allis, C. D., Tetrahymena Histone Acetyltransferase A: A Homolog to Yeast Gcn5p Linking Histone Acetylation to Gene Activation. *Cell* **1996,** *84* (6), 843-851.

8. Hudson, B. P.; Martinez-Yamout, M. A.; Dyson, H. J.; Wright, P. E., Solution structure and acetyl-lysine binding activity of the GCN5 bromodomain1. *J. Mol. Biol.* **2000,** *304* (3), 355-370.

9. Groth, A.; Rocha, W.; Verreault, A.; Almouzni, G., Chromatin Challenges during DNA Replication and Repair. *Cell* **2007,** *128* (4), 721-733.

10. Grunstein, M., Histone acetylation in chromatin structure and transcription. *Nature* **1997,** *389* (6649), 349-352.

11. Kimura, A.; Umehara, T.; Horikoshi, M., Chromosomal gradient of histone acetylation established by Sas2p and Sir2p functions as a shield against gene silencing. *Nat. Genet.* **2002,** *32* (3), 370-377.

12. Lee, K. K.; Workman, J. L., Histone acetyltransferase complexes: one size doesn't fit all. *Nature Reviews Molecular Cell Biology* **2007,** *8*, 284.

13. Brownell, J. E.; Allis, C. D., Special HATs for special occasions: linking histone acetylation to chromatin assembly and gene activation. *Current Opinion in Genetics & Development* **1996,** *6* (2), 176-184.

14. Haigney, A.; Ricketts, M. D.; Marmorstein, R., Dissecting the Molecular Roles of Histone Chaperones in Histone Acetylation by Type B Histone Acetyltransferases (HAT-B). *J. Biol. Chem.* **2015,** *290* (51), 30648-30657.

15. Sun, W.-J.; Zhou, X.; Zheng, J.-H.; Lu, M.-D.; Nie, J.-Y.; Yang, X.-J.; Zheng, Z.-Q., Histone acetyltransferases and deacetylases: molecular and clinical implications to gastrointestinal carcinogenesis. *Acta Biochimica et Biophysica Sinica* **2012,** *44* (1), 80-91.

16. Neuwald, A. F.; Landsman, D., GCN5-related histone N-acetyltransferases belong to a diverse superfamily that includes the yeast SPT10 protein. *Trends in Biochemical Sciences* **1997,** *22* (5), 154-155.

17. Marmorstein, R., Structure and function of histone acetyltransferases. *Cell. Mol. Life Sci.* **2001,** *58* (5-6), 693-703.

18. Yang, X. J., The diverse superfamily of lysine acetyltransferases and their roles in leukemia and other diseases. *Nucleic Acids Res.* **2004,** *32* (3), 959-976.

19. Avvakumov, N.; Cote, J., The MYST family of histone acetyltransferases and their intimate links to cancer. *Oncogene* **2007,** *26* (37), 5395-5407.

20. Sun, Y.; Jiang, X.; Xu, Y.; Ayrapetov, M. K.; Moreau, L. A.; Whetstine, J. R.; Price, B. D., Histone H3 methylation links DNA damage detection to activation of the tumour suppressor Tip60. *Nat Cell Biol* **2009,** *11* (11), 1376-1382.

21. Ullah, M.; Pelletier, N.; Xiao, L.; Zhao, S. P.; Wang, K.; Degerny, C.; Tahmasebi, S.; Cayrou, C.; Doyon, Y.; Goh, S.-L.; Champagne, N.; Côté, J.; Yang, X.-J., Molecular Architecture of Quartet MOZ/MORF Histone Acetyltransferase Complexes. *Molecular and Cellular Biology* **2008,** *28* (22), 6828-6843.

22. Parthun, M. R.; Widom, J.; Gottschling, D. E., The Major Cytoplasmic Histone Acetyltransferase in Yeast: Links to Chromatin Replication and Histone Metabolism. *Cell* **1996,** *87* (1), 85-94.

23. Parthun, M. R., Histone acetyltransferase 1: More than just an enzyme? *Biochimica et Biophysica Acta (BBA) - Gene Regulatory Mechanisms* **2012,** *1819* (3), 256-263.

24. Lu, D., Epigenetic modification enzymes: catalytic mechanisms and inhibitors. *Acta Pharmaceutica Sinica B* **2013,** *3* (3), 141-149.

25. Nagarajan, P.; Ge, Z.; Sirbu, B.; Doughty, C.; Agudelo Garcia, P. A.; Schlederer, M.; Annunziato, A. T.; Cortez, D.; Kenner, L.; Parthun, M. R., Histone Acetyl Transferase 1 Is Essential for Mammalian Development, Genome Stability, and the Processing of Newly Synthesized Histones H3 and H4. *PLoS Genet.* **2013,** *9* (6), e1003518.

26. Parthun, M. R., Hat1: the emerging cellular roles of a type B histone acetyltransferase. *Oncogene* **2007,** *26*, 5319.

27. Tafrova, J. I.; Tafrov, S. T., Human histone acetyltransferase 1 (Hat1) acetylates lysine 5 of histone H2A in vivo. *Mol. Cell. Biochem.* **2014,** *392* (1), 259-272.

28. Ma, X.-J.; Wu, J.; Altheim, B. A.; Schultz, M. C.; Grunstein, M., Deposition-related sites K5/K12 in histone H4 are not required for nucleosome deposition in yeast. *Proceedings of the National Academy of Sciences* **1998,** *95* (12), 6693-6698.

29. Barman, H. K.; Takami, Y.; Ono, T.; Nishijima, H.; Sanematsu, F.; Shibahara, K.-i.; Nakayama, T., Histone acetyltransferase 1 is dispensable for replication-coupled chromatin assembly but contributes to recover DNA damages created following replication blockage in vertebrate cells. *Biochem. Biophys. Res. Commun.* **2006,** *345* (4), 1547-1557.

30. Benson, L. J.; Phillips, J. A.; Gu, Y.; Parthun, M. R.; Hoffman, C. S.; Annunziato, A. T., Properties of the Type B Histone Acetyltransferase Hat1: H4 TAIL INTERACTION, SITE PREFERENCE, AND INVOLVEMENT IN DNA REPAIR. *J. Biol. Chem.* **2007,** *282* (2), 836-842.

31. Liu, H.; Zhang, M.; He, W.; Zhu, Z.; Teng, M.; Gao, Y.; Niu, L., Structural insights into yeast histone chaperone Hif1: a scaffold protein recruiting protein complexes to core histones. *Biochem. J* **2014,** *462* (3), 465-473.

32. Ai, X.; Parthun, M. R., The Nuclear Hat1p/Hat2p Complex: A Molecular Link between Type B Histone Acetyltransferases and Chromatin Assembly. *Mol. Cell* **2004,** *14* (2), 195-205.

33. Yang, X.; Li, L.; Liang, J.; Shi, L.; Yang, J.; Yi, X.; Zhang, D.; Han, X.; Yu, N.; Shang, Y., Histone Acetyltransferase 1 Promotes Homologous Recombination in DNA Repair by Facilitating Histone Turnover. *J. Biol. Chem.* **2013,** *288* (25), 18271-18282.

34. Wu, H.; Moshkina, N.; Min, J.; Zeng, H.; Joshua, J.; Zhou, M.-M.; Plotnikov, A. N., Structural basis for substrate specificity and catalysis of human histone acetyltransferase 1. *Proceedings of the National Academy of Sciences* **2012,** *109* (23), 8925-8930.

35. Jin, X.; Tian, S.; Li, P., Histone Acetyltransferase 1 Promotes Cell Proliferation and Induces Cisplatin Resistance in Hepatocellular Carcinoma. *Oncology Research Featuring Preclinical and Clinical Cancer Therapeutics* **2017,** *25* (6), 939-946.

36. Han, N.; Shi, L.; Guo, Q.; Sun, W.; Yu, Y.; Yang, L.; Zhang, X.; Zhang, M., HAT1 induces lung cancer cell apoptosis via up regulating Fas. *Oncotarget* **2017,** *8* (52), 89970-89977.

37. Liu, D.; Zhang, M.; Xie, W.; Lan, G.; Cheng, H. P.; Gong, D.; Huang, C.; Lv, Y. C.; Yao, F.; Tan, Y. L.; Li, L.; Zheng, X. L.; Tang, C. K., MiR-486 regulates cholesterol efflux by targeting HAT1. *Biochemical and biophysical research communications* **2016,** *472* (3), 418-24.

38. Sadler, A. J.; Suliman, B. A.; Yu, L.; Yuan, X.; Wang, D.; Irving, A. T.; Sarvestani, S. T.; Banerjee, A.; Mansell, A. S.; Liu, J.-P.; Gerondakis, S.; Williams, B. R. G.; Xu, D., The acetyltransferase HAT1 moderates the NF-κB response by regulating the transcription factor PLZF. *Nature Communications* **2015,** *6*, 6795.

39. Seiden-Long, I. M.; Brown, K. R.; Shih, W.; Wigle, D. A.; Radulovich, N.; Jurisica, I.; Tsao, M. S., Transcriptional targets of hepatocyte growth factor signaling and Ki-ras oncogene activation in colorectal cancer. *Oncogene* **2006,** *25* (1), 91-102.

40. Xue, L.; Hou, J.; Wang, Q.; Yao, L.; Xu, S.; Ge, D., RNAi screening identifies HAT1 as a potential drug target in esophageal squamous cell carcinoma. *Int. J. Clin. Exp. Pathol.* **2014,** *7* (7), 3898-907.

41. Pogribny, I. P.; Tryndyak, V. P.; Muskhelishvili, L.; Rusyn, I.; Ross, S. A., Methyl Deficiency, Alterations in Global Histone Modifications, and Carcinogenesis. *The Journal of Nutrition* **2007,** *137* (1), 216S-222S.

42. Timmermann, S.; Lehrmann, H.; Polesskaya, A.; Harel-Bellan, A., Histone acetylation and disease. *Cellular and molecular life sciences : CMLS* **2001,** *58* (5-6), 728-36.

43. Eckschlager, T.; Plch, J.; Stiborova, M.; Hrabeta, J., Histone Deacetylase Inhibitors as Anticancer Drugs. *International Journal of Molecular Sciences* **2017,** *18* (7), 1414.

44. Baell, J. B.; Miao, W., Histone acetyltransferase inhibitors: where art thou? *Future Med. Chem.* **2016,** *8* (13), 1525-1528.

45. Manzo, F.; Tambaro, F. P.; Mai, A.; Altucci, L., Histone acetyltransferase inhibitors and preclinical studies. *Expert Opin. Ther. Pat.* **2009,** *19* (6), 761-774.

46. Horiuchi, K.; Fujimoto, D., Use of phospho-cellulose paper disks for the assay of histone acetyltransferase. *Analytical Biochemistry* **1975,** *69* (2), 491-496.

47. Mizzen, C. A.; Brownell, J. E.; Cook, R. G.; Allis, C. D., Histone acetyltransferases: Preparation of substrates and assay procedures. In *Methods in Enzymology*, Paul M. Wassarman, A. P. W., Ed. Academic Press: 1999; Vol. Volume 304, pp 675-696.

48. Wynne Aherne, G.; Rowlands, M. G.; Stimson, L.; Workman, P., Assays for the identification and evaluation of histone acetyltransferase inhibitors. *Methods* **2002,** *26* (3), 245-253.

49. Turlais, F.; Hardcastle, A.; Rowlands, M.; Newbatt, Y.; Bannister, A.; Kouzarides, T.; Workman, P.; Aherne, G. W., High-Throughput Screening for Identification of Small Molecule Inhibitors of Histone Acetyltransferases Using Scintillating Microplates (FlashPlate). *Anal. Biochem.* **2001,** *298* (1), 62-68.

50. Trievel, R. C.; Li, F.-Y.; Marmorstein, R., Application of a Fluorescent Histone Acetyltransferase Assay to Probe the Substrate Specificity of the Human p300/CBP-Associated Factor. *Anal. Biochem.* **2000,** *287* (2), 319-328.

51. Dahlin, J. L.; Nissink, J. W. M.; Strasser, J. M.; Francis, S.; Higgins, L.; Zhou, H.; Zhang, Z.; Walters, M. A., PAINS in the Assay: Chemical Mechanisms of Assay Interference and Promiscuous Enzymatic Inhibition Observed during a Sulfhydryl-Scavenging HTS. *J. Med. Chem.* **2015,** *58* (5), 2091-2113.

52. Bradner, J. E.; West, N.; Grachan, M. L.; Greenberg, E. F.; Haggarty, S. J.; Warnow, T.; Mazitschek, R., Chemical phylogenetics of histone deacetylases. *Nat Chem Biol* **2010,** *6* (3), 238-243.

53. Kim, S. C.; Sprung, R.; Chen, Y.; Xu, Y.; Ball, H.; Pei, J.; Cheng, T.; Kho, Y.; Xiao, H.; Xiao, L.; Grishin, N. V.; White, M.; Yang, X.-J.; Zhao, Y., Substrate and Functional Diversity of Lysine Acetylation Revealed by a Proteomics Survey. *Mol. Cell* **2006,** *23* (4), 607-618.

54. Lau, O. D.; Courtney, A. D.; Vassilev, A.; Marzilli, L. A.; Cotter, R. J.; Nakatani, Y.; Cole, P. A., p300/CBP-associated Factor Histone Acetyltransferase Processing of a Peptide

Substrate: KINETIC ANALYSIS OF THE CATALYTIC MECHANISM. *Journal of Biological Chemistry* **2000,** *275* (29), 21953-21959.

55. Wu, J.; Xie, N.; Wu, Z.; Zhang, Y.; Zheng, Y. G., Bisubstrate Inhibitors of the MYST HATs Esa1 and Tip60. *Biorg. Med. Chem.* **2009,** *17* (3), 1381-1386.

56. Lau, O. D.; Kundu, T. K.; Soccio, R. E.; Ait-Si-Ali, S.; Khalil, E. M.; Vassilev, A.; Wolffe, A. P.; Nakatani, Y.; Roeder, R. G.; Cole, P. A., HATs off. *Molecular Cell* **2000,** *5* (3), 589-595.

57. Dancy, B. M.; Cole, P. A., Protein Lysine Acetylation by p300/CBP. *Chem. Rev.* **2015,** *115* (6), 2419-2452.

58. Wapenaar, H.; Dekker, F. J., Histone acetyltransferases: challenges in targeting bi-substrate enzymes. *Clin. Epigenetics* **2016,** *8*, 59.

59. Cebrat, M.; Kim, C. M.; Thompson, P. R.; Daugherty, M.; Cole, P. A., Synthesis and analysis of potential prodrugs of coenzyme A analogues for the inhibition of the histone acetyltransferase p300. *Biorg. Med. Chem.* **2003,** *11* (15), 3307-3313.

60. Bandyopadhyay, K.; Banères, J.-L.; Martin, A.; Blonski, C.; Parello, J.; Gjerset, R., Spermidinyl-CoA-based HAT inhibitors block DNA repair and provide cancer- specific chemo- and radiosensitization. *Cell Cycle* **2009,** *8* (17), 2779-2788.

61. Ghizzoni, M.; Boltjes, A.; Graaf, C. d.; Haisma, H. J.; Dekker, F. J., Improved inhibition of the histone acetyltransferase PCAF by an anacardic acid derivative. *Biorg. Med. Chem.* **2010,** *18* (16), 5826-5834.

62. Balasubramanyam, K.; Altaf, M.; Varier, R. A.; Swaminathan, V.; Ravindran, A.; Sadhale, P. P.; Kundu, T. K., Polyisoprenylated Benzophenone, Garcinol, a Natural Histone

Acetyltransferase Inhibitor, Represses Chromatin Transcription and Alters Global Gene Expression. *Journal of Biological Chemistry* **2004,** *279* (32), 33716-33726.

63. Mazumder, A.; Raghavan, K.; Weinstein, J.; Kohn, K. W.; Pommier, Y., Inhibition of human immunodeficiency virus type-1 integrase by curcumin. *Biochemical Pharmacology* **1995,** *49* (8), 1165-1170.

64. Balasubramanyam, K.; Varier, R. A.; Altaf, M.; Swaminathan, V.; Siddappa, N. B.; Ranga, U.; Kundu, T. K., Curcumin, a Novel p300/CREB-binding Protein-specific Inhibitor of Acetyltransferase, Represses the Acetylation of Histone/Nonhistone Proteins and Histone Acetyltransferase-dependent Chromatin Transcription. *Journal of Biological Chemistry* **2004,** *279* (49), 51163-51171.

65. Meyers, R. A., *Epigenetic Regulation and Epigenomics*. John Wiley & Sons Weinheim, Germany 2012.

66. Furdas, S. D.; Kannan, S.; Sippl, W.; Jung, M., Small Molecule Inhibitors of Histone Acetyltransferases as Epigenetic Tools and Drug Candidates. *Archiv der Pharmazie* **2012,** *345* (1), 7-21.

67. Balasubramanyam, K.; Swaminathan, V.; Ranganathan, A.; Kundu, T. K., Small Molecule Modulators of Histone Acetyltransferase p300. *Journal of Biological Chemistry* **2003,** *278* (21), 19134-19140.

68. Stimson, L.; Rowlands, M. G.; Newbatt, Y. M.; Smith, N. F.; Raynaud, F. I.; Rogers, P.; Bavetsias, V.; Gorsuch, S.; Jarman, M.; Bannister, A.; Kouzarides, T.; McDonald, E.; Workman, P.; Aherne, G. W., Isothiazolones as inhibitors of PCAF and p300 histone acetyltransferase activity. *Molecular Cancer Therapeutics* **2005,** *4* (10), 1521-1532.

69. Furdas, S. D.; Shekfeh, S.; Bissinger, E.-M.; Wagner, J. M.; Schlimme, S.; Valkov, V.; Hendzel, M.; Jung, M.; Sippl, W., Synthesis and biological testing of novel pyridoisothiazolones as histone acetyltransferase inhibitors. *Bioorganic & Medicinal Chemistry* **2011,** *19* (12), 3678-3689.

70. Gajer, J. M.; Furdas, S. D.; Grunder, A.; Gothwal, M.; Heinicke, U.; Keller, K.; Colland, F.; Fulda, S.; Pahl, H. L.; Fichtner, I.; Sippl, W.; Jung, M., Histone acetyltransferase inhibitors block neuroblastoma cell growth in vivo. *Oncogenesis* **2015,** *4*, e137.

71. Coffey, K.; Blackburn, T. J.; Cook, S.; Golding, B. T.; Griffin, R. J.; Hardcastle, I. R.; Hewitt, L.; Huberman, K.; McNeill, H. V.; Newell, D. R.; Roche, C.; Ryan-Munden, C. A.; Watson, A.; Robson, C. N., Characterisation of a Tip60 Specific Inhibitor, NU9056, in Prostate Cancer. *PLoS ONE* **2012,** *7* (10), e45539.

72. Bowers, E. M.; Yan, G.; Mukherjee, C.; Orry, A.; Wang, L.; Holbert, M. A.; Crump, N. T.; Hazzalin, C. A.; Liszczak, G.; Yuan, H.; Larocca, C.; Saldanha, S. A.; Abagyan, R.; Sun, Y.; Meyers, D. J.; Marmorstein, R.; Mahadevan, L. C.; Alani, R. M.; Cole, P. A., Virtual Ligand Screening of the p300/CBP Histone Acetyltransferase: Identification of a Selective Small Molecule Inhibitor. *Chem. Biol.* **2010,** *17* (5), 471-482.

73. Santer, F. R.; Höschele, P. P. S.; Oh, S. J.; Erb, H. H. H.; Bouchal, J.; Cavarretta, I. T.; Parson, W.; Meyers, D. J.; Cole, P. A.; Culig, Z., Inhibition of the Acetyltransferases p300 and CBP Reveals a Targetable Function for p300 in the Survival and Invasion Pathways of Prostate Cancer Cell Lines. *Molecular Cancer Therapeutics* **2011,** *10* (9), 1644-1655.

74. Zhu, X.-Y.; Huang, C.-S.; Li, Q.; Chang, R.-m.; Song, Z.-b.; Zou, W.-y.; Guo, Q.-L., p300 exerts an epigenetic role in chronic neuropathic pain through its acetyltransferase activity in rats following chronic constriction injury (CCI). *Molecular Pain* **2012,** *8* (1), 84.

75. Jasial, S.; Hu, Y.; Bajorath, J., How Frequently Are Pan-Assay Interference Compounds Active? Large-Scale Analysis of Screening Data Reveals Diverse Activity Profiles, Low Global Hit Frequency, and Many Consistently Inactive Compounds. *J. Med. Chem.* **2017,** *60* (9), 3879-3886.

76. Baell, J.; Walters, M. A., Chemistry: Chemical con artists foil drug discovery. *Nature* **2014,** *513* (7519), 481-3.

77. Dahlin, J. L.; Nelson, K. M.; Strasser, J. M.; Barsyte-Lovejoy, D.; Szewczyk, M. M.; Organ, S.; Cuellar, M.; Singh, G.; Shrimp, J. H.; Nguyen, N.; Meier, J. L.; Arrowsmith, C. H.; Brown, P. J.; Baell, J. B.; Walters, M. A., Assay interference and off-target liabilities of reported histone acetyltransferase inhibitors. *Nature Communications* **2017,** *8* (1), 1527.

78. Wei, W.; Mao, A.; Tang, B.; Zeng, Q.; Gao, S.; Liu, X.; Lu, L.; Li, W.; Du, J. X.; Li, J.; Wong, J.; Liao, L., Large-Scale Identification of Protein Crotonylation Reveals Its Role in Multiple Cellular Functions. *J. Proteome Res.* **2017,** *16* (4), 1743-1752.

79. Sabari, Benjamin R.; Tang, Z.; Huang, H.; Yong-Gonzalez, V.; Molina, H.; Kong, Ha E.; Dai, L.; Shimada, M.; Cross, Justin R.; Zhao, Y.; Roeder, Robert G.; Allis, C. D., Intracellular Crotonyl-CoA Stimulates Transcription through p300-Catalyzed Histone Crotonylation. *Mol. Cell 58* (2), 203-215.

80. Xu, W.; Wan, J.; Zhan, J.; Li, X.; He, H.; Shi, Z.; Zhang, H., Global profiling of crotonylation on non-histone proteins. *Cell research* **2017,** *27* (7), 946-949.

81. Gusterson, R. J.; Jazrawi, E.; Adcock, I. M.; Latchman, D. S., The Transcriptional Co-activators CREB-binding Protein (CBP) and p300 Play a Critical Role in Cardiac Hypertrophy That Is Dependent on Their Histone Acetyltransferase Activity. *J. Biol. Chem.* **2003,** *278* (9), 6838-6847.

82. Isharwal, S.; Miller, M. C.; Marlow, C.; Makarov, D. V.; Partin, A. W.; Veltri, R. W., p300 (histone acetyltransferase) biomarker predicts prostate cancer biochemical recurrence and correlates with changes in epithelia nuclear size and shape. *The Prostate* **2008,** *68* (10), 1097-1104.

83. Zheng, Y. G.; Wu, J.; Chen, Z.; Goodman, M., Chemical regulation of epigenetic modifications: Opportunities for new cancer therapy. *Med. Res. Rev.* **2008,** *28* (5), 645-687.

84. Berndsen, C. E.; Denu, J. M., Assays for mechanistic investigations of protein/histone acetyltransferases. *Methods* **2005,** *36* (4), 321-31.

85. Wu, S.; Liu, B., Application of Scintillation Proximity Assay in Drug Discovery. *Biodrugs* **2005,** *19* (6), 383-392.

86. Richards, F. M., [1] Reflections. In *Methods Enzymol.*, Meir, W.; Edward, A. B., Eds. Academic Press: 1990; Vol. 184, pp 3-5.

87. Holmberg, A.; Blomstergren, A.; Nord, O.; Lukacs, M.; Lundeberg, J.; Uhlén, M., The biotin-streptavidin interaction can be reversibly broken using water at elevated temperatures. *Electrophoresis* **2005,** *26* (3), 501-510.

88. Berry, J.; Price-Jones, M., Measurement of Radioligand Binding by Scintillation Proximity Assay. In *Receptor Binding Techniques*, Davenport, A., Ed. Humana Press: 2005; Vol. 306, pp 121-138.

89. Wu, J.; Xie, N.; Feng, Y.; Zheng, Y. G., Scintillation Proximity Assay of Arginine Methylation. *J. Biomol. Screen.* **2012,** *17* (2), 237-244.

90. Park, Y.-W.; Cummings, R. T.; Wu, L.; Zheng, S.; Cameron, P. M.; Woods, A.; Zaller, D. M.; Marcy, A. I.; Hermes, J. D., Homogeneous Proximity Tyrosine Kinase Assays:

Scintillation Proximity Assay versus Homogeneous Time-Resolved Fluorescence. *Anal. Biochem.* **1999,** *269* (1), 94-104.

91. Dhayalan, A.; Dimitrova, E.; Rathert, P.; Jeltsch, A., A continuous protein methyltransferase (G9a) assay for enzyme activity measurement and inhibitor screening. *J. Biomol. Screen.* **2009,** *14* (9), 1129-33.

92. Thompson, P. R.; Wang, D.; Wang, L.; Fulco, M.; Pediconi, N.; Zhang, D.; An, W.; Ge, Q.; Roeder, R. G.; Wong, J.; Levrero, M.; Sartorelli, V.; Cotter, R. J.; Cole, P. A., Regulation of the p300 HAT domain via a novel activation loop. *Nat. Struct. Mol. Biol.* **2004,** *11* (4), 308-315.

93. Cook, N. D., Scintillation proximity assay: A versatile high-throughput screening technology. *Drug Discovery Today* **1996,** *1* (7), 287-294.

94. Bowers, E. M.; Yan, G.; Mukherjee, C.; Orry, A.; Wang, L.; Holbert, M. A.; Crump, N. T.; Hazzalin, C. A.; Liszczak, G.; Yuan, H.; Larocca, C.; Saldanha, S. A.; Abagyan, R.; Sun, Y.; Meyers, D. J.; Marmorstein, R.; Mahadevan, L. C.; Alani, R. M.; Cole, P. A., Virtual ligand screening of the p300/CBP histone acetyltransferase: identification of a selective small molecule inhibitor. *Chem. Biol.* **2010,** *17* (5), 471-82.

95. Copeland, R. A., *Evaluation of Enzyme Inhibitors in Drug Discovery. A Guide for Medicinal Chemists and Pharmacologists*. John Wiley & Sons, Inc.: Hoboken, New Jersey 2005; Vol. 46, p 1-265.

96. Zhang, J. H.; Chung, T. D.; Oldenburg, K. R., A Simple Statistical Parameter for Use in Evaluation and Validation of High Throughput Screening Assays. *J. Biomol. Screen.* **1999,** *4* (2), 67-73.

97. Ait-Si-Ali, S.; Ramirez, S.; Robin, P.; Trouche, D.; Harel-Bellan, A., A rapid and sensitive assay for histone acetyl-transferase activity. *Nucleic Acids Res.* **1998,** *26* (16), 3869-70.

98. Turlais, F.; Hardcastle, A.; Rowlands, M.; Newbatt, Y.; Bannister, A.; Kouzarides, T.; Workman, P.; Aherne, G. W., High-throughput screening for identification of small molecule inhibitors of histone acetyltransferases using scintillating microplates (FlashPlate). *Anal Biochem* **2001,** *298* (1), 62-8.

99. Aherne, G. W.; Rowlands, M. G.; Stimson, L.; Workman, P., Assays for the identification and evaluation of histone acetyltransferase inhibitors. *Methods* **2002,** *26* (3), 245-253.

100. Mizzen, C. A.; Brownell, J. E.; Cook, R. G.; Allis, C. D., Histone acetyltransferases: preparation of substrates and assay procedures. *Methods Enzymol.* **1999,** *304*, 675-96.

101. Wong, L. J.; Patton, W. F., Salt inhibition of nuclear histone acetyltransferase from calf thymus. *Int. J. Biochem.* **1985,** *17* (1), 123-6.

102. Hagihara, Y.; Aimoto, S.; Fink, A. L.; Goto, Y., Guanidine Hydrochloride-induced Folding of Proteins. *J. Mol. Biol.* **1993,** *231* (2), 180-184.

103. Tanford, C., Protein Denaturation. In *Adv. Protein Chem.*, C.B. Anfinsen, M. L. A. J. T. E.; Frederic, M. R., Eds. Academic Press: 1968; Vol. 23, pp 121-282.

104. Kleff, S.; Andrulis, E. D.; Anderson, C. W.; Sternglanz, R., Identification of a gene encoding a yeast histone H4 acetyltransferase. *J. Biol. Chem.* **1995,** *270* (42), 24674-7.

105. Gelato Kathy, A.; Fischle, W., Role of histone modifications in defining chromatin structure and function. In *Biol. Chem.*, 2008; Vol. 389, p 353.

106. Miglena, K.; Michael, S.; Marc, D., Role of Histone Acetylation in Cell Cycle Regulation. *Curr. Top. Med. Chem.* **2016,** *16* (7), 732-744.

107. Sun, X.-J.; Man, N.; Tan, Y.; Nimer, S. D.; Wang, L., The Role of Histone Acetyltransferases in Normal and Malignant Hematopoiesis. *Front. Oncol.* **2015,** *5*, 108.

108. Seiden-Long, I. M.; Brown, K. R.; Shih, W.; Wigle, D. A.; Radulovich, N.; Jurisica, I.; Tsao, M. S., Transcriptional targets of hepatocyte growth factor signaling and Ki-ras oncogene activation in colorectal cancer. *Oncogene* **2005,** *25*, 91.

109. Espíndola, M. S.; Soares, L. S.; Galvão-Lima, L. J.; Zambuzi, F. A.; Cacemiro, M. C.; Brauer, V. S.; Marzocchi-Machado, C. M.; de Souza Gomes, M.; Amaral, L. R.; Martins-Filho, O. A.; Bollela, V. R.; Frantz, F. G., Epigenetic alterations are associated with monocyte immune dysfunctions in HIV-1 infection. *Sci. Rep.* **2018,** *8* (1), 5505.

110. Zheng, Y.; Thompson, P. R.; Cebrat, M.; Wang, L.; Devlin, M. K.; Alani, R. M.; Cole, P. A., Selective HAT inhibitors as mechanistic tools for protein acetylation. *Methods Enzymol.* **2004,** *376*, 188-99.

111. Zheng, Y. G.; Wu, J.; Chen, Z.; Goodman, M., Chemical regulation of epigenetic modifications: Opportunities for new cancer therapy. *Med. Res. Rev.* **2008,** *28* (5), 645-687.

112. Luan, Y., Ngo, L., Han, Z., Wang, X., Qu, M., Zheng, Y. G., Histone Acetyltransferases: Enzymes, Assays, and Inhibitors. In *Epigenetic Technological Applications*, Zheng, Y. G., Ed. Academic Press: San Diego, 2015; pp 291-317.

113. Lau, O. D.; Kundu, T. K.; Soccio, R. E.; Ait-Si-Ali, S.; Khalil, E. M.; Vassilev, A.; Wolffe, A. P.; Nakatani, Y.; Roeder, R. G.; Cole, P. A., HATs off: Selective Synthetic Inhibitors of the Histone Acetyltransferases p300 and PCAF. *Mol. Cell* **2000,** *5* (3), 589-595.

114. Yang, C.; Ngo, L.; Zheng, Y. G., Rational Design of Substrate- Based Multivalent Inhibitors of the Histone Acetyltransferase Tip60. *ChemMedChem* **2014,** *9* (3), 537-541.

115. Yuan, H.; Rossetto, D.; Mellert, H.; Dang, W.; Srinivasan, M.; Johnson, J.; Hodawadekar, S.; Ding, E. C.; Speicher, K.; Abshiru, N.; Perry, R.; Wu, J.; Yang, C.; Zheng, Y. G.; Speicher, D. W.; Thibault, P.; Verreault, A.; Johnson, F. B.; Berger, S. L.; Sternglanz, R.; McMahon, S. B.; Cote, J.; Marmorstein, R., MYST protein acetyltransferase activity requires active site lysine autoacetylation. *EMBO J.* **2012,** *31* (1), 58-70.

116. Poux, A. N.; Cebrat, M.; Kim, C. M.; Cole, P. A.; Marmorstein, R., Structure of the GCN5 histone acetyltransferase bound to a bisubstrate inhibitor. *Proc. Natl. Acad. Sci. U. S. A.* **2002,** *99* (22), 14065-70.

117. Makowski, A. M.; Dutnall, R. N.; Annunziato, A. T., Effects of acetylation of histone H4 at lysines 8 and 16 on activity of the Hat1 histone acetyltransferase. *J. Biol. Chem.* **2001,** *276* (47), 43499-502.

118. Ngo, L.; Wu, J.; Yang, C.; Zheng, Y. G., Effective Quenchers Are Required to Eliminate the Interference of Substrate: Cofactor Binding in the HAT Scintillation Proximity Assay. *Assay Drug Dev. Technol.* **2015,** *13* (4), 210-220.

119. Copeland, R. A., *Tight Binding Inhibition. In Evaluation of Enzyme Inhibitors in Drug Discovery.* . 2013.

120. He, M.; Han, Z.; Liu, L.; Zheng, Y. G., Chemical Biology Approaches for Investigating the Functions of Lysine Acetyltransferases. *Angew. Chem.* **2018,** *57* (5), 1162-1184.

121. Duggleby, R. G., Determination of inhibition constants, I50 values and the type of inhibition for enzyme-catalyzed reactions. *Biochem. Med. Metab. Biol.* **1988,** *40* (2), 204-212.

122. Lau, O. D.; Courtney, A. D.; Vassilev, A.; Marzilli, L. A.; Cotter, R. J.; Nakatani, Y.; Cole, P. A., p300/CBP-associated factor histone acetyltransferase processing of a peptide substrate. Kinetic analysis of the catalytic mechanism. *J. Biol. Chem.* **2000,** *275* (29), 21953-9.

123. Yu, M.; Magalhaes, M. L.; Cook, P. F.; Blanchard, J. S., Bisubstrate inhibition: Theory and application to N-acetyltransferases. *Biochemistry* **2006,** *45* (49), 14788-94.

124. Khalil, E. M.; Cole, P. A., A potent inhibitor of the melatonin rhythm enzyme. *J. Am. Chem. Soc.* **1998,** *120* (24), 6195-6196.

125. Wapenaar, H.; Dekker, F. J., Histone acetyltransferases: challenges in targeting bi-substrate enzymes. *Clin. Epigenetics* **2016,** *8* (1), 59.

126. Duan, G.; Walther, D., The Roles of Post-translational Modifications in the Context of Protein Interaction Networks. *PLoS Comp. Biol.* **2015,** *11* (2), e1004049.

127. Mahlknecht, U.; Hoelzer, D., Histone acetylation modifiers in the pathogenesis of malignant disease. *Mol. Med.* **2000,** *6* (8), 623-44.

128. Wang, Y.; Miao, X.; Liu, Y.; Li, F.; Liu, Q.; Sun, J.; Cai, L., Dysregulation of Histone Acetyltransferases and Deacetylases in Cardiovascular Diseases. *Oxid. Med. Cell. Longev.* **2014,** *2014*, 11.

129. Beekum, O. V.; Kalkhoven, E., Aberrant Forms of Histone Acetyltransferases in Human Disease. In *Chromatin and Disease*, Kundu, T. K.; Bittman, R.; Dasgupta, D.; Engelhardt, H.; Flohe, L.; Herrmann, H.; Holzenburg, A.; Nasheuer, H. P.; Rottem, S.; Wyss, M.; Zwickl, P., Eds. Springer Netherlands: Dordrecht, 2007; pp 235-268.

130. Chen, Y.; Sprung, R.; Tang, Y.; Ball, H.; Sangras, B.; Kim, S. C.; Falck, J. R.; Peng, J.; Gu, W.; Zhao, Y., Lysine Propionylation and Butyrylation Are Novel Post-translational Modifications in Histones. *Mol. Cell. Proteomics* **2007,** *6* (5), 812-819.

131. Kaczmarska, Z.; Ortega, E.; Goudarzi, A.; Huang, H.; Kim, S.; Márquez, J. A.; Zhao, Y.; Khochbin, S.; Panne, D., Structure of p300 in complex with acyl-CoA variants. *Nat. Chem. Biol.* **2016,** *13*, 21.

132. Sabari, B. R.; Zhang, D.; Allis, C. D.; Zhao, Y., Metabolic regulation of gene expression through histone acylations. *Nature Reviews Molecular Cell Biology* **2016,** *18*, 90.

133. Tan, M.; Luo, H.; Lee, S.; Jin, F.; Yang, Jeong S.; Montellier, E.; Buchou, T.; Cheng, Z.; Rousseaux, S.; Rajagopal, N.; Lu, Z.; Ye, Z.; Zhu, Q.; Wysocka, J.; Ye, Y.; Khochbin, S.; Ren, B.; Zhao, Y., Identification of 67 Histone Marks and Histone Lysine Crotonylation as a New Type of Histone Modification. *Cell* **2011,** *146* (6), 1016-1028.

134. Liu, X.; Wei, W.; Liu, Y.; Yang, X.; Wu, J.; Zhang, Y.; Zhang, Q.; Shi, T.; Du, J. X.; Zhao, Y.; Lei, M.; Zhou, J.-Q.; Li, J.; Wong, J., MOF as an evolutionarily conserved histone crotonyltransferase and transcriptional activation by histone acetyltransferase-deficient and crotonyltransferase-competent CBP/p300. *Cell Discovery* **2017,** *3*, 17016.

135. Xu, W.; Wan, J.; Zhan, J.; Li, X.; He, H.; Shi, Z.; Zhang, H., Global profiling of crotonylation on non-histone proteins. *Cell Res.* **2017,** *27*, 946.

136. Feldman, J. L.; Baeza, J.; Denu, J. M., Activation of the Protein Deacetylase SIRT6 by Long-chain Fatty Acids and Widespread Deacylation by Mammalian Sirtuins. *The Journal of Biological Chemistry* **2013,** *288* (43), 31350-31356.

137. Bao, X.; Wang, Y.; Li, X.; Li, X.-M.; Liu, Z.; Yang, T.; Wong, C. F.; Zhang, J.; Hao, Q.; Li, X. D., Identification of 'erasers' for lysine crotonylated histone marks using a chemical proteomics approach. *eLife* **2014,** *3*, e02999.

138. Tan, M.; Luo, H.; Lee, S.; Jin, F.; Yang, Jeong S.; Montellier, E.; Buchou, T.; Cheng, Z.; Rousseaux, S.; Rajagopal, N.; Lu, Z.; Ye, Z.; Zhu, Q.; Wysocka, J.; Ye, Y.; Khochbin, S.; Ren,

B.; Zhao, Y., Identification of 67 Histone Marks and Histone Lysine Crotonylation as a New Type of Histone Modification. *Cell 146* (6), 1016-1028.

139. Liu, S.; Yu, H.; Liu, Y.; Liu, X.; Zhang, Y.; Bu, C.; Yuan, S.; Chen, Z.; Xie, G.; Li, W.; Xu, B.; Yang, J.; He, L.; Jin, T.; Xiong, Y.; Sun, L.; Liu, X.; Han, C.; Cheng, Z.; Liang, J.; Shang, Y., Chromodomain Protein CDYL Acts as a Crotonyl-CoA Hydratase to Regulate Histone Crotonylation and Spermatogenesis. *Mol. Cell 67* (5), 853-866.e5.

140. Emilie, M.; Sophie, R.; Yingming, Z.; Saadi, K., Histone crotonylation specifically marks the haploid male germ cell gene expression program. *Bioessays* **2012,** *34* (3), 187-193.

141. Ruiz-Andres, O.; Sanchez-Niño, M. D.; Cannata-Ortiz, P.; Ruiz-Ortega, M.; Egido, J.; Ortiz, A.; Sanz, A. B., Histone lysine crotonylation during acute kidney injury in mice. *Disease Models & Mechanisms* **2016,** *9* (6), 633.

142. Fellows, R.; Denizot, J.; Stellato, C.; Cuomo, A.; Jain, P.; Stoyanova, E.; Balázsi, S.; Hajnády, Z.; Liebert, A.; Kazakevych, J.; Blackburn, H.; Corrêa, R. O.; Fachi, J. L.; Sato, F. T.; Ribeiro, W. R.; Ferreira, C. M.; Perée, H.; Spagnuolo, M.; Mattiuz, R.; Matolcsi, C.; Guedes, J.; Clark, J.; Veldhoen, M.; Bonaldi, T.; Vinolo, M. A. R.; Varga-Weisz, P., Microbiota derived short chain fatty acids promote histone crotonylation in the colon through histone deacetylases. *Nature Communications* **2018,** *9* (1), 105.

143. Ruiz-Andres, O.; Sanchez-Niño, M. D.; Cannata-Ortiz, P.; Ruiz-Ortega, M.; Egido, J.; Ortiz, A.; Sanz, A. B., Histone lysine crotonylation during acute kidney injury in mice. *Disease Models & Mechanisms* **2016,** *9* (6), 633-645.

144. Agudelo Garcia, P. A.; Hoover, M. E.; Zhang, P.; Nagarajan, P.; Freitas, M. A.; Parthun, M. R., Identification of multiple roles for histone acetyltransferase 1 in replication-coupled chromatin assembly. *Nucleic Acids Research* **2017,** *45* (16), 9319-9335.

145. Nagamori, I.; Cruickshank, V. A.; Sassone-Corsi, P., Regulation of an RNA granule during spermatogenesis: acetylation of MVH in the chromatoid body of germ cells. *J. Cell Sci.* **2011,** *124* (24), 4346-4355.

146. Thompson, P. R.; Wang, D.; Wang, L.; Fulco, M.; Pediconi, N.; Zhang, D.; An, W.; Ge, Q.; Roeder, R. G.; Wong, J.; Levrero, M.; Sartorelli, V.; Cotter, R. J.; Cole, P. A., Regulation of the p300 HAT domain via a novel activation loop. *Nature Structural &Amp; Molecular Biology* **2004,** *11*, 308.

147. Deng, W.; Wang, C.; Zhang, Y.; Xu, Y.; Zhang, S.; Liu, Z.; Xue, Y., GPS-PAIL: prediction of lysine acetyltransferase-specific modification sites from protein sequences. *Sci. Rep.* **2016,** *6*, 39787.

148. Liu, X.; Wei, W.; Liu, Y.; Yang, X.; Wu, J.; Zhang, Y.; Zhang, Q.; Shi, T.; Du, J. X.; Zhao, Y.; Lei, M.; Zhou, J. Q.; Li, J.; Wong, J., MOF as an evolutionarily conserved histone crotonyltransferase and transcriptional activation by histone acetyltransferase-deficient and crotonyltransferase-competent CBP/p300. *Cell discovery* **2017,** *3*, 17016.

149. Wu, H.; Moshkina, N.; Min, J.; Zeng, H.; Joshua, J.; Zhou, M. M.; Plotnikov, A. N., Structural basis for substrate specificity and catalysis of human histone acetyltransferase 1. *Proc Natl Acad Sci U S A* **2012,** *109* (23), 8925-30.

150. Yang, C.; Mi, J.; Feng, Y.; Ngo, L.; Gao, T.; Yan, L.; Zheng, Y. G., Labeling Lysine Acetyltransferase Substrates with Engineered Enzymes and Functionalized Cofactor Surrogates. *Journal of the American Chemical Society* **2013,** *135* (21), 7791-7794.

151. Han, Z.; Chou, C.-w.; Yang, X.; Bartlett, M. G.; Zheng, Y. G., Profiling Cellular Substrates of Lysine Acetyltransferases GCN5 and p300 with Orthogonal Labeling and Click Chemistry. *ACS Chemical Biology* **2017,** *12* (6), 1547-1555.

152. Paik, W. K.; Pearson, D.; Lee, H. W.; Kim, S., Nonenzymatic acetylation of histones with acetyl-CoA. *Biochimica et Biophysica Acta (BBA) - Nucleic Acids and Protein Synthesis* **1970,** *213* (2), 513-522.

153. Wagner, G. R.; Hirschey, M. D., Non-enzymatic protein acylation as a carbon stress regulated by sirtuin deacylases. *Molecular cell* **2014,** *54* (1), 5-16.

154. Yang, X.-J.; Seto, E., Lysine Acetylation: Codified Crosstalk with Other Posttranslational Modifications. *Mol. Cell* **2008,** *31* (4), 449-461.

155. Strahl, B. D.; Allis, C. D., The language of covalent histone modifications. *Nature* **2000,** *403*, 41.

156. Zhang, C.; Zhong, J. F.; Stucky, A.; Chen, X.-L.; Press, M. F.; Zhang, X., Histone acetylation: novel target for the treatment of acute lymphoblastic leukemia. *Clin. Epigenetics* **2015,** *7*, 117.